M-Pos69 RAPID RELEASE OF OCCLUDED ^{86}Rb FROM THE Na PUMP. Bliss Forbush III, (Intro. by S. Dissing), Dept. of Physiol., Yale University, New Haven, CT 06510.

K or Rb ions which are tightly bound to Na,K-ATPase are presumed to represent an "occluded state" in which the ions are inaccessible to solutions on both sides of the membrane (Glynn and Richards, J. Physiol. 330:17,1982). For this to be a normal state of the transport cycle, on the addition of ATP, the release of ions must occur at least as rapidly as the turnover rate of the pump: about 15 sec^{-1} at 20°C. I have used a rapid pressure filtration apparatus to continuously monitor the ^{86}Rb that is released from the Na,K-ATPase. A sample of membrane-bound purified Na,K-ATPase (1-2 mg/ml) is incubated with 2 mM $MgCl_2$, 2 mM ^{86}Rb, in 4 ul of 25 mM imidazole, then diluted in cold buffer and filtered onto the surface of a cellulose ester filter. Following a brief wash, the wet filter is transferred to the pressure filtration device where flow of warm buffer (20°C) is begun, and after an additional 0.1 s, the solution is switched to one containing ATP or other ligand. The solution passes through the filter and into a row of rapidly moving cuvettes. The time resolution of the apparatus, including the time for 90% complete change of solutions, is about 15 ms. In the presence of 50 mM NaCl, 25 mM imidazole (pH 7.5), occluded ^{86}Rb is released with a rate constant of 18 $\pm$ 2 sec^{-1} after addition of MgATP ($K_{1/2}$ = 0.4 mM). De-occlusion is slowed two fold in the absence of Mg^{++} or in the presence of millimolar concentrations of free Mg^{++}. ADP and P_i also promote de-occlusion with maximal rates of 3.7 sec^{-1} and 11 sec^{-1} respectively under the above conditions. The rate of Rb release following addition of MgATP, while 3-fold lower than the value that has been inferred from fluorescence measurements, is consistent with de-occlusion as the rate limiting step in Na,K transport.

M-Pos70 VANADIUM METABOLISM IN *S. cerevisiae*. Gail R. Willsky, Deborah A. Preischel and Barbara C. McCabe, Dept. of Biochemistry, SUNY at Buffalo, 14215.

Vanadium metabolism may be involved in the normal control of various cellular processes. Vanadate (V), a potent inhibitor of the Na,K-ATPase, is reduced to the less inhibitory vanadyl (IV) by cellular glutathione. In addition, recent work has implicated vanadate as a stimulator of various cellular processes in cell culture systems. We have investigated vanadium metabolism in yeast, since this organism contains a plasma membrane Mg(2+)ATPase similar in mechanism to the Na,K-ATPase and is easily manipulated. In yeast vanadate stopped cell growth while vanadyl stimulated cell growth. Both ions inhibited the plasma membrane Mg(2+)ATPase (but vanadate was a more potent inhibitor) and were transported into the cell (as shown with radiolabeled vanadate and vanadyl ions). EPR spectroscopy was used to monitor the cell associated paramagnetic vanadyl ions and 51(V)-NMR to monitor other cell associated vanadium ions. Cells were exposed to both toxic (1mM) and nontoxic (5mM) concentrations of vanadate in the media. EPR spectra showed that in both media vanadate became cell associated and was converted to vanadyl, which was excreted into the media. In the presence of 5 mM vanadate 51(V)-NMR studies have shown the accumulation of new cellular vanadium resonances (distinct from the orthovanadate signal) which are not present in cells exposed to 1 mM vanadate and appear to be associated with cell toxicity. These studies imply that the vanadyl ion may be involved in the stimulatory effects observed when vanadate is added to cultured cells and provide the starting point for learning if vanadium metabolism is involved in the control of the Na,K-ATPase *in vivo*.

M-Pos71 INTERNAL SITES ARE RESPONSIBLE FOR pH SENSITIVITY OF SODIUM PUMP FLUXES. G. E. Breitwieser and J. M. Russell. Department of Physiology and Biophysics, University of Texas Medical Branch, Galveston, Texas 77550

We have previously reported (Biophys. J., 41, 71a (1983)) that ouabain-sensitive sodium efflux (i.e. sodium pump flux), in squid giant axons is modulated by pH changes of the intracellular, but not extracellular fluid. Thus, ouabain-sensitive Na efflux is maximum at an intracellular pH of about 7.4, and is reduced by pH_i changes in either the acidic or alkaline directions (over the range 6.1-8.6). We now report that ouabain-sensitive potassium influx is likewise modulated by internal pH changes, while being relatively insensitive to variations of external pH (over the range 6.0-8.1). The near-identical dependence of both fluxes upon pH_i suggests a common mechanism of action of protons on the two Na^+ pump fluxes. Clearly, this action is mediated at an intracellular site since these experiments were conducted in internally dialyzed squid giant axons, a technique which permits relatively independent control of internal and external pH. The characteristic "bell-shaped" dependence of both Na and K fluxes on pH_i suggests that at least two pH-sensitive sites exist on the cytoplasmic face of the membrane. Presently available data do not reveal the identity of these sites. However, likely candidates would be the internal Na binding site and/or the ATP binding site. The latter site seems less likely inasmuch as we used 20 mM ATP, thus exceeding published $K_{\frac{1}{2}}$ values by a factor of 100. Alternatively, the sites affected by changing pH_i could be distinct from any of the documented substrate sites, perhaps affecting overall sodium pump activity by altering the pump's ability to undergo required conformational changes. (Supported by DHHS NS 11946).

M-Pos72 MECHANISMS OF ATP HYDROLYSIS BY Na,K-ATPase FROM Mg^{++} INHIBITION PATTERNS, L.Beaugé and C.H.Pedemonte, División de Biofísica, Instituto M. y M. Ferreyra, 5000 Córdoba, Argentina

The hydrolysis of ATP catalyzed by purified Na,K-ATPase from pig kidneys was more sensitive to Mg^{++} inhibition in the presence of Na+K (Na,K-ATPase) than in the presence of Na alone, either at high (Na,Na-ATPase) or low (Na,0-ATPase) Na concentrations. This was seen with 3 mM and 0.003 mM ATP, but Mg^{++} inhibition was more marked at low ATP concentration. In the presence of other monovalent cations in addition to Na, the K_i for Mg^{++} followed the sequence: none > Li > NH_4 > K > Rb; the K_i were lower in the uM than in the mM ATP range, but the sequence was not altered. The $K_{0.5}$ for ATP activation followed the sequence: none < Li < NH_4 < K < Rb; the $K_{0.5}$ were lower at 0.05 mM than at 10 mM Mg^{++} but the order was not modified. With 150 mM ChCl and Mg^{++} but with no K, trypsin inactivation of Na,K-ATPase agreed with the pattern described for the E_1 state; the addition of K changed the pattern into that observed with the E_2 enzyme form. These results concur with two mechanisms for Mg^{++} inhibition of Na,K-ATPase: "product " and dead-end; the first is favoured by all conditions stabilizing the E_2-occluded state, whereas the second would be brought by an enzyme-Mg complex with the enzyme in the E_1 state. The results are also consistent with a model where (i) in the ATP ase cycle the route towards rephosphorylation is different in spontaneous and cation-induced dephosphorylation, (ii) ATP accelerates disocclusion but has no effect on the E_2-E_1 transformation, and (iii) the affinity of the E_2 enzyme form for ATP is determined not by the E_2 state but by the "degree" of occlusion of the dephosphorylating cation. (Supported by Grants from CONICET, CONICOR and Fundación Lucio Cherny).

M-Pos73 RADIATION TARGET SIZE OF Na-K PUMP AND Na-K ATPase OF HUMAN ERYTHROCYTES. Jong-Sik Hah, John Cuppoletti, and Chan Y. Jung (intr. C.R. Zobel), VA Medical Center and Biophysical Sciences, SUNY/AB, Buffalo, NY 14215, and Department of Medicine, UCLA, Los Angeles, CA 90073.

Previous biochemical studies indicate that the Na-K ATPase is composed of two subunits, α and β, in a form of $\alpha_2\beta_2$ with a molecular weight of approximately 300,000 daltons. There is also suggestive evidence that the Na-K pump in human erythrocytes occurs in complex with some glycolytic enzymes. We assessed here in situ assembly size of the Na-K pump and Na-K ATPase of human erythrocytes by applying classical target theory to radiation inactivation data of the ouabain-sensitive sodium flux and ATP hydrolysis of intact cells and ghosts. Cells (in the presence of cryoprotective agent) and ghosts were irradiated at -40 to -50°C with an increasing dose of a 1.5 MeV electron beam, and after thawing, the pump and/or enzyme activities were assayed. Each activity measured was inactivated as a simple exponential function of radiation dose, from which a radiation sensitive volume (target size) was calculated. When intact cells were used, the target size of both Na-K pump and Na-K ATPase was found to be approximately 600,000 dalton. This target size of the ATPase was reduced to approximately 325,000 dalton if the cells were pretreated with strophantidin. When ghosts were used, the ATPase target size was again approximately 325,000 daltons. Our target size measurement suggests that, in intact cells, the Na-K ATPase pump exists either as a dimer of ($\alpha_2\beta_2$) which is a functional unit or as a monomer of ($\alpha_1\beta_2$) but in tight complex with other enzyme or enzymes. The results also suggest that this dimeric or heterocomplex association is dissociated during ghost preparation and strophantidin treatment.
This work was supported by NIH grant AM13376.

M-Pos74 EFFECTS OF CALCIUM AND POTASSIUM ON THE ATP-ADP EXCHANGE CATALYZED BY Na,K-ATPase, L. Beaugé and Marta Campos, División de Biofísica, Instituto M. y M. Ferreyra, 5000 Córdoba, Argentina

In contraposition to the findings in microsomes of Electrophorus electricus (Fahn et al. J.Biol. Chem. 241:1882,1966) $CaCl_2$, in the absence of $MgCl_2$, stimulates a Na-dependent-ouabain-sensitive ATP-ADP exchange catalyzed by purified Na,K-ATPase from pig kidneys. As a function of the divalent cation concentration this exchange follows a biphasic curve with a maximun at about 20 uM ionized (3 mM ATP-0.75 mM ADP). In absolute values the exchange is larger in Mg^{++} than in Ca^{++}, but the ratio Ca-activated/Mg-activated increases at high concentrations where Mg^{++} becomes more inhibitory than Ca^{++}. The Na dependence of the ATP-ADP exchange varies with the divalent cation present: with Mg^{++} there is a partial inhibition at 2.5-10 mM-Na which is not seen with Ca^{++}. In the presence of Na, K ions (at a Na/K ratio = 10/1) stimulate a ouabain-sensitive ATP-ADP exchange (see also Banerjee & Wong, J.Biol.Chem.247:5409,1972); this stimulation is more manifested in Mg^{++} than in Ca^{++}. In Mg^{++}, the K stimulation is observed at ATP/ADP concentrations of 3 mM/0.75 mM, but is replaced by inhibition at 0.04 mM/0.01 mM and, even more marked , at 0.003 mM/0.001 mM. With 3 mM ATP/0.75 mM ADP, the $K_{0.5}$ for K stimulation is about 0.25 mM at 20 mM-Na and around 0.7 mM at 120 mM-Na. These results suggest that K ions stimulation of ouabain-sensitive ATP-ADP exchange takes place at extracellular sites, perhaps through an increase in the concentration of the E_1 enzyme form following the acceleration of the hydrolytic cycle. (Supported by Grants from CONICET, CONICOR and PNUD/UNESCO).

M-Pos75 EFFECT OF Ca^{2+} ON PHOSPHORYLATION OF (Na,K)-ATPase FROM P_i. Robert L. Post and H. Bernard Stewart*, Physiology Dept., Vanderbilt Univ. Med. Sch., Nashville, TN, 37232.

Ca^{2+} had two separate actions: (1) it inhibited catalysis of phosphorylation by Mg^{2+}; and (2) it formed a stable calcium-dephosphoenzyme complex, (Ca)E, that accepted phosphate from P_i in the presence of Mg^{2+}. The resulting phosphoenzyme, (Ca)E-P, exchanged its phosphate group with P_i immediately at 0°C, thus resembling the (K)E-P complex (Post et al. JBC 250, 691). Na^+ competitively inhibited formation of (Ca)E and (K)E. Experiments were done at 0°C at pH 7.2 in 40mM imidazole/MOPS, 1mM $^{32}P_i$, and 1 mg/ml enzyme from dog kidney. Order of addition of cations and chelators was varied. Reactions were terminated with acid and [^{32}P]phosphopeptides overlapping the active site were solubilized by peptic digestion and isolated by paper electrophoresis. E-P formation with 0.5-3mM Ca^{2+} was < 1 percent of that with 1-3mM Mg^{2+}; combinations of these cations gave intermediate levels supporting action (1) above. Action (2) was demonstrated by preincubating enzyme with variable [Na^+] and 2mM Mg^{2+} ± 2mM Ca^{2+}. Phosphorylation for 6 s was started with P_i plus EGTA to chelate the free Ca^{2+}. In the presence of 0, 3, or 10 mM NaCl without Ca^{2+}, E-P was 54, 16, or 2 percent and with Ca^{2+}, it was 30, 28 or 19 percent of phosphorylation capacity respectively. In the absence of Ca^{2+} a CDTA chase of E-P gave a rate constant of dephosphorylation of .12/s but a chase of (Ca)E-P gave a rate constant of > .7/s. Unlabeled (Ca)E-P was completely labeled < 4 s after radioactive P_i was added. K(1/2) for Ca^{2+} was about 20-30μM. We suggest that Ca^{2+} can replace K^+ as a ligand in the monovalent cation binding center of (Na,K)-ATPase. Supported by grant 5R01 HL-01974 from NHLBI and fellowship CA 07088 from NCI.

M-Pos76 ON THE RELATIONSHIP BETWEEN GLYCOLYSIS AND Na-K-ATPase IN CULTURED CELLS. R.S. Balaban and J.P. Bader, NHLBI, LKEM and NCI Bethesda, MD 20205

In several tissues a distinct coupling between glycolysis and Na-K-ATPase has been observed. We report here on studies concerning the coupling of glycolysis and Na-K-ATPase in Rous transformed Hamster cells (HTcBH) and Erhlich ascites tumor cells. The rate of Na-K-ATPase was estimated in the intact cells from the initial rate of ouabain-sensitive K-influx after K reintroduction to K-depleted cells using an extracellular K^+ electrode. Experiments were performed with cells producing ATP via oxidative phosphorylation alone (i.e. lactate sole substrate), glycolysis alone (i.e. glucose as substrate in the absence of oxygen or with antimycin A), or glycolysis and oxidative phosphorylation (i.e. glucose and lactate as substrates in the presence of oxygen). The calculated ATP production rates by the cells were within 10% under these conditions. However, the maximum rate of Na-K-ATPase was two-fold higher (43.5 ± 2.5 to 98.3 ± 10.1 N moles/min mg (N = 10) in HTcBH cells) under both conditions where glycolysis was a source of ATP. The steady state chemical gradient for K across the plasma membrane was also increased with glycolysis. Aerobic glycolysis results in a net efflux of 33.4 ± 1.4 N moles H^+/min/mg in HTcBH cells due to the production of lactic acid. Thus, it is possible that Na^+-H^+ exchange could increase Na^+-K^+ ATPase activity by increasing cell Na^+. However, 1 mM amiloride, an inhibitor of Na^+-H^+ exchange, had no effect on proton efflux or on K influx. Other transport proceses associated with glycolysis, such as Na glucose cotransport and K^+-H^+ exchange, were also experimentally ruled out as mediators of the glycolysis effect on Na-K-ATPase activity. These data suggest that glycolysis is more effectively coupled to Na-K-ATPase than oxidative phosphorylation in these cultured cells.

M-Pos77 ADP STIMULATES RELEASE OF INORGANIC PHOSPHATE FROM E_2-P FORMED BY (Na,K)-ATPase AND Ca-ATPase FROM SARCOPLASMIC RETICULUM. A.S. Hobbs and R.W. Albers, NINCDS, NIH, Bethesda, MD 20205; P.F. Heller and J.P. Froehlich, NIA, NIH, Baltimore, MD 21224.

Incubation of (Na,K)-ATPase from eel electroplax for 116 msec with 10 μM ATP, 25 mM NaCl and 1 mM $MgCl_2$ results in the production of a high level of phosphorylated protein (E-P), an intermediate in ATPase and Na pump turnover. Under these conditions the phosphoenzyme is presumably in E_2-P, the K sensitive form, as opposed to E_1-P, the ADP sensitive form. When we subsequently added 5 mM ADP plus 10 mM EDTA (to prevent rephosphorylation), two phases were seen in the disappearance of E-P, a rapid phase with a rate greater than 50 sec^{-1}, which accounted for 15% or more of the E-P and was accompanied by apparent stoichiometric amounts of P_i release, and a slower phase with a rate of about 4 sec^{-1}, which had less than stoichiometric amounts of P_i associated with it. The rate of decay of the rapid phase was faster than the measured rate of E-P turnover under the phosphorylation conditions, indicating stimulation of turnover by ADP. Similar results were obtained with the Ca-ATPase of sarcoplasmic reticulum phosphorylated at low (0.1 mM) Mg in the absence of KCl. These results suggest that ADP can have a K-like effect on the rate of decomposition of E_2-P in both the (Na,K)- and Ca-ATPases and indicate the need for caution in interpreting results of experiments measuring ADP sensitive E-P when P_i release is not determined stimultaneously.

M-Pos78 CHARACTERIZATION OF PORCINE SKELETAL MUSCLE SARCOLEMMA. James R. Mickelson, Esther M. Gallant and Charles F. Louis. Department of Veterinary Biology, University of Minnesota, St. Paul, Minnesota 55108.

Sarcolemma (SL) was isolated from porcine skeletal muscle by the procedure of Barchi et al. (Biochim. Biophys. Acta 550, 59-76, 1979). The SL was characterized by its high cholesterol (257 µg/mg) and phospholipid content (78 µg P/mg) as well as its adenylate cyclase (basal = 0.14 pmoles/mg/min, NaF-activated = 1.02 nmoles/mg/min) and latent ouabain-sensitive ($Na^+ + K^+$)-ATPase activities (45 µmoles Pi/mg/hr). These values compare favorably with those of skeletal muscle SL preparations from other species. Latent ($Na^+ + K^+$)-ATPase, acetylcholinesterase and K^+-p-nitrophenylphosphatase values indicate that approx. 70% of the SL vesicles are oriented inside-out. The Ca^{2+}-ATPase activity of SL (55 nmoles Pi/mg/min at 37°C) was stimulated 20% by 1 µM calmodulin. In contrast to sarcoplasmic reticulum (SR), ATP-supported Ca uptake by SL was linear for up to 2 min (12 nmoles Ca/mg/min at 37°C); the initial rate of SL Ca uptake was stimulated 40% by 1 µM calmodulin. Oxalate, which enhanced the initial rate of SR Ca uptake to 2 µmoles/mg/min, had no effect on the initial rate of SL Ca uptake. However, the maximal Ca capacity of SL (90 nmoles/mg) was increased 25% by 5mM oxalate. When SL was loaded with Ca by the Ca^{2+}-ATPase Ca pump, approx 40% of the Ca could be rapidly released by the addition of 30 mM NaCl. We conclude that porcine skeletal muscle SL contains both calmodulin-dependent Ca^{2+}-ATPase/Ca^{2+} pump, and Na/Ca exchange activities. (Supported by the Muscular Dystrophy Association).

M-Pos79 CALCIUM UPTAKE IN SQUID OPTIC NERVE MEMBRANE VESICLES. L. Osses, M. Condrescu and R. DiPolo. IVIC. Caracas, Venezuela.

Previous work in dialysed squid giant axons has demonstrated the existence of two membrane mechanisms that regulate the intracellular calcium concentration: the Ca pump and the Na/Ca exchange (DiPolo and Beaugé, Nature 278, 271-273, 1979). Here we report evidence for the presence of these two mechanisms in an axolemma rich plasma membrane fraction from squid optic nerves wich shows ($Ca^{2+} + Mg^{2+}$)-ATPase activity. This fraction is composed of 63% inside-out vesicles, as found by Con A - Sepharose chromatography and detergent treatment (Nonidet P-40 and Triton X-100). Calcium uptake experiments have been performed in this preparation using the millipore filtration technique or a Ca-sensitive electrode. An active calcium accumulation of 1 nmol $\cdot$ mg^{-1} $\cdot$ min^{-1} was observed in the presence of 2 mM ATP and 4 µM free calcium concentration; the accumulated Ca^{2+} could be released by A 23187 ionophore (10 g/ml). When the membrane vesicles were preloaded with sodium (300mM NaCl) and further diluted in a medium containing 100 µM Ca^{2+} they accumulated 27 nmol Ca^{2+} $\cdot$ mg^{-1} $\cdot$ min^{-1} in the absence of ATP. Experiments with vesicles preloaded with different Na concentrations (0 - 300 mM) indicated that the $K_{1/2}$ for the Na_i-Ca_o exchange is 60 mM. Ca uptake was not observed when vesicles were preloaded with KCl or N-methyl-D-glucamine chloride instead of NaCl. These results indicate the presence of both Ca pump and Na/Ca exchange in our membrane vesicle preparation with characteristics resembling the in vivo Ca transport. (Supported by CONICIT S1-1144. L. Osses is a recipient of a fellowship from "Fundación Vollmer", Venezuela).

M-Pos80 FURTHER CHARACTERIZATION OF THE GASTRIC Ca^{+2}-ATPase FOLLOWING COMPLETE SEPARATION FROM THE MICROSOMAL H^+, K^+-ATPase ACTIVITY. Tushar K. Ray and Jyotirmoy Nandi, Department of Surgery, S.U.N.Y. - Upstate Medical Center, Syracuse, New York 13210.

Purified dog gastric microsomes free from any enzymatically detectable basolateral and mitochondrial contaminants are highly enriched in secretory membrane located H^+, K^+-ATPase and were also demonstrated (Fed. Proc. 42, 1936, 1983) to have both high ($Ka=5x10^{-7}M$) and low ($Ka=5x10^{-4}M$) affinity Ca^{+2}-stimulated ATPase activities which are insensitive to NaN_3 and calmodulin. Based on some new evidences the K^+-stimulated and Ca^{+2}-stimulated components have been clearly suggested to be separate enzymic activities associated with the gastric microsomal vesicles. Thus, unlike the H^+, K^+-ATPase activity the Ca^{+2}-ATPase does not seem to be critically dependent on exogenous Mg^{+2}. Vanadate at 10 uM inhibits about 90% of the K^+-stimulated activity without affecting the Ca^{+2}-stimulated ATPase(s). SDS (0.033%) extraction with sonication at pH 8.0 followed by equillibrium sucrose density gradient centrifugation produced three distinct fractions; namely, a heavy membrane band (boyant density, 1.11) containing nearly "pure" and highly active H^+, K^+-ATPase, a light membrane band (boyant density, 1.08) containing all of the microsomal Mg^{+2} or Ca^{+2}-ATPase activities and a soluble fraction devoid of any ATPase and accounting for about 60% of the microsomal proteins. SDS-PAGE revealed a striking similarity between the H^+, K^+-ATPase and Ca^{+2}-ATPase containing membranes with respect to some proteins such as the 100,000 dalton thought to be characteristic of H^+, K^+-ATPase and a distinct glycoprotein of 85,000 daltons. Such similarities raise fundamental questions regarding the molecular identity of various ATPase activities associated with gastric microsomes. Some noteworthy features of the high and low affinity Ca^{+2}-ATPase include their differential sensitivity to pH and various inhibitors like EEDQ, DCCD and phenothiazines.

M-Pos81 PLASMA MEMBRANE Ca^{2+} TRANSPORT: INHIBITION BY MODEL HEPATOTOXINS IN VIVO. J.O. Tsokos-Kuhn, E.L. Todd, J.R. Mitchell and J.B. McMillin-Wood. Baylor Coll. Med. Houston, Tx. 77030.

Lethal cell injury from hepatotoxic drugs is postulated to result from an alteration in cell Ca^{2+} homeostasis. The ATP-dependent Ca^{2+} pump of the plasma membrane (PM) has high Ca^{2+} affinity and is the first defense against elevated cystolic $[Ca^{2+}]$. If the pump were a target of chemically reactive drug intermediates, cells could not maintain Ca^{2+} homeostasis. Thus, we studied the effect of model alkylating hepatotoxins given in vivo on Ca^{2+} transport by PM vesicles from livers of adult male rats. Ca^{2+} transport was decreased 55 ± 5% by bromobenzene (BrB) (1.5 nmol/kg i.p. in corn oil; 3 day pretreatment with 80 mg/kg phenobarbital; fasted 18h before dose; killed 4h post-dose), 70 ± 7% kg acetaminophen (PHAA) 2g/kg p.o. 20% in Tween 80; 1 day pretreatment with 3-methylcholanthrene; fasted; killed 2.5h), and 80 ± 4% by CCl_4 (2 ml/kg i.p. in corn oil; otherwise as for BrB). Diquat (35 mg/kg i.p. in saline; fasted; killed 4 h), which produces only oxidative stress in the liver, had no effect. However, the high affinity (Ca^{2+} + Mg^{2+})ATPase of liver PM [Lotersztajn et al., J. Biol. Chem. 257, 6638 (1982)], presumed but not yet demonstrated to be responsible for pumping Ca^{2+}, was much less affected by hepatotoxins. Only CCl_4 treatment produced as much as 50% (Ca^{2+} + Mg^{2+}) ATPase inhibition (contrasted to 80% reduction of Ca^{2+} transport); PHAA affected (Ca^{2+} + Mg^{2+})ATPase activity only slightly and BrB and diquat not at all. These data suggest either 1) uncoupling of ATPase from Ca^{2+} transport or 2) alterations in membrane Ca^{2+} permeabilities from drug-treated animals. Supported by GM26611 and GM13901.

M-Pos82 LIGAND INTERACTIONS WITH THE Ca PUMP and Na/Ca EXCHANGE IN DIALYZED SQUID AXONS. R. DiPolo and L. Beaugé. IVIC Caracas Venezuela and M.Y.M. Ferreyra Córdoba Argentina.

In squid axons, the extrusion of Ca is accomplished by two different mechanism: The Ca pump and the Na/Ca exchange. We have studied the interaction of physiological ligands other than Na_i and Ca_i with these two transport systems in internally dialyzed squid axons. The results show: 1) Internal Mg^{2+} is a potent inhibitor of the Na_o-dependent Ca efflux. At physiological Mg_i^{2+} (4 mM) the inhibition amounts to about 50%. The inhibition is partial, noncompetive with Ca_i and not affected by Na_i and ATP. The ATP dependent uncoupled efflux is unaffected by Mg_i up to 20 mM. Both components require Mg_i^{2+} for their activation by ATP. 2) At constant membrane potential, K_i^+ is an important cofactor for the uncoupled Ca efflux. 3) Orthophosphate (P_i) activates the Na_o-dependent Ca efflux without affecting the uncoupled component. Activation by P_i occurs only in the presence of ATP or hydrolizable ATP analogs. 4) ADP is a potent inhibitor of the uncoupled Ca efflux. The Na_o-dependent component is inhibited by ADP only at much higher concentrations. These results indicate: first, depending on the concentration of Ca_i^{2+}, Na_i^+, Mg_i^{2+} and P_i, the Na/Ca carrier can operate under a low or a high rate regime; second, the interactions of Mg_i, P_i Na_i and ATP with the carrier are not interdependent; third, the effect of P_i resembles the stimulation of the Na_o-dependent Ca efflux by internal vanadate.
(Supported by CONICIT S1-1144 and NSF-BNS 8025570).

M-Pos83 THE PH DEPENDENCE OF THE KM AND VM OF BOVINE CARDIAC SARCOLEMMAL CA^{2+}-ATPASE PUMP. Deborah Dixon, Dept. of Pharmacology, Univ. of Miami School of Medicine, Miami, Florida 33101.

The Km and Vm were investigated to obtain information on the translocator enzyme. Active uptake in inside-out vesicles was studied by addition of 1 mM Mg-ATP to sarcolemmal vesicles (0.07 mg prot./ml) following preincubation in a medium containing 160 mM KCl, 20 mM MOPS, 50 mM Tris at 37°C and various pH values. The $[Ca^{2+}]_o$ was set at the desired level with Ca-EGTA. Active uptake was measured by chlorotetracycline (1×10^{-6}M) fluorescence which was shown to be proportional to $[Ca^{2+}]_i$ by calibration experiments performed at each pH. A plot of log 1/Km vs. pH gave a curve with two straight line segments. A slope of 1.59 ± 0.06 was seen between pH values 6.2 and 7.8 and of 0.7 ± 0.02 between pH 7.8 and 8.2. These data suggest that 2 H^+ compete with one Ca^{2+} for the binding site on the translocator. Furthermore, a pK value in the region of 7.8 is suggested. The Vm, shows a pH optimum of 7.4 with a maximum value of 4 mM/min. These observations will be compared to data from rabbit skeletal sarcoplasmic reticulum obtained in comparable experiments. The data are quite similar, demonstrating only quantitative differences. Skeletal sarcoplasmic reticulum displays a pK of 7.0 as compared to that in the region of 7.8 for sarcolemma, and a much greater Vm; 6.5 mM/sec. as compared to a sarcolemmal rate of 4 mM/min. Supported by GM23990 and Training Grant HL07188.

M-Pos84 IDENTIFICATION AND PARTIAL PURIFICATION OF THE CARDIAC SODIUM-CALCIUM EXCHANGER. Calvin C. Hale, Robert S. Slaughter, Diane Ahrens and John P. Reeves. Roche Institute of Molecular Biology, Roche Research Center, Nutley, NJ 07110.

Cardiac sarcolemmal (SL) vesicles were solubilized in 2% cholate, 0.5 M NaCl, 25 mg/ml soybean phospholipids and reconstituted following the procedure of Miayamoto and Racker (J. Biol. Chem. 255: 2656, 1980). Initial rates of Na-Ca exchange in the reconstituted proteoliposomes were approximately 20-fold higher than in the native vesicles. Total recovery of exchange activity (specific activity x total protein) exceeded 100%, indicating that the exchange system had been activated by the reconstitution procedure. Examination of native and reconstituted vesicles by SDS-PAGE revealed two protein bands that were substantially enriched in the reconstituted system: one at 48 kD and a diffuse band centered at 82kD. A cholate extract of SL vesicles was applied to a Sephacryl S-300 column and the various eluted fractions were reconstituted, assayed for Na-Ca exchange and examined by SDS-PAGE. The activity profile, after correcting for loss of activity on the column, showed a good correlation with the diffuse 82 kD band. A cholate extract of SL vesicles was treated with 1 mg/ml pronase for 10 min at 37°C and reconstituted using a procedure similar to that described by Wakabayashi and Goshima (Biochim. Biophys. Acta 693: 125, 1982). The resulting proteoliposomes catalyzed Na-Ca exchange with a specific activity 30- to 100-fold greater than that of native vesicles. Upon examination by SDS-PAGE, these proteoliposomes exhibited a single major band at 82 kD with several minor bands at lower molecular weights that migrated identically to the components of pronase. The results provide strong evidence that the 82 kD band represents the cardiac Na-Ca exchange protein.

M-Pos85 AMILORIDE ANALOGS, NON-COMPETITIVE INHIBITORS OF SODIUM-CALCIUM EXCHANGE IN CARDIAC SARCOLEMMAL VESICLES. Robert Slaughter, Pilar de la Peña, John P. Reeves, Edward Cragoe* and Gregory J. Kaczorowski*. Roche Institute of Molecular Biology, Roche Research Center, Nutley, NJ 07110, and *Merck Institute for Therapeutic Research, Rahway, NJ 07065.

Benzamil, an amiloride derivative, inhibited Na_i-dependent Ca uptake in cardiac sarcolemmal vesicles in a non-competitive manner with respect to Ca (K_i=400 μM). It also inhibited Ca_i-dependent ^{45}Ca uptake (Ca-Ca exchange) although in this case, a mixed type of inhibition was observed. Inhibition of Ca-Ca exchange was more pronounced in sucrose than in 160 mM KCl: The non-competitive K_i for benzamil in sucrose was 52 μM and in 160 mM KCl, it was 190 μM. In addition, benzamil (200 μM) inhibited Na_i-dependent ^{22}Na uptake (Na-Na exchange) by approximately 50% at 5 mM Na_o. A 2-methoxy-5-nitrobenzyl derivative of amiloride was tested as a possible photoaffinity probe of the Na-Ca exchanger. In the dark, this derivative inhibited Na-Ca exchange reversibly in a manner similar to benzamil. Irradiation of vesicles at 313 nm in the presence of this derivative (in 160 mM KCl) resulted in a time- and concentration-dependent loss of Na-Ca exchange activity which was not reversed by extensive washing (50% inhibition after 15 min. irradiation at 100 μM inhibitor). Controls incubated with the inhibitor in the dark or irradiated in the absence of inhibitor showed no loss of activity. The presence of 160 mM NaCl during photolysis protected the exchanger against inactivation although the presence of 5 mM $CaCl_2$ did not. The results suggest that amiloride analogs may interact with the site on the exchanger that binds the third Na ion during Na-Ca exchange; this may also be the site responsible for monovalent cation stimulation of Ca-Ca exchange.

M-Pos86 INACTIVATION OF THE CARDIAC SODIUM-CALCIUM EXCHANGE SYSTEM WITH QUINACRINE MUSTARD. Pilar de la Peña and John P. Reeves. Roche Institute of Molecular Biology, Roche Research Center, Nutley, NJ 07110.

Quinacrine, an acridine derivative and potent local anesthetic, inhibited both Na_i-dependent Ca^{2+} uptake (Na-Ca exchange) and Ca_i-dependent Ca^{2+} uptake (Ca-Ca exchange) in cardiac sarcolemmal vesicles in a competitive manner with respect to Ca^{2+} with a K_i of 10-20 μM. Inhibition was fully reversible. Quinacrine also inhibited Na_o-dependent $^{45}Ca^{2+}$ efflux as well as Na-Na exchange activity. Moreover, at concentrations of up to 200 μM, quinacrine did not affect ATP-dependent Ca^{2+} uptake. Quinacrine mustard (20 μM), an alkylating derivative of quinacrine, produced an irreversible inhibition of Na-Ca exchange activity after 10 min. of incubation with the vesicles in 160 mM KCl at 37°C. The inactivation was maintained after subsequent solubilization and reconstitution of the exchanger according to the procedure of Miyamoto and Racker (J. Biol. Chem. 255: 2656-2658, 1980). The presence of 5 mM $CaCl_2$ in the reaction medium protected Na-Ca exchange activity against inactivation with quinacrine mustard; NaCl (160 mM) partially protected against inactivation but was less effective than $CaCl_2$. The results indicate that quinacrine and quinacrine mustard interact with the Ca^{2+} binding site of the Na-Ca exchanger carrier. The apparent alkylation of the carrier by quinacrine mustard and the protection afforded by $CaCl_2$, should be useful properties for specifically labeling and identifying the exchange carrier.

M-Pos87 STOICHIOMETRY OF THE CARDIAC SODIUM-CALCIUM EXCHANGE SYSTEM. John P. Reeves and Calvin C. Hale, Roche Institute of Molecular Biology, Roche Research Center, Nutley, NJ 07110.

A thermodynamic approach was adopted for determining the stoichiometry of the cardiac Na-Ca exchange system. Cardiac sarcolemmal vesicles were equilibrated with 0.1 mM $^{45}CaCl_2$ in a medium containing 30 mM NaCl, 20 mM KCl and 110 mM LiCl. The vesicles were then treated with valinomycin and diluted into media containing the same $^{45}CaCl_2$ and NaCl concentrations as in the equilibration medium but with the external KCl concentration adjusted so as to impose either positive or negative membrane potentials ($\Delta\Psi$). $^{45}Ca^{2+}$ uptake ensued upon establishing a positive (inside) $\Delta\Psi$, whereas $^{45}Ca^{2+}$ efflux was observed for a negative $\Delta\Psi$. Those $\Delta\Psi$-dependent Ca^{2+} movements did not occur if NaCl was omitted from the medium, indicating that they were mediated by the Na-Ca exchange system. High concentrations of either NaCl or $CaCl_2$ inhibited the $\Delta\Psi$-dependent Ca^{2+} movements. This presumably reflects the competition between Na^+ and Ca^{2+} for the active site of the exchange carrier: Since $\Delta\Psi$-dependent Ca^{2+} movements require the interaction of both Na^+ and Ca^{2+} with the exchanger, conditions that strongly favor either the Ca-bound form or the Na-bound from will inhibit these movements. To determine the exchange stoichiometry, a series of Na^+ gradients were established across the vesicle membrane so as to oppose the effects of a constant $\Delta\Psi$ (either positive or negative) on Ca^{2+} movements. The stoichiometry n could be determined from the magnitude of the Na^+ gradient that exactly compensated for $\Delta\Psi$ such that no net Ca^{2+} movements occurred. This point is defined by the relation $(n-2)\Delta\Psi = nE_{Na}$ where E_{Na} is the equilibrium potential for Na^+ under these conditions. The value of n ($\pm$SE) determined in this way was 2.94 $\pm$ 0.04 (N = 6).

M-Pos88 Ca-STIMULATED Na FLUXES IN HUMAN (H) AND RABBIT (R) RED BLOOD CELLS (RBC): AMILORIDE SENSITIVITY. Nelson Escobales and Mitzy Canessa, Department of Physiology and Biophysics, Harvard Medical School, Boston, Massachusetts 02115

The effect of Ca on Na fluxes in fresh RBC was studied. RBC were incubated in (mM): 75 KCl + (75 choline or NaCl), 0.12 $MgCl_2$, 10 Tris-MOPS (pH 7.4 at 37°C), 10 glucose, 0.1 ouabain and 0.01 bumetamide. RBC Ca content (Ca_i) was increased using the ionophore A23187 (I). In HRBC at I = 25 µmol/L cells + Ca_o = 0, or at I = 0 + Ca_o = 1 mM, Na efflux and influx (mmol/L cells x hour = FU) were amiloride insensitive. When Ca_o was raised from 0 to 200 µM (I = 25 µmol/L cells), both the Na efflux into a 75 K-choline medium and Na influx were stimulated (from 0.2 to 1 FU and from 1 to 4 FU respectively). The Ca-stimulated Na fluxes were inhibited 30-60% by 1 mM amiloride (ID50 = 10 µM) and 100% EGTA. Mg did not mimic the effect of Ca on Na fluxes and A23187 alone did not mediate Na transport. Amiloride did not affect the Ca-dependent K efflux, nor influenced ^{45}Ca uptake. The activation of Na fluxes by Ca in HRBC was a function of internal Na (Na_i). Increasing Na_i with nystatin loading (10-90 mmol/L cells) enhanced Ca-stimulated Na efflux from 1 to 7 FU. The amiloride-sensitive (AS) component of Na efflux half-saturated at 18 mmol/L cells and reached a V_{max} of 1 FU at Na_i = 50 mmol/L cells. The activation of the AS Na pathway seems to require metabolic substrate(s) as Ca and A23187 did not activate the AS fluxes in starved HRBC. In RRBC, Na efflux was 67% AS in the absence of I + Ca. This AS Na efflux was abolished by I + EGTA and stimulated by 100 µM Ca + I to values ten times higher than those observed in HRBC. It appears that Ca_i modulates an AS Na pathway which is not operative at low Ca_i. These results are consistent with a modulation by Ca_i of a Na/H or Na/Na exchange system via several mechanisms (i.e., phosphorylation). Supported by Am. Physiol. Soc., Univ. Puerto Rico (NE), NIH grant GM-25686 and Harvard University (MC).

M-Pos89 ELECTRONEUTRAL EXCHANGE COULD THEORETICALLY AFFECT MEMBRANE POTENTIAL. R. Jacob, D. Piwnica-Worms, C.R. Horres, M. Lieberman. Dept. Physiology, Duke Univ Med Ctr Durham, NC 27710.

Transmembrane electroneutral transport mechanisms (e.g. Na/H and Cl/HCO_3 exchanges, (K+Cl) cotransport) have recently been identified in a variety of cells. We discuss how, in the presence of an electrogenic pump, these transporters can affect the steady-state membrane potential (E_m) when electrodiffusion of Cl is negligible i.e., net electroneutral Cl flux by Cl/HCO_3 exchange and (K+Cl) cotransport is zero. When the exchanges sum to give an electroneutral Na/K exchange, E_m will be hyperpolarized beyond the value calculated by the Mullins-Noda (MN) eqn. (J. Gen. Physiol. (1963) 47:117-132): E_m could even be driven beyond E_K when the electroneutral exchange is very rapid. The eqn. describing this phenomenon has the same form as the MN eqn. but the Na/K pump stoichiometry (r) is replaced by $r/(1+\beta(1-r))$ where β is the ratio of electroneutral Na exchange flux to Na pump flux. In this case, Na/H exchange is exactly balanced by Cl/HCO_3 exchange and is incapable of extruding metabolically produced H^+. However, when Na/H exchange exceeds Cl/HCO_3 exchange, the MN eqn. is modified by replacing r with $r/(1+\beta(1-r)+\varepsilon)$ to give

$$E_m = \frac{RT}{F}\cdot\ln\left(\frac{(r/(1+\beta(1-r)+\varepsilon))\cdot P_K\cdot K_o + P_{Na}\cdot Na_o}{(r/(1+\beta(1-r)+\varepsilon))\cdot P_K\cdot K_i + P_{Na}\cdot Na_i}\right)$$

ε has the same meaning as β but is a measure of the excess Na/H exchange which is not balanced by Cl/HCO_3 exchange. Depending on the relative magnitudes of the two Na/H exchange components, E_m can now either be hyperpolarized or depolarized from the value calculated using the MN eqn. Supported in part by NIH grants HL27105, HL17670, HL07101, GM07171.

M-Pos90 PHOSPHORYLATION OF THE GASTRIC (H^++K^+)ATPase BY INORGANIC PHOSPHATE. Jackson, R.J. and Saccomani, G. (Intr. by M. Goodall) Lab. Membrane Biology, Univ. of Alabama Birmingham, AL 35294

The (H^++K^+) ATPase is a membrane bound enzyme which catalyses the hydrolysis of ATP during the course of transporting protons in exchange for K^+. Labelling the enzyme with fluorescein isothiocyanate (FITC) revealed the enzyme exists in two major conformational states (E_1 and E_2). Addition of Mg^{++} and inorganic phosphate (iP) induced a large fluorescent change when added to FITC enzyme suggesting enzyme phosphorylation. The amount of phosphoenzyme (E-P) formed from unlabelled enzyme was quantitated using (^{32}P) iP. Shifting the equilibrium from E_1 to E_2 was accomplished using appropriate buffers and temperature. In 50mM imidazole buffer pH 7.5 at 22°C approximately 2nmol/mg E-P was formed with 1mM Mg^{++} and 1mM iP. The substrate saturation curve for iP in the presence of 1mM Mg^{++} in imidazole buffer at 22°C revealed normal Michaelis Menton kenetics with a K_m of approximately 60 μM and a V_{max} of 2.35 nmole E-P/mg protein. The level of E-P could be further increased to 2.5-2.7 nmol/mg at 37°C. E-P was chased by the addition of 4 mM KCL in the presence of 10 mM CDTA. At 0°C two rate constants were detected. Extrapolation of the slower rate (0.051 s^{-1}) constant to 0 time revealed 50% of E-P was slowly dephosphorylated. The addition of 1mM ADP + 10 mM CDTA did not enhance dephosphorylation. The fact only 1.5 nmole/mg E-P can be detected by phosphorylation from ATP (high affinity site) and the present finding of almost twice the sites suggests that while the enzyme has the potential to form 3 nmol/mg acidstable E-P at equivalent sites from iP, during ATP catalysis only half the sites are available for E-P formation and half (low affinity ATP) proceed via an alternate hydrolytic mechanism (NIH Support).

M-Pos91 TOPOLOGY OF THE LAC CARRIER PROTEIN IN THE MEMBRANE OF ESCHERICHIA COLI. N. Carrasco, D. Herzlinger, S. DeChiara, W. Danho*, T.F. Gabriel* and H.R. Kaback, Roche Inst. Mol. Biol. and *The Biology Dept. of Hoffmann-La Roche, Inc., Roche Research Ctr., Nutley, NJ 07110

The lac carrier protein, an intrinsic membrane protein encoded by the lac y gene that catalyzes H^+:lactose symport, has been purified to homogeneity in a completely functional state. The protein is a 46.5 Kdalton polypeptide containing 417 amino acid residues of known sequence. A secondary structure model has been proposed based both on CD measurements indicating that the protein is ≈85% α-helix and on the hydropathic profile of the protein along its primary sequence. Accordingly, the protein consists of 12-13 α-helical segments that traverse the bilayer (in a zig-zag fashion), connected by shorter hydrophilic "loops". The polypeptide spans the bilayer, and monoclonal antibodies against the purified protein have been prepared and characterized. One of the antibodies binds to an epitope on the external surface of the membrane, inhibiting H^+:lactose symport without altering the ability of the protein to bind substrate or catalyze exchange. Recent efforts to study the topology of the protein are focused on the use of site-directed polyclonal antibodies. For this purpose, polypeptides 10-15 residues in length corresponding to the N-terminus, the C-terminus and portions of loops 2, 5 and 7 have been synthesized and coupled to thyroglobulin. Antibodies against the peptides were purified by affinity chromatography and radiolabeled with ^{125}I. Each antibody binds specifically to the appropriate polypeptide and to the intact lac carrier protein. Preliminary experiments with right-side-out and inside-out membrane vesicles suggest that the C-terminus is accesible from the cytoplasmic surface of the membrane while loop 2 is inaccesible from either surface.

M-Pos92 KINETIC DETERMINATION OF BIOGENIC AMINE ACCUMULATION INTO ISOLATED CHROMAFFIN GRANULES. Robert G. Johnson, Adam Pallant, Tom Vaughan, Sally E. Carty, and Antonio Scarpa, Dept. Biochemistry and Biophysics, University of Pennsylvania School of Medicine, Philadelphia, PA 19104

In view of the confusion and contradictions existing in the literature, the kinetic parameters of catecholamine uptake by chromaffin granules have been investigated using: a) a highly purified preparation of bovine chromaffin ghosts whose internal composition and transmembrane pH and potential gradients could be manipulated and controlled for long periods of time; b) a glassy carbon electrode which permits on-line continuous quantitative measurement of uptake of various amines. When ghosts were suspended in 185 mM KCl, 10 mM Hepes, pH 7.00 at 37°, the addition of MgATP resulted in the acidification of the intravesicular space, which was constant at pH 5.90-6.00 for over 30 min. Each of the various amines studied, when introduced into this incubation medium, produced a rapid initial deflection of the electrode tracing which then dissipated in a time-dependent manner corresponding to kinetic accumulation of the exogenous amine into the chromaffin ghosts. In all cases the initial rate of amine accumulation was linear over the first 60 seconds. Quantitation of the initial rates of accumulation for each amine permitted precise determination of K_M (and V_{max}) values as follows: dopamine, 14.6±3.6 μM (12.2±3.0 nmoles/min/mg protein); norepinephrine, 32.1±5.6 (16.2±3.6); epinephrine, 35.5±7.5 (15.7±5.8); (+)α-methyl-dopamine, 17.2±1.2 (10.9±1.7); (-)α-methyl-dopamine, 35.7±8.8 (7.8±2.4), α-methyl-norepinephrine, 35.3±1.4 (7.8±2.4), and serotonin, 3.5±1.1 (7.0±2.2). The exact determination of these kinetic parameters under strictly defined conditions also provides for a better understanding of the relationship between extra- and intravesicular pH and the overall molecular mechanism of catecholamine accumulation into adrenal chromaffin granules. Supported by NIH HL-18708.

M-Pos93 MEASUREMENT OF pCa AND pH IN ISOLATED MYXICOLA AXOPLASM. Ronald F. Abercrombie. Department of Physiology, Emory University School of Medicine, Atlanta, Georgia 30322.

Ion-selective electrodes recorded the pH and pCa of isolated Myxicola axoplasm contained within a 760 μm diameter plastic tube. Resting pH and pCa in axoplasm was 7.49 ± 0.05 (n=8) and 6.81 ± 0.06 (n=23), respectively. Reducing axoplasmic pH 0.97 ± 0.095 by injection of 4 nmoles HCl reduced pCa 0.33 ± 0.07 (n=5). Reducing axoplasmic pCa 2.51 ± 0.48 (n=3) by injection of 40 pmoles $CaCl_2$ had only a small effect on pH, which is the result of axoplasm's greater ability to buffer protons versus calcium. In other experiments, two Ca electrodes measured the calcium activity 125 μm and 375 μm from the site of $CaCl_2$ injection. Evidence of calcium "buffering" was demonstrated when the calcium activity at these two locations was below that expected for free calcium diffusion. Centrifuged axoplasm (100,000 xg) taken from the bottom of the centrifuge tube had a somewhat greater calcium buffering capacity than that taken from the top of the tube. Ruthenium red (40 μg/ml) greatly reduced calcium buffering. After each successive injection of 40 pmoles of $CaCl_2$ into uninhibited axoplasm, calcium activity increased by a greater amount, suggesting saturation of calcium buffers. These data may be described by a numerical model which assumes the presence of two calcium buffers. One has a K_d of 1.0 μM (k_r/k_f = 0.0001/100), a capacity of ~1 mM, and is inhibited by ruthenium red. The other has a K_d of 0.8 μm (k_r/k_f = 0.01/12,000), a capacity of ~0.1 mM, and is insensitive to ruthenium red. Supported by NIH NS19194.

M-Pos94 THE MODULATORY ACTION OF 5-HYDROXYTRYPTAMINE ON SODIUM EFFLUX: THE BARNACLE MUSCLE FIBER AS A MODEL SYSTEM. E. Edward Bittar and Geoffrey Chambers, Department of Physiology, University of Wisconsin, Madison, Wisconsin 53706.

The Na efflux from unpoisoned and ouabain-poisoned barnacle fibers is often responsive to externally applied 5-hydroxytryptamine (5-HT). Evidence that this has a physiological basis is provided by the observation that these fibers are responsive to concentrations of 5-HT as low as 10^{-9}M, and that analysis by gc-mass spectrometry indicates the presence of 5-HT in barnacles. The kinetics of the response to 5-HT resemble those seen following cAMP injection, i.e. the response develops promptly but begins to decay 20 minutes later. However, whereas barnacle fibers are always responsive to injected cAMP, the same is not true when 5-HT is applied externally. A likely explanation for this is desensitization. This stems from the observation that insensitive fibers can be rendered sensitive by preinjecting Gpp(NH)p into them. Desensitization also explains why the response to 5-HT is transitory. This is borne out by the fact that external application of 5-HT to fibers preinjected with Gpp(NH)p leads to *sustained* stimulation of the ouabain-insensitive Na efflux. The role of cAMP-PDE in decay of the 5-HT response is unclear. Though PMX (a xanthine derivative) augments the response, it fails to stop it from decaying. Since PMX augments the response to injected cAMP and stops it from decaying, the inference is that the membrane-bound form of PDE is PMX refractory. The question now is: Does 5-HT interact with a receptor, and does this lead to activation of Ca^{2+}channels and/or membrane adenylate cyclase? Experiments show a lack of effect with methysergide and a marked effect with cyproheptadine. They also show that verapamil, Cd^{2+} and WB-4101 are ineffective. The finding that preinjection of PKI or Mg^{2+} reduces the 5-HT response is further evidence favoring the idea that the response is due to activation of cAMP-PK by newly formed cAMP.

M-Pos95 CHLORIDE DISTRIBUTION AND EXCHANGE IN HUMAN LYMPHOCYTES. William Negendank. University of Pennsylvania Cancer Center and Philadelphia VA Medical Center, Philadelphia, PA 19104.

Recent studies in human lymphocytes suggested a model in which most of the normal high level of K reflects K adsorbed onto intracellular fixed charges, while the normal low level of Na reflects primarily the relative exclusion of Na from ordered cellular water. Both Na and K are dissolved within cellular water at equilibrium concentrations less than in the external medium, and both exchange rapidly ($t_{1/2}$ 2-4 min) with ions in the external medium, while adsorbed ions exchange more slowly ($t_{1/2}$ 60-400 min) with ions in cellular water (Bioch. Biophys. Acta 694:123,1982). Blood lymphocytes were incubated 24-48 hr in Hank's medium containing 136 mM Cl, packed at 6000g, trapped space measured with ^{14}C-PEG, and total cell Cl determined by a Cl-sensitive electrode in an 0.1 N nitric acid extract. Cellular Cl was 94.7 +/- 7.8 mM (SE,n=11) at 37° C, 104 +/- 3.7 mM at 0° C, 150 +/- 17 mM in ouabain, and 203 +/- 22 mM with ATP-depletion. However, cells washed in solutions low in Cl immediately lost up to two-thirds of their Cl. This fraction of Cl bore a ratio to external Cl of 0.5. It was also evident in cells incubated in medium containing 20 mM Cl, 22 mM Na, in which total cellular Cl was 33.0 +/- 4.0 mM at 48 hours. The fast and slow fractions of cellular Cl were documented by steady-state isotopic (^{36}Cl) efflux studies, in which the fast fraction of self-exchange of Cl, like that of Na and K, had a $t_{1/2}$ of 2 min, while the dominant slower fraction of self-exchange of Cl had a $t_{1/2}$ of 120-150 min. These results are important in the assessment of the various possible mechanisms underlying ionic distributions between cells and their external media, and in the assessment of the relation between anionic distributions and the cellular potential of lymphocytes.

M-Pos96 DEPENDENCE OF TAURINE EFFLUX ON INTERNAL TAURINE CONCENTRATION IN DIALYZED MYXICOLA GIANT AXON. Lyle W. Horn. Temple University, Philadelphia.

The efflux of taurine was measured at 10°C from internally dialyzed axons which were washed continually in normal, taurine-free sea water. Membrane potential was constant for each axon (range -60 to -65 mV). Internal Na was constant at 100 mM. Internal taurine was varied between 5 and 200 mM. The apparent leak permeability was estimated from the efflux measured at high taurine concentrations and found to be 7.8×10^{-9} cm/sec. A plot of the leak-corrected efflux vs. taurine concentration shows saturation at about 2.56 pmoles/cm^2 sec and a $K_{\frac{1}{2}}$ of about 19.8 mM. The curve is S-shaped and can be fit with a second order Hill equation (correlation coefficient r = 0.99990), which gives an apparent V_{max} = 1.59 pmoles/cm^2 sec and a $K_{\frac{1}{2}}$ = 18.5 mM. The shape of the efflux curve can not be attributed to axoplasmic binding because: 1) efflux was measured at steady state by internal dialysis; 2) significant taurine binding by axoplasm can not be detected by direct measurements; 3) the taurine diffusivity in axoplasm was determined to be $4.4 \pm 1.2 \times 10^{-6}$ cm^2/sec compared to a predicted value for dilute solution of 6.1×10^{-6} cm^2/sec; and the measured ratio of axoplasmic taurine to sucrose diffusivities is 1.97 $\pm$ 0.26 compared to a predicted ratio of 1.79. The second order flux relation could be due to cooperative binding of two taurines per carrier, or to the lack of rapid equilibrium binding of taurine with the carrier. (Supported by NIH Grant NS18868).

M-Pos97 Na-K-Cl COTRANSPORT IN VASCULAR ENDOTHELIAL CELLS: REGULATION BY VASOACTIVE PEPTIDES. Tommy A. Brock, Carlo Brugnara, Mitzy Canessa and Michael A. Gimbrone, Jr., Department of Pathology, Brigham and Women's Hospital and Department of Physiology and Biophysics, Harvard Medical School, Boston, MA 02115.

We have identified a Na-K-Cl cotransport system in cultured bovine aortic endothelial cells (EC). This was demonstrated by the inhibition of ouabain-resistant (OR) ^{86}Rb influx by furosemide (IC_{50}=20 μM) and bumetanide (IC_{50}=0.5 μM) in media containing (mM): NaCl, 115; KCl, 0-20; $MgCl_2$, 1; $CaCl_2$, 2. The OR, furosemide-sensitive (FS), ^{86}Rb influx in EC was 2-3 times greater than ouabain-sensitive ^{86}Rb influx. The FS and bumetanide-sensitive (BS) ^{86}Rb influx was equal to the OR, external Na (Na_o)-stimulated ^{86}Rb influx and to the OR, chloride-dependent (nitrate substitution) ^{86}Rb influx. The OR ^{22}Na influx measured in the same conditions was also FS, BS, cis-stimulated by external K (K_o) and chloride dependent. At K_o=0, net Na extrusion occurred through the Na-K cotransport pathway. Net Na influx occurred with K_o over 0.5 mM. The stoichiometry of ^{86}Rb/^{22}Na influxes was 3K:1Na for cells with normal and low Na content. Assuming that Na-K-Cl cotransport in vascular EC is electroneutral, net influx of Na,K and Cl will occur under physiological ionic conditions. Vasopressin (1 μM) and Bradykinin (10 μM) markedly stimulated ^{86}Rb influx (FS, BS, Nao-stimulated and chloride-dependent), ^{22}Na influx (FS and BS) and ^{36}Cl influx (BS). In contrast, Isoproterenol, PGE_1 and Forskolin had no effect, thus suggesting that the effect of vasopressin and bradykinin was probably not mediated by prostaglandins or cyclic AMP. The physiological importance of the Na-K-Cl cotransport system in EC is currently under investigation.

M-Pos98 COMPARTMENTAL ANALYSIS OF $^{45}Ca^{2+}$ TRANSPORT IN MYOCYTES ISOLATED FROM ADULT RAT HEART: EFFECTS OF Na^+ AND K^+. M. Desilets and M. Horackova (Intr. by J.A. DeSimone). Dept. of Physiology and Biophysics, Dalhousie University, Halifax, N.S., Canada B3H 4H7.

$^{45}Ca^{2+}$ flux studies on isolated cardiac myocytes were performed as previously described (Desilets and Horackova, BBA 721:144-157, 1982). Under steady-state conditions, kinetic analyses of both $^{45}Ca^{2+}$ uptake and efflux experiments indicated the presence of two distinct cellular compartments with rate constants of 0.4 ("fast component") and 0.02 min^{-1} ("slow component").

The uptake studies in normal $[Na^+]_o$ showed that increasing $[Ca^{2+}]_o$ (from 0.1 to 0.55 mM) or $[K^+]_o$ (from 5 to 60 mM) caused an augmentation of Ca^{2+} uptake by stimulating specifically the slow component. On the other hand, the effect of reducing $[Na^+]_o$ (isotonic replacement of 109 mM NaCl with LiCl or Tris-HCl) seemed to be solely related to a transient stimulation of the fast component. Furthermore, in 17 mM $[Na^+]_o$, high $[K^+]_o$ had an additional effect by increasing the uptake related to this fast component. $^{45}Ca^{2+}$ efflux was inhibited by reducing $[Na^+]_o$ and both Ca^{2+} compartments seemed to be affected under these conditions, while high $[K^+]_o$ had an opposite effect by causing an apparent stimulation of $^{45}Ca^{2+}$ efflux from the isolated cells.

In order to explain the various effects of $[Na^+]_o$ and $[K^+]_o$ on $^{45}Ca^{2+}$ uptake and efflux, a model consisting of two intracellular compartments exchanging Ca^{2+} with the sarcoplasm has been postulated. Such a model is also consistent with the presence of a voltage-dependent Na-Ca exchange mechanism at the sarcolemmal level. In addition, these results suggest that altering $[Na^+]_o$ and $[K^+]_o$ may affect the kinetic properties of the compartments located intracellularly. (Supported by a grant from Nova Scotia Heart Foundation and grant MT-4128 from the MRC of Canada.)

M-Pos99 MITOGENS INCREASE INTRACELLULAR pH and Ca^{+2} IN HUMAN FIBROBLASTS. Leslie L. Mix, Robert J. Dinerstein and Mitchel L. Villereal. Dept. of Pharmacol. and Physiol. Sciences, Univ. of Chicago, Chicago, IL 60637, USA.

We have measured intracellular pH and free calcium concentration in human fibroblasts (HSWP) using the pH-sensitive fluorescent dye 6-carboxy,4,5-dimethylfluorescein and the Ca^{+2}-dependent fluorescent probe Quin 2. HSWP cells plated on glass coverslips were serum deprived for 4 hours, loaded with indicator, and the fluorescence monitored with a microspectrofluorimeter. Addition of a combination of peptide mitogens that maximally stimulates Na^+ influx and DNA synthesis in HSWP cells induces intracellular alkalinization. This alkalinization is blocked by amiloride or by replacement of Na^+ with choline, suggesting that it occurs via a Na^+/H^+ exchange. An increase in pH is also obtained with the divalent cation ionophore A23187, an effect which is inhibited by amiloride or Na^+-free medium. Addition of mitogens also causes an immediate increase in the Quin 2 fluorescent signal. This increase is inhibited by 8-(N,N-diethylamino)octyl-3,4,5-trimethoxybenzoate (TMB-8), a compound that has been suggested to block mobilization of intracellular calcium. The mitogen-induced alkalinization is also inhibited by TMB-8. Although both mitogens and A23187 induce an increase in pH without an initial acidification, acid loading has been reported to activate the Na^+/H^+ exchange in fibroblasts. When HSWP cells are acid loaded by preincubating with NH_4Cl followed by its removal, they recover from the internal acidification within 3 minutes. This recovery is almost completely blocked by removal of Na^+ or by 3 mM amiloride, and is also inhibited by TMB-8. These observations support our hypothesis that mitogen activation of Na^+/H^+ exchange is mediated by a rise in intracellular Ca^{+2} and suggest that recovery from an acid load may occur by a similar mechanism. [Supported by grant GM28359, RCDA AM01182 (MLV) and 5 T32 GM07151 fellowship].

M-Pos100 INSULIN INCREASES THE ENERGY STATE OF THE CELL. Richard D. Moore, SUNY, Plattsburgh, N.Y. Dept of Physiology and Biophysics, Given Bldg, College of Medicine, Univ of Vermont

It has been proposed that the action of insulin is characterized by an 'energization', or increased energy level of the cell.[1] Since insulin increases intracellular pH, pH_i,[1] and since H^+ is a product of ATP hydrolysis, the increase in pH_i results in an increase in the energy intensity of ATP hydrolysis, i.e. ΔG per molecule of ATP.

The elevation of pH_i by insulin has been demonstrated in frog sartorius by ^{14}C-DMO,[1] by ^{31}P-NMR,[2] and pH-sensitive microelectrodes.[3] This increase in pH_i is a result of acid extrusion by Na:H.[3] Insulin also increases pH_i in frog oocytes.[4] There have been 2 reports, both based upon ^{31}P-NMR, that insulin does not increase pH_i in mammalian muscle.[5,6] However, a third group[7] found that in isolated rat diaphrams, insulin increased pH_i as determined by ^{31}P-NMR. Moreover, provided a serum factor, EGF, is present, insulin increases pH_i as measured by a fluorescent indicator in human fibroblasts.[8] Finally, when plasma insulin is moderately decreased in live rats, pH_i decreases without a decrease in blood pH.[9,10] This suggests that the energy state of cells is decreased in diabetes.

1)Moore, R.D. 1983, Biochim Biophys Acta 737:1. 2)Moore, R.D., and Gupta, R.K. 1981, Int J Quantum Chem: Quantum Biol Symp 7:83. 3)Putnam, R.W. and Roos, A. 1983, Cell Physiol I A-70. 4)Morrill, G. et al. 1983, Fed Proc 42:1791. 5)Bailey, I.A. et al. 1983, Biochem Biophys Res Commun 720:17. 6)Meyer, R.A. et al. 1983, Fed Proc a1248. 7)Podo, R. det al. 1982, X Intl Conf on Mag Res in Biol Syst 1982, p14. 8)Moolenaar, W.H. et al. 1983, Nature 304:645. 9)Brunder, D.G. et al. 1983, J Gen Physiol 82:15a. 10)Clancy, R.L. et al. 1983, Cell Physiol II A-107.

M-Pos101 Inhibition of Na^+ - Dependent P_i Transport by H^+ in Ehrlich Ascites Tumor Cells. Jesse W. Bowen and Charles Levinson. University of Texas Health Science Center, Department of Physiology, San Antonio, TX. 78284.

Na^+-dependent P_i transport in Ehrlich cells is inhibited following prolonged incubation below an extracellular pH (pH_o) of 6.9. Upon return to pH_o 7.4 inhibition of transport is relieved. Since incubation of these cells below pH_o 7.4 results in internal acidification, it was not clear whether the inhibition of P_i transport developed as a consequence of increased $[H^+]$ on either or both sides of the membrane. To investigate the effect of H^+ on P_i transport, cells were equilibrated at pH_o 7.4 and pH_o was acutely changed to 5.5 by the addition of a small volume of isoosmotic MES buffer (pH~4). Steady state P_i exchange flux was calculated from the uptake of ^{32}P and intracellular pH (pH_i) was simultaneously estimated from the distribution ratio of [^{14}C]DMO. Rapid reduction of pH_o from 7.4 to 5.5 does not initially result in inhibition of P_i transport but rather transiently stimulates P_i exchange by 20-50%. However, inhibition of P_i transport becomes apparent when pH_i falls below ~6.5. The inhibition of P_i transport progressively increases to 50% of the control rate as pH_i decreases to 6.2. We tested the hypothesis that inhibition of P_i transport occurs as a result of interaction between H^+ and the Na^+ binding site on the Na-P_i carrier. Transport data, collected from cells equilibrated at various pHo's and medium $[Na^+]$ in the presence of a saturating medium $[P_i]$, were analyzed by the method of Hunter and Downs. Plots of the relationships between I(1-i)/i and cell $[Na^+]$, where i is fractional inhibition of P_i transport and I is the intracellular $[H^+]$, have a slope greater than zero. This is consistent with competition between H^+ and Na^+ for binding to the Na-P_i carrier at the cytoplasmic side of the membrane. (Supported in part by USPHS Grant CA28287)

M-Pos102 MICROELECTRODES CONTAINING THE NEUTRAL LIGAND ETH-1117 CAN BE USED FOR MEASURING CYTOPLASMIC FREE MAGNESIUM. S. M. Gamiño and F. J. Alvarez-Leefmans. Laboratory of Neurobiology. Department of Pharmacology. CINVESTAV-IPN. Ap. Postal 14-740. Mexico 07000, D.F.

Mg^{2+}-sensitive microelectrodes (MgSE), with tips < 1 μm, have been prepared with a liquid sensor based on the neutral ligand ETH-1117 (Lanter, F. et al, Anal. Chem. 52: 2400, 1980). These electrodes have DC resistances between 15 and 40 GΩ and show significant interference from K^+, at concentrations in which this cation is found intracellularly. Therefore to calibrate MgSE properly, in solutions resembling the cytosolic environment, it is indispensable first to obtain an accurate value for $[K^+]_i$ in the same cells (or cells of the same batch) in which $[Mg^{2+}]_i$ is wished to be measured. In cell bodies of Helix aspersa neurones, using ion selective microelectrode techniques we have measured the following mean intracellular free ion concentrations: K^+, 91 mM; Na^+, 7.5 mM and Ca^{2+}, 170 nM. Consequently we have been calibrating MgSE in solutions containing (mM): K^+, 91, Na^+, 7.5; HEPES, 5 (pH=7.5) and various concentrations of Mg^{2+} (0, 0.2, 0.5, 1, 2, 5, 10). Electrode response in these solutions, although sub-nernstian, shows adequate amplitude and stability for reliable intracellular measurements of $[Mg^{2+}]_i$. The deviation from nernstian behaviour is mainly due to K^+ interference. Ca^{2+} and Na^+ at concentrations found intracellularly produce negligible interference on MgSE response. With the above precautions, MgSE can be used for measuring $[Mg^{2+}]_i$ and constitute a promising tool for studying Mg regulation and transport in cells. We have already reported a basal $[Mg^{2+}]_i$ of 0.66 mM ± 0.05 ($\bar{x}$ ± S.E., n=7) in cell bodies of identified neurones of Helix aspersa (Alvarez- Leefmans, F.J., Gamiño, S.M. and Rink, T.J. J. Physiol. in the Press).

M-Pos103 DETERMINATION OF INTRACELLULAR PH, CA^{++} and ZN^{++} FROM SAME SUSPENSION OF EHRLICH ASCITES TUMOR CELLS USING ^{31}P AND ^{19}F NMR SPECTROSCOPY. Gillies, R.J., Powell, D.A., and Drury, Dept. of Biochemistry, Colorado State University, Ft. Collins, Colorado 80523

We have used the techniques of ^{31}P and ^{19}F NMR spectroscopy to determine intracellular pH, pCa and pZn of Ehrlich ascites cells under serum-starved and serum-stimulated conditions. The spectrometer used was a Nicolet NT-360-WB housed at the CSU/NSF Regional NMR center (Dept. Chemistry, CSU). The probe employed was a modified 20mm configuration, containing 2 Helmholz coils: tuned to 145 MHz (^{31}P) on the inside coil and 338 MHz (^{19}F) on the outside coil. Manual switching between frequencies took approx. 2 minutes and alternating ^{19}F and ^{31}P spectra were generated every 15 minutes. Cells were suspended in a home-made turbine driven spinner/hollow fiber perfusion system demonstrated to maintain physiologically viable suspensions for up to 18 hours.

In the absence of serum, intracellular pH (pH^{in}) was measured at 7.26 from the chemical shift of the intracellular orthophosphate (P_i^{in}) peak. pH^{in} increased to 7.45 in the presence of 10% serum (n = 3). This increase in pH^{in} was accompanied by an increase in the size of the P_i^{in} peak. Intracellular pCa (pCa^{in}) and pZn (pZn^{in}) were estimated using ^{19}F NMR of 5-fluoro-BAPTA (Smith et al., 1982). Under serum-starved conditions, pCa^{in} was 7.33 and pZn^{in} was 8.99. Addition of 10% serum caused a drop in pCa to 6.84, whereas pZn was not significantly changed at 8.87. (Supported by The Research Corporation, Burroughs-Wellcome and NSF PCM #8215608.)

Smith, G.A., Hesketh, J.R. and Metcalfe, J.C. (1982) pp. 65-76 in "Ions, Cell Proliferation and Cancer", Academic Press.

M-Pos104 TEMPERATURE EFFECTS ON ANION PERMEABILITY OF ISOLATED RINGER PERFUSED MAMMALIAN VENTRICLE. Donald D. Macchia and Patrick W. Bankston. Indiana University School of Medicine, Northwest Center for Medical Education, Gary, Indiana 46408.

Recently, it has been shown that isolated skeletal muscles incubated in Ringer's have anion permeability properties which are significantly different than in situ muscles or muscles incubated in plasma. In an effort to assess the effects of perfusing cardiac tissue with protein free Ringer (22 -36) we have examined the anion permeability and tissue morphology of isolated perfused rat, guinea pig and hamster hearts. One group of hearts from each animal were perfused and superfused for 90 min before the tissues were prepared for EM examination of ventricular tissue and vascular morphology and morphometric determination of extracellular volume, ECV. The anion permeability of the ventricular tissue were determined from the sulfate distribution in a second group of hearts following 120 min of perfusion with a $^{35}SO_4^{-2}$ labelled Ringer's. When the temperature of the perfusate was 22 C, the sulfate space of rat, guinea pig and hamster hearts were found to be 2-3 times larger than the morphometric space in these tissues. When the perfusate temperature was increased to 36 C, the sulfate space was significantly smaller than measured at 22 C and, in the case of the rat and guinea pig, was found to be similar to the morphometric space. Since no significant difference was noted in the morphometric space for hearts perfused-superfused at the different temperatures, it was suggested that the increased sulfate space in hearts perfused with 22 C Ringer's represented an increase in the anion permeability of these tissues. This would permit the large impermeant sulfate anion to enter the cellular compartment thereby resulting in a falsely elevated sulfate space. (Supported by the AHA, Indiana Affiliate and NIH Grant AM27148).

M-Pos105 DISSOCIATION OF CALCINEURIN FROM LYMPHOCYTE PLASMA MEMBRANES. Peter D. Chantler. Department of Anatomy, Medical College of Pennsylvania, Philadelphia, PA. 19129.

Plasma membranes, prepared from pig mesenteric lymph node lymphocytes by homogenization of cell suspensions followed by sucrose density gradient centrifugation, were subjected to alkaline urea/acrylamide gel electrophoresis, both in the presence (1mM calcium) and absence (5mM EGTA) of calcium. Electrophoresis of preparations in 8M urea, 10% acrylamide gels, produced a characteristic pattern including an acidic protein band which was present irrespective of the presence or absence of calcium. In 4M or 6M urea gels, however, this band was only apparent in the absence of calcium indicating a calcium-dependent association with other plasma membrane components under these reduced urea concentrations. Similar results were observed using plasma membrane preparations from rat thymic lymphocytes and a variety of human lymphoblastoid cell lines (Bri 8 ; MST ; Daudi; Maja). Electrophoretic elution of this acidic protein from the urea gel, followed by SDS gel electrophoresis, indicated the presence of 64K and 14K peptides, suggestive of calcineurin. Western transfer of this complex from the urea gel to nitrocellulose paper and development of the immunoblots with anti-calmodulin and anti-calcineurin revealed the presence of both calmodulin and calcineurin in the plasma membrane preparation and confirmed the identity of the acidic protein band as calcineurin. This is the first demonstration in lymphocytes of calcineurin, a protein phosphatase capable of cleaving phosphotyrosine. I thank Dr. Claude Klee for generously supplying the antibodies. Supported by the Office of Mental Health of the Commonwealth of Pennsylvania.

M-Pos106 LIGHT-SCATTERING MICROSCOPIC MEASUREMENT OF THE KINETICS OF EXOCYTOSIS IN ISOLATED PLANAR CORTICES FROM EGGS OF THE SEA URCHIN STRONGYLOCENTROTUS PURPURATUS: Retardation of Rate with Hyperosmotic Solutions. J. Zimmerberg, Physical Sciences Lab., DCRT, NIH, Bethesda, MD 20205

Rupturing and washing a monolayer of eggs attached to a planar surface leaves a planar cortex--plasma membrane with associated secretory organelles, cytoskeletal elements, and extracellular proteins (V. D. Vacquier. 1975. Devel. Biol. 43:62-74). Subsequent addition of micromolar Ca^{+2} results in exocytosis of the cortical vesicles (M. J. Whitaker and P. F. Baker. 1983. Proc. R. Soc. Lond. B. 218:397-413; J. Zimmerberg, C. Sardet, and D. Epel, in prep.). I have found, in dark field low magnification microscopy, that each cortical granule becomes a scattering center against a dark background; the disappearance of cortical granules during exocytosis causes a linearly proportional diminution in total scattered light as detected by a photovoltaic cell in the camera tube of the microscope. Approximately 10^6 secretory granules were continuously monitored per experiment with low, nonperturbing light levels. Solutions could be rapidly changed while recording.

Both the extent and rate of exocytosis was dependent upon calcium concentration in isoosmotic milieu. When cortices were treated with hyperosmotic sucrose solutions of $\geq$4.4 Osmolal and then exposed to elevated Ca^{+2}, (a) exocytosis was dramatically slower than in isoosmotic solutions with identical $[Ca^{+2}]$, (b) the rate of exocytosis was no longer calcium dependent, and (c) phase-contrast microscopy revealed granule swelling following calcium addition. Thus, hyperosmotic milieu prolong an intermediate state of exocytosis. I suggest that calcium, among other things, triggers a swelling of cortical granule contents, first within the granule leading to exocytosis, and then within the perivitelline space leading to fertilization envelope elevation.

M-Pos107 APPLICATION OF TIME RESOLVED SPATIAL PHOTOMETRY (TRSP) TO MEASUREMENT OF LATERAL MOTION IN MEMBRANES. H.G. Kapitza, G. McGregor and K.A. Jacobson. Laboratories for Cell Biology/ Department of Anatomy/University of North Carolina at Chapel Hill/Chapel Hill, NC 27514

Previously research in our laboratory has been focussed on the lateral motion of membrane components as this relates to cell structure and function. Currently we are developing a new experimental approach which allows the quantitative analysis of variations in two-dimensional intensity distributions in time. The new system incorporates a microfluorometer using a microchannel-plate image intensifier video camera coupled with a software-based image analysis system for the detection of very low light levels. This system corrects for detector non-idealities, performs optical enhancement of displayed images and controls the timing of the experiments directly to provide minimum exposure of the specimen to light. Our first experiments have been directed toward examining redistribution of fluorescent membrane markers following spot photobleaching with the aim of detecting possible anisotropic diffusion and/or convective flow. Preliminary VIDEO FRAP experiments have shown that (a) Lipid probes in multibilayers made from DMPC below the main transition temperature exhibit marked anisotropic transport related to the grain boundaries in the $P_{\beta'}$-Phase. (b) Fluorescence-conjugated lectins (S-Con A, Con A, WGA) appear to diffuse isotropically immediately after labelling but display anisotropic lateral transport (i.e., clearing from the cell periphery) after prolonged residence of the lectin.

This work was supported by grants from NIH (GM 29234), the American Cancer Society (CD-181) and the DFG (Ka 617/1-1) of West Germany.

M-Pos108 BIOENERGETIC STUDIES OF MITOCHONDRIAL OXIDATIVE PHOSPHORYLATION BY ^{31}P NMR SPECTROSCOPY L. Gyulai, Z. Roth, J. S. Leigh Jr. and B. Chance Department of Biochemistry and Biophysics, University of Pennsylvania, Philadelphia PA 19104

In view of the extensive use of the phosphocreatine-inorganic phosphate ratio (PCr/P_i) as a bioenergetic index *in vivo* (1,2), the relationship between PCr/P_i, and ATPase activity was investigated on isolated mitochondria in order to evaluate their thermodynamic capabilities. Isolated rat heart mitochondria were suspended at low concentration in oxygenated KCl-sucrose-HEPES medium at 25°C with pyruvate-malate as substrates. PCr, ATP, P_i and Mg were added to physiological levels. Changes in extramitochondrial phosphorus compounds were followed by ^{31}P NMR using Bruker 360 WH spectrometer operating at 145.732 MHz for phosphorus. The ATPase activity was varied by addition of potato apyrase and ATPase activity was assayed both by enzymatic assay and using NMR. A logarithmic plot of PCr/P_i vs. ATPase rate is approximately linear, with an extrapolated maximum value of $PCr/P_i \geq 20$, in accord with values found *in vivo* (1,2) in state 4 of > 10. The calculated maximum phosphorylation ratio was between $3.3-7 \times 10^6$M, corresponding to $\Delta G_{ATP} \sim 16$ kcal/mole.

1) Chance, B. et al (1981), P.N.A.S., USA, 78:6714
2) Chance, B. et al (1982), P.N.A.S., USA, 79:7714

M-Pos109 LATERAL MOBILITY OF CYTOCHROME *c* IN COUPLED MITOCHONDRIA. Grzegorz Maniara, Jane M. Vanderkooi, and Maria Erecinska, Departments of Biochemistry & Biophysics and of Pharmacology, Univ. of Pennsylvania, Philadelphia, PA 19104.

Lateral motion of cytochrome *c* bound to giant (2 to 6 u, diameter) mitochondria isolated from *Lethocerus indicus* was examined using the technique of fluorescence recovery after photobleaching (FRAP). Fluorescent cytochrome *c* was exchanged from native cytochrome *c* through partly damaged outer membrane. Recovery profiles were not statistically different when the fluorescence from iron-free cytochrome *c* or fluorescein labeled cytochrome *c* was used and were essentially the same in the presence or absence of an uncoupler (1799). In the presence of excess cytochrome *c* (0.02 mM to 1.8 mg/ml mitochondria) the apparent diffusion coefficient was $6x10^{-11}$ cm^2/s in 0.3 M sucrose-mannitol-EDTA and $2X10^{-10}$ cm^2/s in 0.075 M KCl-0.15 M sucrose. In both cases the recovery curves were better fit to a three dimensional rather than two-dimensional diffusion model and we interpret the recovery to be due to exchange of cytochrome *c* from solution. At concentrations of cytochrome *c* which are stoichiometric with the oxidase and for mitochondria in which excess cytochrome *c* was washed away, two components were observed in the recovery profile. The diffusion coefficient of the fast component was $1x10^{-10}$ cm^2/s and increased little with increase in KCl. The second component showed no recovery during the time scale of measurement ($D<10^{-12}$ cm^2/s). We speculate that the outer mitochondrial membrane may influence the organization of the inner membrane components. (Supported by NIH HL-18708).

M-Pos110 SELECTIVE INACTIVATION OF H^+-PUMP ACTIVITY IN CYTOCHROME *C* OXIDASE FROM THERMOPHILIC BACTERIUM PS3. N. Sone and P. Nicholls, Biological Sciences, Brock University, St. Catharines, Ontario, Canada, L2S 3A1.

An aa_3-type terminal oxidase of the thermophilic bacterium PS3 has been purified and reconstituted into liposomes which showed active H^+ pumping accompanying cytochrome *c* oxidation (J.Biol.Chem. 257. 12600). The enzyme is composed of only three subunits (56,000, 38,000 and 22,000 daltons) and contains two hemes, two coppers and heme *c* as prosthetic groups (Biochem.Biophys.Acta 682: 216). The oxidase activity is stable upto 62°C, while H^+ pumping activity can be selectively inactivated at 55-60°C. This heat treatment induces no significant change in the absorption spectra (reduced, resting, oxi-ferri, cyano aa_3, azide aa_3), the binding of exogenous cytochrome *c*, the oxidase activity and the respiratory control ratio (indicating membrane potential formation), but induces a disappearance of the 213 cm^{-1} line of the Resonance Raman spectrum (441.6 nm excited), probably associated with a Fe-histidine stretching mode of the ferrous high spin a_3-heme, while almost all other Raman lines remain unchanged. These data indicate that H^+ movement observed is not due to a redox-dependent scalar H^+ release from a cytochrome *c*-phospholipid complex (Mitchell, P., FEBS Lett. 151:167) but is due to the H^+ pumping activity of cytochrome oxidase itself. Conformational changes of the enzyme may play important roles in this process and the histidine liganding to heme *a* may initiate it. In the case of beef heart cytochrome oxidase selective inactivation of H^+ pumping can also be induced by heat treatment at 43°C.

M-Pos111 ATP-DEPENDENT K^+ FLUX INTO RAT LIVER MITOCHONDRIA. Junsung Choi and Joyce J. Diwan, Biology Department, Rensselaer Polytechnic Institute, Troy, NY 12181.

The process of respiration-dependent K^+ flux into rat liver mitochondria has been well characterized (e.g. Diwan & Lehrer, Membr. Biochem. 1: 43, 1978). According to the chemiosmotic view, the respiration-dependence of K^+ influx is explained in terms of passive cation entry driven by a membrane potential arising from H^+ ejection (Jung et al., Arch. Biochem. Biophys. 183: 452, 1977). Thus it should be possible to energize K^+ influx also via ATPase-linked H^+ ejection. Experiments utilizing the radioisotope ^{42}K and the silicone sampling technique have shown that, compared to K^+ influx rates energized by succinate, K^+ influx rates in the presence of ATP are very low and exhibit only partial sensitivity to oligomycin. However when mitochondria are suspended in a buffered sucrose medium at pH 7.5 containing 3 mM K^+, 1.5 mM ATP and 1.5 mM Mg^{++}, with rotenone present to block endogenous respiration, the rate of unidirectional K^+ influx is approximately doubled when creatine phosphate and creatine kinase are included in the medium as an "ADP trap". For example, in one expt. K^+ influx increased from 0.16 to 0.35 nmol K^+/mg protein/min. Parallel studies have shown the creatine kinase system to be capable of preventing stimulation of respiration by ADP under the conditions used. The enhancement of K^+ influx by creatine phosphate plus creatine kinase is blocked by oligomycin and/or by carboxyatractyloside. The data are consistent with the interpretation that product inhibition of ATPase activity by ADP may limit the rate of ATP-supported K^+ influx. The possible role of other factors controlling ATPase activity is being investigated. (Supported by USPHS grant GM-20726)

M-Pos112 CK KINETICS IN PHOSPHOCREATINE DEPLETED RAT HEARTS. Ronald A. Meyer, Truman R. Brown, Fox Chase Cancer Center, Philadelphia, PA 19111, and Martin J. Kushmerick, Department of Physiology, Harvard Medical School, Boston, MA 02115

It has been proposed that phosphocreatine (PCr) mediates the transfer of high energy phosphate from mitochondria to myofibrils in cardiac muscle by a "creatine shuttle" mechanism. In this study, PCr was depleted from rat hearts by feeding the creatine analogue β-guanidinopropionate (βGPA - 2% of diet for 6 months), which is known to be a poor substrate for creatine kinase ($V_{max\ GPA} < 1\%\ V_{max\ creatine}$). ^{31}P-NMR spectra of isolated, Langendorff-perfused hearts, and of skeletal muscle in situ (by surface coil), showed PCr levels less than 10% of controls, with corresponding accumulation of phosphorylated βGPA (βGPAP). Mechanical performance and oxygen consumption (2.9 ± .3 μmole O_2/g/min) of perfused control and βGPA treated hearts were not significantly different, and the addition of isoproterenol (0.1 μg/ml) to the perfusate increased oxygen consumption by up to 100% in both groups. In the hearts, saturation transfer revealed no detectable exchange of phosphate between the γ-phosphate of ATP and βGPAP (unidirectional flux βGPAP→ATP < 0.1 μmole/g/sec). Therefore, although βGPAP was slowly hydrolyzed during cardiac ischemia or skeletal muscle contraction, βGPAP could not mediate the steady state ATP turnover predicted from the cardiac oxygen consumption (.3 to .6 μmole/g/sec, assuming $P/O_2 = 6.2$). In one analogue treated heart with sufficient PCr remaining to permit the saturation transfer measurement, the unidirectional rate constant for exchange from PCr to ATP was not significantly different from controls (.61 and .53 sec^{-1}, respectively). Therefore, it is also unlikely that the remaining PCr could mediate the ATP turnover. We conclude that PCr is not an obligatory intermediate in high energy phosphate transport in the rat heart.

M-Pos113 Mg^{2+} INDUCES A REGULATORY FUNCTION OF ADP TIGHTLY BOUND WITHOUT P_i ON CF_1 ATPase. Richard I. Feldman and Paul D. Boyer, Molecular Biology Institute, UCLA, Los Angeles, CA. 90024.

Isolated chloroplast ATPase (CF_1 ATPase) after prolonged exposure to [^{3}H]ADP retains about one tightly bound ADP per mole of enzyme. Uncertainty has remained as to whether this ADP is principally at catalytic or noncatalytic sites. Experiments to be reported show that most or all of such tightly bound ADP is at catalytic sites. When the CF_1 ATPase with tightly bound [^{3}H]ADP present is exposed to Mg^{2+} or Ca^{2+} prior to addition of MgATP or CaATP a pronounced lag in onset of ATP hydrolysis is observed, with only slow replacement of the bound [^{3}H]ADP. However, when MgATP or CaATP is added to Mg^{2+} and Ca^{2+} depleted ATPase the onset of ATP hydrolysis occurs without a lag and most of the tightly bound [^{3}H]ADP is rapidly replaced. Although Mg^{2+} induces ATPase inhibition within a few seconds, reactivation of the enzyme when Mg^{2+} is removed with EDTA requires up to an hour. The Mg^{2+} induced inhibition of ATPase and tightly bound ADP replacement can be overcome by prior exposure of the enzyme to P_i.

These and other results can be explained if enzyme catalysis is greatly hindered when MgADP without P_i is tightly bound at one of the 3 alternating catalytic sites on the enzyme. Such a complex does not arise during steady state catalysis but can be formed after removal of medium MgATP by hydrolysis of the tightly bound ATP to tightly bound ADP and P_i, with slow loss of the P_i. During net MgATP hydrolysis, both ADP and P_i are present only transitorily as tightly bound products and are converted to loosely bound forms as ATP binds to an alternate catalytic site. ADP when tightly bound at a catalytic site without concomitant binding of P_i when exposed to Mg^{2+} exerts an apparent regulatory function.

M-Pos114 SUBMITOCHONDRIAL PARTICLES CORECONSTITUTED WITH BACTERIORHODOPSIN: A VESICLE SYSTEM CAPABLE OF BOTH REDOX- AND PHOTON-DRIVEN ENERGY COUPLING. Rita Casadio[+] and Maria Catia Sorgato'.
[+]Inst.of Botany,University of Bologna and 'CNR Unit,Inst.of Biol.Chemistry,University of Padova,Italy.

Purple membranes reconstituted into phospholipid vesicles(phospholipid(PL) bacteriorhodopsin(BR) molar ratio 100:1) were fused to submitochondrial particles(SMP) by means of a freeze-thaw sonication technique.The new SMP/BR/PL system characteristically showed a BR content of 10-20% of the total protein ; lipid phosphorus was 1.0-1.5 μmoles per mg protein. Evidence that after such procedure mitochondrial ATP-synthase and redox pumps as well as BR were present and operating in a new coupled system was based on the following experimental data:a)The fused population was recovered as a single band after sucrose density gradient and in the presence of 400 mM NaCl to prevent aggregation;b)DpH evaluated under steady state conditions from the fluorescence quenching of 9-aminoacridine and sustained by the light-driven proton pump was usually less than that due to succinate oxidation;these two individual contributions were not additive in that their sum total was the same regardless the initial mode of energization(by light or by succinate oxidation).Furthemore,the contribution of BR activity to the total DpH(about 1.8 units in the presence of K^+ and valinomycin) increased as the succinate-generated DpH was progressively diminished upon titration with malonate;c)FCCP and/or oligomycin-sensitive ATP synthesis was elicited by succinate oxidation as well as by light.This system is suited to test newly proposed models for energy transduction challenging a pure chemiosmosis.

M-Pos115 ENZYME KINETICS OF ATPase AND TRANSLOCASE IN MITOCHONDRIA. R. Strasser and A. Darszon. Dept. of Bioenergetics, Univ. of Stuttgart, Fed. Rep. Ger. and Dept. of Biochem, CINVESTAV-IPN, México, City.

Experiments where the P/O ratio is determined in chloroplasts and mitochondria contain information about the stoichiometry of ATP synthesized per electron transferred. A new method (Jahn and Strasser, 1983) derives from these experiments in chloroplasts information about the properties of the ATPase (K_m, V_m). This approach has now been applied to rat liver mitochondria. Oxygen consumption was measured with an oxygen electrode, the signal stored on line with a microcomputer and processed using multiparameter analysis. Respiration was stimulated upon addition of ADP until it was consumed. This analysis allows the derivation of a function related to the rate of ATP synthesis versus the ADP concentration at any time. During one P/O experiment the full enzyme kinetics (Menten type) are revealed. However the presence of the translocator in mitochondria could influence the enzyme kinetics. Atractiloside at a concentration that inhibits 50 % of the oxygen consumption stimulated by ADP, decreases the observed V_m and increases K_m. Mathematical equations of the system (translocator, ATPase, electron transport) indicate that according to the conditions, the enzyme characteristics of the ATPase or the translocase can be measured. Under normal conditions in mitochondria, we interpret the data as indicating that ATP synthesis is limited by the ATPase. However when the translocator activity is altered, its enzyme properties can be measured and the question of if it becomes the limiting factor at low ADP concentrations can be addressed.

M-Pos116 THE USE OF TETRAPHENYLPHOSPHONIUM (TPP^+) TO MEASURE MEMBRANE POTENTIALS IN MITOCHONDRIA: MEMBRANE BINDING AND RESPIRATORY EFFECTS. B.D. Jensen* and T. E. Gunter, University of Rochester, Rochester, New York 14642

TPP^+ has been used to measure membrane potentials ($\Delta\Psi$) in both cellular and subcellular systems in the concentration range 1 nM to 0.6 mM. It is almost universally accepted that TPP^+ binds to biological membranes. While it is generally assumed that this binding saturates at a low concentration, resulting in a constant amount of TPP^+ bound, this has not been demonstrated. The binding of TPP^+ was investigated using a TPP^+ cation selective electrode. The effect of TPP^+ on mitochondrial respiration was examined using a Clark polarigraphic oxygen electrode. TPP^+ binding to deenergized mitochondria was found to be concentration dependent and was not saturated at 0.7 mM. This concentration dependence can be used to show that binding is strongly dependent on $\Delta\Psi$. Concentrations in excess of 10 μM TPP^+ were shown to adversely affect state III respiration, but not state IV respiration. The data suggest that TPP^+ may partially inhibit the proton ATPase above 10 μM. It is concluded that TPP^+ must be used at or below 10 μM with mitochondria. Various approaches to calibration of membrane-TPP^+ binding are discussed.

*Present Address: Smith Kline & French Laboratories, Swedeland, PA, 19479.
This work has been supported by DOE contract DE-AC02-76EV03490 and NIH Grant AM-20359.

M-Pos117 ^{31}P NMR STUDIES OF A CYTOCHROME b DEFICIENT SKELETAL TISSUE. B. Chance, Biochem/Biophys. Univ. of Penna., S. Eleff, Dept. Anesthesiology, Univ. of Penna., Phila, PA; N . Buist & N. Kennaway, Depts.Medical Genetics & Pediatrics, Oregon Health Sci., Univ. of Oregon, Portland, OR

NMR examination of resting states and of recovery from functional activity of body tissues are combined with manipulation of their metabolic and redox states in humans having vascular and genetic problems thereby to optimize energy metabolism at rest and in limited activity. ^{31}P NMR study of resting and exercised skeletal tissues have defined the physiological limits to the thermodynamically related parameter PCr/P_i from a maximum at rest (state 4) of greater than 10 and to its limit for the fully activated state 3 metabolism set by painful lactic acidosis (~1). The energy cost of quantified muscle work is linearly related to PCr/P_i from state 4 to state 3 to state 3 (1). Failure to produce cytochrome b subunits in a 17 year old female leads to inhibited oxidative metabolism, blood lactic acidosis of approx 10 mM and a resting PCr/P_i of 1-2. Calibrated exercise in the Cybex ergometer leads to further decreases of PCr/P_i to less than 1 with significant discomfort and a slow recovery over a 20 min interval as compared with normal recoveries of <1 min. In order to bypass cytochrome b we have employed standard dietary levels of menadione and ascorbic acid expecting reduction of menadione by the ubiquinone pool and ascorbate by the menadione and of cytochrome c by the latter and activation of electron transport. Increases in the resting level of PCr/P_i to approx 4 together with a 10-fold increase recovery rate are observed. The effect of the mediators in vivo seems at least as effective if not more than in vitro controls. The possibilities for using more active redox mediators such as duroquinone and ubiquinone afford opportunities to apply in vitro bioenergetics to an important in vivo problem.

(1) Darley-Usmar, V.M. (1983) Proc.Natl.Acad.Sci. In press.

M-Pos118 OXIDATION STATES OF MANGANESE IN GRAM-POSITIVE BACTERIA: ESR AND ^{31}P-NMR STUDY. F. S. Ezra, D. S. Lucas and A. F. Russell, The Procter and Gamble Company, Miami Valley Laboratories, Cincinnati, Ohio 45247.

ESR and ^{31}P-NMR spectra have been obtained of Gram-positive bacteria grown in BHI. In the facultative anaerobes, S. aureus and S. epidermis, the intensity of the ESR sextet due to Mn^{2+} hexaquo ions decreases in the presence of O_2 or H_2O_2 and is subsequently restored under anaerobic conditions. Concurrently, the linewidth of the ^{31}P-NMR resonance due to intracellular phosphate decreases under aerobic conditions and increases progressively in the absence of oxygen. The results are attributed to changes in the oxidation state of manganese. The Mn^{2+} ions are oxidized to Mn^{3+} (or higher oxidation states) in oxygenated cells and the latter are reduced to Mn^{2+} during anaerobiosis. In M. luteus, these changes in the oxidation states of manganese affect the linewidth of the ^{31}P-NMR resonance due to cell wall polyphosphate. In the catalase-negative aerotolerant anaerobes, L. plantarum and S. faecalis, manganese remains predominantly in the divalent state. Nevertheless, a decrease in the ESR sextet is detected during oxygenation.

The implications of these results concerning the role of manganese in oxygen metabolism by Gram-positive bacteria will be discussed.

M-Pos119 PROPAGATION VELOCITY AND FREQUENCY OF SPONTANEOUS MICROSCOPIC WAVES IN INTACT RAT PAPILLARY MUSCLES ARE Ca^{2+}-DEPENDENT. A.A. Kort and E.G. Lakatta. Gerontology Research Center, NIA, Baltimore, MD, Intr. by J.P. Froehlich.

Spontaneous propagated contractile waves occur in unstimulated rat papillary muscles. While the fluctuations of scattered coherent light (characterized by the reciprocal of the decay time of its autocorrelation function, f1/2) monitor the magnitude of motion associated with these waves, information is lost. We studied these waves directly in thin isolated rat muscles (29°C at L_{max}) by placing two pinhole covered photoresistors over the high magnification video image of the incoherently illuminated preparation. Propagation velocity was determined by the cross correlation of these signals and the frequency of wave occurence was obtained by the fourier transform of the digitized signal. f1/2 was measured during intermittent He-Ne laser illumination. The frequency of wave occurence (figure), f1/2, and wave propagation velocity (table, mean ± SE, n=4) increased with bathing Ca^{2+}. Caffeine 10mM both reduced the amplitude of video motion to 2.1 ± 1.3% of control and abolished f1/2. We conclude that the previously measured effects of caffeine and Ca^{2+} on f1/2 (J Gen Physiol 82: 119-153, 183) may be explained by the effects of these interventions on the amplitude, frequency and propagation velocity of the waves.

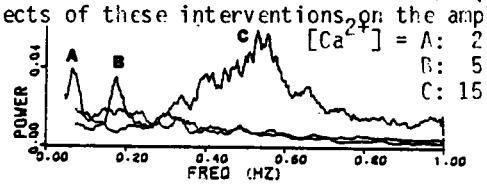

Bath Ca^{2+} (mM)	2	5	15
Wave velocity (μ/sec)	33±4	49±8	86±17
f1/2(Hz)	2.3±0.1	4.0±0.3	6.3±0.6

M-Pos120 SPONTANEOUS CONTRACTILE WAVES AND STIMULATED CONTRACTIONS EXHIBIT THE SAME Ca^{++} AND SPECIES DEPENDENCE IN ISOLATED CARDIAC MYOCYTES AND PAPILLARY MUSCLES. M.C. Capogrossi, A.A. Kort, M.A. Spurgeon, E.A. Suarez-Isla and E.G. Lakatta. Gerontology Research Center, NIA, Baltimore, MD.

In intact papillary muscle both stimulated synchronous contractions (C) and spontaneous contractile activity which propagates as a wave (W) exhibit Ca^{++} and species dependence (J. Physiol. 1981, 315: 369; J. Gen. Physiol. 1983, 82: 119). In the present experiments we varied $[Ca^{++}]_o$ in single cardiac myocytes isolated with collagenase and thin papillary muscles from adult rabbits and rats. The experiments were in oxygenated Hepes buffer (37°C, pH 7.4) in 7 different $[Ca^{++}]_o$'s in rat (0.25-4 mM) and in 10 different $[Ca^{++}]_o$'s in rabbit (0.25-30 mM). (1) At field stimulation of 2 min^{-1} the $[Ca^{++}]_o$ for maximal developed force in papillary muscles and extent of shortening in myocytes was approximately 1.5 mM in rat and 20 mM in rabbit. Within species there was a correlation between extent of shortening and developed force (r = 0.84 in rat and r = 0.97 in rabbit). (2) In the absence of stimulation the propagation of each W along the cell produced a depolarization of 1-3 mV from a resting membrane potential of -76±3.3 mV (n=32). W frequency was measured directly in myocytes and using scattered light intensity fluctuation in papillary muscles. In rat W was detectable at $[Ca^{++}]_o$ of 0.25 mM in myocytes and 0.5 mM in papillary muscles. In rabbit a higher $[Ca^{++}]_o$ (> 10 mM) was necessary. The changes in W frequency in myocytes and scattered light intensity fluctuations in papillary muscles were correlated within species (r = 0.99 in rat and r = 0.94 in rabbit). These effects of Ca^{++} were fully reversible. We conclude that the Ca^{++}-dependence of W frequency and C are similar in myocytes and papillary muscles and that W in myocytes reflects a property of intact papillary muscles.

M-Pos121 PROPAGATED CONTRACTILE WAVES IN SINGLE CARDIAC MYOCYTES MODELED AS REGENERATIVE CALCIUM INDUCED CALCIUM RELEASE FROM THE SARCOPLASMIC RETICULUM. M.D. Stern, M.C. Capogrossi and E.G. Lakatta. Gerontology Res. Ctr., NIA, Baltimore MD, Intr. by W.E. Jacobus.

Intact isolated cardiac myocytes from rats demonstrate spontaneous solitary waves (W) of contraction which originate at localized sites and propagate the length of the cell at velocities of 50-150 μm/sec. The frequency and velocity of W increase with $[Ca^{++}]_o$. Caffeine (10 mM) or ryanodine (1 μM) abolish W. Passage of a wave produces periods of absolute and relative refractoriness to propagation of a subsequent wave. We modeled these W by a partial differential equation describing diffusion of Ca^{++} in the myoplasm, augmented by release of Ca^{++} from the SR via a Ca^{++}-gated channel. Steadily propagated solitary waves are solutions of a nonlinear eigenvalue problem with the velocity as a parameter. For a phenomenalogical SR channel which releases Ca^{++} at a constant rate, the model is analytically soluble; wave velocity varies as the square root of rate of Ca^{++} release, wave amplitude is proportional to duration of release, and a delay in channel opening gives rise to a minimum velocity at which a sustained W can propagate. For a "realistic" SR channel, described by an arbitrary system of differential equations, we have developed an iterative least squares method of solution. Simple models using a two state channel with immediate control by a Ca^{++} binding site can give rise to waves of the proper velocity and to spontaneous oscillations. Inhibition of Ca^{++} release by high applied Ca^{++} in skinned cells (Fabiato, 1983) appears to require at least a four state channel with time-dependent activation, prior inactivation and highly cooperative Ca^{++} binding sites. We conclude that regenerative calcium-induced calcium release is a plausible mechanism for the observed waves.

M-Pos122 SODIUM DISTRIBUTION IN SKELETAL MUSCLE CELLS. David Maughan, Department of Physiology & Biophysics, University of Vermont, Burlington, VT 05405

I used a microsampling and X-ray spectroscopic method to measure what fraction of total intracellular sodium in frog semitendinosus muscle is freely diffusible. Single muscle fiber segments were manually skinned under water-saturated mineral oil (20°C) and 0.2 nl droplets of isosmotic solution (0.25 M sucrose + 5 uM EGTA) were placed on each fiber and allowed to equilibrate with the cell fluid. X-ray spectroscopic analysis of fluid droplets from 24 fibers yielded 6.4 ± 3.7 mmol per liter of diffusible Na (mean ± 1 S.D.) in the intracellular fluid. Na efflux experiments on 6 whole muscles (washout into a series of tubes containing 1 mM ouabain Ringer in which Na was replaced by choline) yielded 13.9 ± 1.3 mmol per kg wet weight. For total Na analysis, 24 whole muscles were dried and ashed, and the residue dissolved in citric acid. X-ray spectroscopic analysis of those fluid samples (neutralized with ammonium hydroxide) yielded 21 ± 7 mmol Na per kg wet weight. In all experiments, extracellular fluid was removed by centrifuging the muscles. These results suggest that approximately a third of the total intracellular Na [i.e., about 6.4 mM/21 mM] is freely diffusible and equilibrates with a microdroplet. Perhaps another third [i.e., about (13.9 mM - 6.4 mM)/21 mM] is restricted as counterions of charges on fixed proteins and can be washed out along with the freely diffusible fraction into a large volume of Na-free solution. The remaining third may be tightly bound to or incorporated into fixed proteins and organelles in muscles. Supported by AHA 79-165 and NBREPM, C. Lechene, Director.

M-Pos123 EFFECTS OF OUABAIN AND EXTERNAL K^+ CONCENTRATION ON METABOLISM AND FORCE PRODUCTION IN RAT ANOCOCCYGEUS SMOOTH MUSCLE. S. Davidheiser, Dept. of Animal Biology, Sch. of Vet. Med., Univ. of PA., Phila., PA 19104.

In isolated, chemically-denervated rat anococcygeus smooth muscle (ASM) incubated at 37°C, removal of external K^+ $[K^+]_o$ resulted in a biphasic response in lactate production (J_{lac}, μmoles/min·g); a large increase during the initial hour, followed by a decrease below the resting rate after 3-4 hr. Under these conditions force production was minimal and oxygen utilization (J_{O_2}) did not change. (Davidheiser, et al., Biophys. J. 41: 248a, 1983). In ASM treated with ouabain (10^{-3}M), the initial rise in J_{lac} was not prevented (J_{lac}:K^+-free medium/J_{lac}:normal medium=2.92 S.E.±0.09, n=9, control; 3.49±0.28,n=5, ouabain-treated). After 4 hr. in K^+-free medium J_{lac} fell below the resting rate in both the control and ouabain-treated tissues (0.55±0.07,n=8; 0.17±0.05,n=5, respectively), and the rise in J_{lac} that occurred in control muscles upon restoration of K^+ (3.58±0.14, n=8) was prevented by ouabain (0.67±0.05,n=5). Subsequent removal of ouabain then resulted in an increase in J_{lac} (3.52±0.28,n=5). Ouabain did not significantly affect J_{O_2} or produce a contraction in denervated ASM incubated in normal or K^+-free medium. Therefore, the decrease in J_{lac} observed after prolonged incubation in K^+-free medium and the increase in J_{lac} after restoration of $[K^+]_o$, but not the initial increase in J_{lac} following removal of $[K^+]_o$, seemed to be related to activity of the Na^+-K^+ pump. In other experiments a logarithmic relationship between J_{lac} and $[K^+]_o$ was found with 5.9,4,3,2,1 and 0.5mM $[K^+]_o$ (J_{lac}, μmoles/min·g=0.80-0.32 ln $[K^+mM]_o$, r=0.98,n=8-17). This suggested that changes in the J_{lac} of ASM were due to alterations in glucose metabolism that occurred following changes in the resting membrane potential. (Supported by NIH grant AM-32682).

M-Pos124 THE GELATION OF PLATELET EXTRACTS, C.J. Jen, L.V. McIntire and D.M. Peterson, Biomedical Engineering Lab., Rice University, Houston, Texas 77251

The kinetics of the gelation process that occurs upon warming cold platelet extracts were studied using a sensitive rheometer. At micromolar free Ca^{2+} concentration and in the presence of 1 mM ATP the gel rigidity curves showed several peaks, indicating that platelet extract proteins went through network assembling/disassembling cycles during gelation. The gelation kinetics were accelerated with increasing free Ca^{2+} concentration up to about 2 μM. At 4-15 μM free Ca^{2+} the gelation cycles were completely abolished except the first peak. The gelation process became monotonically increasing at millimolar free Ca^{2+} concentrations. Trifluoperazine (50 μM), a calmodulin inhibitor, did not affect gelation at micromolar free Ca^{2+} concentrations. Except the first gelation step, which was completed within 5 minutes after warming, the rest of the gelation process was found to be affected by K^+, ATP, cytochalasin E and colchicine. K^+ ions higher than 10 mM retarded the gelation kinetics. Extracts prepared with low ATP (0.1 mM) content showed impaired gelation and this was partially reversed by adding 1 mM ATP but not 1mM adenylylimidodiphosphate (AMPPNP). Both cytochalasin E (1 μM) and colchicine (1 mM) impaired the gelation process. Results from 2-dimensional electrophoresis gels of platelet extracts demonstrated that most of the proteins which participated in network formation did so within the first 5 minutes and subsequent gel rigidity changes were probably due to rearrangements of these proteins.

M-Pos125 INHIBITION AND STIMULATION OF THE ACTOMYOSIN ATPase BY FODRIN
Paul D. Wagner, Laboratory of Biochemistry, NCI, NIH, Bethesda, MD 20205

Fodrin, a spectrin like protein isolated from brain, binds to and cross-links F-actin. The effects of fodrin on the actin-activated ATPase of skeletal muscle myosin have been examined. Fodrin caused this actomyosin ATPase to be calcium sensitive. When added to actin and myosin before ATP, fodrin stimulated the actomyosin ATPase almost three-fold in Ca^{2+}, but by less than 50% in EGTA. Several minutes after ATP addition, the amount of stimulation in Ca^{2+} was reduced, and in EGTA the actomyosin ATPased was substantially inhibited. Stimulation is thought to result from fodrin cross-linking F-actin. When added after ATP, fodrin inhibited the actomyosin ATPase. More fodrin was required for inhibition in Ca^{2+} than in EGTA. Complete inhibition in EGTA occurred at about one fodrin to 200 actins. Whether added before or after ATP, fodrin inhibited the actin-activated ATPase of myosin subfragment-1. This inhibition by fodrin was more effective in EGTA than in Ca^{2+}. There was no obvious correlation between inhibition of ATPase activity and F-actin cross-linking. The inability of fodrin to stimulate the actin-activated ATPase of S1 and the unlikelihood of fodrin interacting with actin in the absence of ATP in vivo suggest that inhibition may be more physiologically important than stimulation.

M-Pos126 LITHIUM INHIBITION OF REACTIVATED SPERM MOTILITY IS REVERSED BY cAMP. Barbara H. Gibbons and I. R. Gibbons. Pacific Biomedical Research Center, University of Hawaii, Honolulu, HI 96822.

The motility of demembranated sea urchin sperm flagella of T. gratilla reactivated in 0.20 M K acetate, 0.5 mM MgATP and 0.1 mM free Mg^{2+}, pH 8.3, is inhibited completely within <10 sec after addition of 6 mM Li^{+}(acetate). Subsequent dilution of the sperm 100-fold into fresh reactivating solution fully restores their motility. The inhibition by Li^{+} appears to be competitive with Mg^{2+}, with 20 mM Li^{+} being required to obtain complete inhibition in the presence of 2 mM free Mg^{2+}. When tested under either set of ionic conditions, concentrations of Li^{+} up to 64 mM have little (<20%) effect on the latent and Triton-activated ATPase activities of solubilized dynein 1. Addition of 10 μM cAMP to sperm inhibited by 6 mM Li^{+} induces highly asymmetric beating in 30-70% of the sperm, whereas 10 μM cGMP has little effect. This concentration of cAMP has no effect on sperm motility in the absence of Li^{+} under the conditions used. Brief digestion of Li^{+}-inhibited sperm flagella with 0.2 μg/ml trypsin restores their motility, with the rate of motility restoration being approximately the same as the rate at which trypsin eliminates Ca^{2+}-induced asymmetry of flagellar waveform. Our preliminary conclusion is that Li^{+}-inhibition of flagellar motility occurs through the interaction of $LiATP^{3-}$ or Li^{+} with the regulatory site through which Ca^{2+} modulates the asymmetry of flagellar beating, and does not block the dynein arm cross-bridge cycle directly. Although Li^{+} is known to inhibit adenylate cyclases (Thams and Geisler, Acta Pharm. Toxicol. 48, 397 (1981)), and we have found conditions under which it apparently prevents the formation of the cAMP required for initial activation of motility, our overall evidence indicates that this is probably not its principal mode of action when used to inhibit sperm during the course of normal motility and the mechanism of cAMP reversal of Li^{+} inhibition remains obscure. Supported by NIH grants HD 06565 and GM 30401.

M-Pos127 CALCIUM EFFECTS ON PHOSPHATIDYLINOSITOL AND PROTEIN PHOSPHORYLATION IN *MYTILUS* GILL CILIA. E. W. Stommel and R. E. Stephens, Marine Biological Laboratory, Woods Hole, MA 02543.

High salt (1.5 M) treatment of *Mytilus edulis* gill filaments in the presence of 10^{-7} M 5HT releases lateral (L) cilia; further treatment with EDTA-seawater releases the remaining cilia types. Using γ-^{32}P-labeled ATP, the two classes of cilia were incubated in low Ca^{++} medium (5 mM EGTA), where L cilia activate but abfrontal (AF) cilia are immotile, and in high Ca^{++} where L cilia arrest 2 μM) but AF cilia activate (50 μM). These cilia are separated into axoneme and membrane fractions by detergent extraction, subjected to SDS-PAGE on 5-15% gels, and autoradiographed. The L cilia show no Ca^{++}-dependent phosphorylation of specific proteins nor does trifluoperazine (TFP) influence phosphorylation at these Ca^{++} levels. However, under Ca^{++} arrest conditions there is a marked increase in phosphorylation of lipid, identified by thin-layer chromatography as diphosphoinositide (DPI). Lipid phosphorylation is not affected by TFP, but Ca^{++} levels higher than 2 μ M may be required for TFP to have an influence. In contrast, lipid phosphorylation is not Ca^{++} dependent in the remaining cilia and general protein phosphorylation increases several fold in high Ca^{++}, with proteins at 40K and in the 100K-150K dalton range being labeled selectively. Thus Ca^{++} activation of AF cilia, but not Ca^{++} arrest of L cilia, may result from protein phosphorylation. Varsanyi et al. (EMBO J. 2: 1543, 1983) recently showed that a Ca^{++}-dependent increase in DPI activates the Ca^{++}-ATPase of sarcoplasmic reticulum. Neomycin or PI, which decrease DPI, and theophylline, which increases cAMP, respectively prolong and shorten the arrest response that follows mechanical stimulation of L cilia. Perhaps 5HT, which activates lateral cilia, simply acts by raising cAMP levels, activating a PI kinase and thus stimulating the Ca^{++}-ATPase pump. Support: NIH Grant GM 29,503.

M-Pos128 INTRACELLULAR pH DURING HYPOXIA AFFECTS THE CREATINE KINASE EQUILIBRIUM IN THE PERFUSED RABBIT HEART. A P-31 NMR STUDY. Michael V. Miceli, and William E. Jacobus, Medicine and Physiological Chemistry, Johns Hopkins School of Medicine, Baltimore, Md. 21205, and Phil L. Hawley, Physiology, University of Illinois at Chicago, Chicago, Ill, 60613.

P-31 NMR was used to determine intracellular pH and high energy phosphate content during hypoxia in the perfused, isovolumic, beating rabbit heart. Hearts weighing 4.7±.8gm were Langendorff perfused in the NMR magnet at 37°C at a constant flow of 35 ml/min and paced at a rate of 175 bpm. Developed pressure (DP) was measured using a intraventricular fluid-filled balloon. Initial DP was 125± 4.5mm Hg. 5 min spectra were recorded during a control period, for 60 min of N_2 hypoxia (pO_2 40-50 mm Hg), and for 40 min of reoxygenation. Normoxic pH_i determined from the Pi chemical shift was 7.14±.02. Hearts perfused with 18.8 mM bicarbonate buffer (pH 7.40 at the cannula) exhibited a pH_i during hypoxia of 6.95±.01 with 16 mM glucose (n=3) and 6.96±.01 with 5 mM glucose (n=3). Hearts perfused with 10 mM Tris (pH 7.40 at 37°C) exhibited a hypoxic intracellular pH of 6.99±.01 with 16 mM glucose (n=4) and 7.00±.01 with 5 mM glucose (n=4). The effect of changing pH_i during hypoxia was determined by varying the pH of the hypoxic buffer using 10 mM Tris at pH 7.0 (n=4) and 8.0 (n=4) with 5 mM glucose. pHi during hypoxia was 6.77 and 7.22 respectively, compared with 6.99 for pH 7.4 buffer. The PCr content showed a strong dependence upon pH_i during hypoxia being 44.8, 32.8 and 22.2% of control (for all three groups $P<.05$) at pHi of 7.22, 6.99 and 6.77 respectively. Functonal recovery in the three groups was 45.8±3.1, 53.6±3.3 and 73.0%±4.1% respectively. These data are consistent with a pH induced shift in the creatine kinase equilibrium. During mild acidosis this pH dependence of the CK reaction may help maintain ATP pools at the expense of PCr and may contribute to the protective effect of acidosis during hypoxia.

M-Pos129 GALVANOTAXIS AND MAGNETOTAXIS OF MOUSE FIBROBLASTS. W. C. Parkinson, Department of Physics, The University of Michigan, Ann Arbor, Michigan 48109.

The motility in vitro of mouse fibroblasts (CCL 1.1 from American Type Culture Collection) has been studied in some detail as a function of temperature in the absence of gradients[1] and also in a temperature gradient (thermotaxis)[2]. Galvanotaxis has been observed for a wide variety of cells plated in vitro[3]. In general the cells elongate and align with the long axis perpendicular to the electric field, and above a threshold field move in the direction of the field. Magnetotaxis is less well investigated.

The motion of mouse fibroblasts is being studied in both static electric fields and static magnetic fields. Preliminary results indicate that for electric fields up to 5 volts per cm no alignment is observed. Similarly no effect on the motion is observed in a 30 gauss (3×10^{-3} T) static magnetic field. Quantative results of these measurements will be reported.

Measurements of the transmembrane potential with and without an electric field are in progress.

1) W. C. Parkinson (1983), Biophys. J. 42, 17.
2) W. C. Parkinson (1983), Aust. J. Phys. 36, #5 (in press).
3) C. A. Erickson and R. Nuccitelli (1982), J. Cell Biol. 95, 314a. M. S. Cooper and R. E. Keller (1983), Biophys. J. 41, 128a; see also Carol A. Erickson and Richard Nuccitelli, (1983) J. Cell Biol. (in press); M. S. Cooper and R. E. Keller, (1983) Proc. Natl. Acad. Sci. (in press).

M-Pos130 APPLIED CURRENT EFFECTS ON CELLULAR MORPHOLOGY, ALIGNMENT AND PROLIFERATION. Stephen M. Ross and Jack M. Ferrier, MRC Group in Periodontal Physiology, 4384 Medical Sciences Building, University of Toronto, Toronto, Ontario, Canada M5S 1A8.

We have carried out studies on the effects of applied extracellular currents on cultured connective tissue cells, including fibroblasts and osteoblast-like clones. Current densities from 1 uA cm^{-2} to 20 mA cm^{-2} have been applied to cells in chambers adapted for light microscopy to observe short term (up to 24 h) morphological changes. Cellular alignment is observed at high current densities. Results are also described for longer term experiments on the effect on cellular proliferation of the following: uniform current, a steep gradient of current density and current intended to simulate the low frequency ion concentration waves known to be emitted by some bone cells.

M-Pos131 PERSISTENT MOTILITY OF FISH EPIDERMAL CELLS IN THE PRESENCE AND ABSENCE OF DC ELECTRIC FIELDS. M.S. Cooper and M. Schliwa*, Biophysics Group and Department of Zoology*, University of California, Berkeley, CA 94720 (Intro. by H.J. Bremermann)

Fish epidermal cells exhibit strongly persistent migration in culture, maintaining their general direction of locomotion for several hundred microns. The cells, approximately 20 X 40 μm, migrate perpendicular to their long axis at speeds of 30-40 μm/min. Their leading edge is a broad canoe-shaped lamellipodium, with the nucleus and all organelles confined to a globular cell body. 1 mM La^{3+}, a calcium channel blocking agent, reversibly inhibits lamellipodial extension and cell locomotion. In electric fields of $\geq$ 2 V/cm, these cells migrate directionally towards the cathode. Actin staining with phalloidin shows a somewhat regular array of criss-crossing fibers in the leading lamellipodium. Tubulin immunofluorescence shows microtubules to be confined to the perinuclear area. Disassembly of these microtubules with 2 μg/ml nocadozole and cold treatment (4°C) has no effect on cell morphology, motility, or the ability to be guided by a DC electric field. We suggest that externally applied DC fields guide the motility of these epidermal cells by biasing an endogenous ionic current which may be driven through the cells as they normally migrate. Ion fluxes through the cell membrane associated with this currrent, such as Ca^{+2}, could control the contractile activity of the actomyosin network which generates the force for cell locomotion. Such an endogenous current has been observed by Nuccitelli et al. (J. Gen. Physiol. (1977) 69:743) in migrating amoebae, which also exhibit cathodal galvanotaxis in applied fields. Our results lend support to the suggestion by Barker et al. (Am. J. Physiol.(1982) 242:R358) that epidermal cell galvanotaxis might occur at wound sites where DC fields of up to 2 V/cm are known to exist.

M-Pos132 PHOSPHORYLATION OF SKELETAL MYOSIN LIGHT CHAINS DECREASES THE VELOCITY OF CONTRACTION OF GLYCERINATED MUSCLE FIBERS. R. Cooke, K. Franks and J.T. Stull*. Dept. of Biochemistry and Biophysics, University of California, San Francisco, and *Dept. of Pharmacology, University of Texas, Dallas, TX 75235.

Rabbit psoas muscle was glycerinated in the presence and absence of 4 mM ATP and stored at -20°. The degree of phosphorylation of the myosin P-light chain was determined by isoelectric focusing. Fibers glycerinated in the absence of ATP were initially partially phosphorylated, and the level of phosphorylation decreased to a low value over a period of approximately one week. Fibers glycerinated in the presence of ATP maintained high levels of phosphorylation 60-80% for periods of several months. If these fibers were transferred to an ATP free glycerination medium, their level of phosphorylation also decreased to low levels within several weeks. Thus by altering the glycerination conditions, one can prepare fibers with dephosphorylated myosin or phosphorylated myosin, and one can dephosphorylate the initially phosphorylated myosin. The isometric ATPase activitiy of the fibers with phosphorylated myosin was less than those of control fibers. Single fibers were mounted on a tensiometer and isometric tensions and isotonic contraction velocities were measured. The isometric tension was not changed by phosphorylation. The isotonic velocity was decreased by about 30% ±10% at all velocities. Dephosphorylation of the fibers returned both the ATPase activities and isotonic velocities to their control values. The effect of phosphorylation was considerably less at 25° than at 35°. We conclude that in skeletal muscle phosphorylation decreases the cycling rate of myosin cross-bridges. Supported by grants from the USPHS HL 16683 and AM 00479 to R.C. and HL23990 to JTS.

M-Pos133 MYOSIN LIGHT CHAIN PHOSPHORYLATION IN NORMAL AND HYPERTENSIVE CANINE ARTERIAL SMOOTH MUSCLE. S.P. Driska, K.A. Szymanski, and R. Porter, Department of Physiology and Biophysics, Medical College of Virginia, Richmond, VA 23298.

Phosphorylation of the 20,000 dalton light chain of smooth muscle myosin is thought to play an important role in the regulation of smooth muscle contraction. For this reason it is important to know if myosin phosphorylation is altered in pathological states such as hypertension. Dogs were made hypertensive (HT) by unilateral nephrectomy and renal artery stenosis. Renal artery strips were frozen in various contractile states at their optimum lengths for force development. Phosphorylation was measured by densitometry of two-dimensional isoelectric-focusing/SDS-electrophoresis gels of the muscle homogenates as described previously and was expressed as a percentage of the total 20,000 dalton light chain. Levels of phosphorylation were low in unstimulated strips from both normal (11.7 ± 2.8%,SD, n=7) and HT (13.5 ±2.9%, SD,n=4) animals. Phosphorylation time courses were measured after stimulation with 10 uM norepinephrine, and peak values of phosphorylation were found after 1 minute of stimulation in both normal and HT strips. Levels of phosphorylation in both normal and HT strips declined after this peak even though isometric force was maintained for 30 minutes. Peak levels of phosphorylation (at 1 minute) were 58.7 ± 8.6%, SD, n=7 for normal arteries and 61.0 ± 7.8%, SD, n=4 for HT arteries. Levels of phosphorylation were also similar for the two groups of arteries after 30 minutes of stimulation. These results suggest that there is no obvious change in the mechanisms regulating light chain phosphorylation in this model of hypertension. Supported by NIH grants HL-24881 and HL-25383. S.P.D. is the recipient of NIH RCDA HL-01198.

M-Pos134 A STUDY OF 'HYSTERESIS' IN THE FORCE-pCa RELATION IN MUSCLE. D.A. Williams and D.G. Stephenson, Zoology Department, La Trobe University, Melbourne, Australia, 3083.

It has been recently suggested that a type of hysteresis may exist within the force generating processes of barnacle muscle (Ridgway et.al. Science 219, 1075-77, 1983) which implies that the relation between force and calcium is not unique since increasing force may increase Ca^{++} sensitivity. As such a phenomenon would be of great importance in the understanding of how force is regulated in muscle, it was therefore of interest to expand upon these observations to incorporate a variety of muscle types from mammals, amphibians and arthropods. Single muscle fibres were mechanically skinned and activated in strongly buffered Ca^{++} containing solutions. The activation protocol involved obtaining a submaximal force response followed immediately by a maximal force response. The fibre was then returned to the same submaximally activating solution and finally completely relaxed. This series was repeated for a number of submaximal forces. Each submaximum force response was compared with the same post-maximum response with any elevation in force in the later response being considered as hysteresis. The steady-state results obtained for mammalian fast-and slow-twitch and toad twitch skinned muscle fibres showed no evidence of hysteresis. The force-pCa curves calculated from pre-maximum force responses coincide with those from post-maximum responses in these muscle types. The situation with arthropod skinned fibres is more complex. A time-dependent hysteresis may be evident but is complicated by a progressive deterioration in the Ca-sensitivity of the force-pCa relation and the non-uniformity of the initial sarcomere lengths within the fibre. We propose that this 'hysteresis' may in fact be associated with a type of catch -like mechanism in these multiply innervated muscle fibres. (Supported by NHF Australia and ARGS).

M-Pos135 EPR AS A PROBE OF MYOSIN"S CONFORMATIONAL STATE IN GLYCERINATED MUSCLE FIBERS.

Vincent A. Barnett, Eric. C. Svensson, and David D. Thomas, Dept. of Biochemistry, University of Minnesota Medical School, Minneapolis, MN 55455.

We have used EPR as a probe of the conformational dynamics of spin-labeled myosin in glycerinated rabbit psoas muscle fibers. An iodoacetamide spin-label was attached covalently and specifically to sulfhydryl-1 (SH1) on the myosin heads in these fibers. Its EPR spectrum provided a direct measure of the fraction of myosin heads in the conformational state corresponding to M**.-ADP.Pi (Seidel et al., 1970, Biochemistry, 9:3265-3272). In parallel experiments, a maleimide spin-label provided a measure of the fraction of myosin heads attached to actin (Thomas and Cooke, 1980, Biophys. J., 32:891-896). In both types of labeled fibers, a majority of the myosin heads were labeled, and physiological properties (isometric tension, velocity/force, ATPase) were not significantly inhibited (Crowder and Cooke, 1983, Biophys. J., 41:149a). During the recording of EPR spectra, fiber bundles were perfused with solutions containing ATP or ATP analogues, such as ADP-vanadate, AMPPNP, and pyrophosphate. In a solution containing 5 mM MgADP and 5 mM vanadate, no significant fraction of myosin heads are either detached from actin or in the M** state, even after a 40 h incubation. This is in contrast to insect flight muscle which yields relaxed x-ray diffraction patterns within 24 hours of incubation in MgADP-vanadate. In the presence of 5 mM MgATP and 5 mM vanadate, the heads are all detached and all in the M** state. In the presence of 5 mM MgATP (relaxation), the heads are similarly detached but not all in the M** state. These and other results will be discussed in relation to the molecular dynamics of the mechanism of energy transduction in muscle.

M-Pos136 ORIENTATION OF SPIN LABEL NUCLEOTIDE IN VERTEBRATE STRIATED MUSCLE. Mark S. Crowder and Roger Cooke. Department of Biochemsitry and Biophysics, and CVRI, University of California, San Francisco, CA 94143

A nitroxide spin label analogue of adenosine triphosphate has been used to examine the orientation of nucleotides bound to myosin in glycerinated psoas muscle fibers. Spin label ATP (SL-ATP) exists as isomers with the nitroxide free radical moiety attached by an ester linkage to either the 2' or 3' position of the ribose group of ATP (BBA 601:34, 1980). SL-ADP has a binding constant of $\sim 10^5$ with myosin and $\sim 2 \times 10^3$ in muscle fibers. When muscle fibers are incubated in 100-200 μM SL-ADP, the resultant EPR spectrum is characterized by two spectral components. The major component gives rise to three narrow peaks which are characteristic of unbound spin label. The other component is highly oriented and we interpret this to represent SL-ADP bound to myosin. Analysis of the hyperfine anisotropy is consistent with these spin probes subtending an angle of $\sim 45°$ with respect to the fiber axis. The relative molecular geometry of SL-ADP and myosin is unknown. Preliminary experients have indicated the probe angle does not change when tension is applied to the muscle fibers. Tension induces some broadening which is tentatively assigned as a small increase in the width of the angular distribution of the probes. SL-ATP will induce relaxation and will support fiber contraction. Tension and velocity measurements indicate that SL-ATP is ~60% as effective as ATP. However, SL-ADP is a poor substrate for both pyruvate and creatine kinase. This work is supported by USPHS HL 30868 and AM 00479.

M-Pos137 MYOFILAMENT LATTICE INSTABILITY IN SKINNED PSOAS MUSCLE FIBERS.

Takashi Matsuda and Richard J. Podolsky, Laboratory of Physical Biology, NIADDK, National Institutes of Health, Bethesda, MD 20205.

To study the factors involved in maintaining the double hexagonal myofilament lattice structure of relaxed muscle fibers, we recorded the equatorial and layer line X-ray patterns of skinned rabbit psoas muscle fibers over a range of pH and ionic strength. At 120 mM ionic strength, the lattice spacing and equatorial intensities I_{10} and I_{11} were insensitive to pH between 7.0 to 6.0. However, I_{11} fell abruptly at about pH 5.8 and disappeared at about 5.2, while the background intensity increased; the lattice spacing d_{10} decreased about 20% over this pH range. I_{10} changed very little although the reflection broadened at low pH (5.0 to 6.0). The pH at which I_{11} fell abruptly was not affected by ionic strength (60 to 170 mM). These changes were almost completely reversible unless the pH was reduced below 5.0. When the ionic strength was reduced from 120 mM to 60 mM, the midpoint of the lattice spacing curve shifted from pH 5.7 to 6.0. The actin layer lines and the myosin off-meridional layer lines became weaker when the pH was reduced from 7.0 to 5.3. These results show that "electrostatic" lattice shrinkage and thin filament disorder are closely linked. This could happen because electrostatic forces that normally order the thin filaments decrease significantly at pH 5.8. However another possibility is that thick filament projections collide with, and disorder, the thin filaments at small lattice spacings ($d_{10} \sim 335$ Å).

M-Pos138 EFFECTS OF LOW IONIC STRENGTH ON INTERFILAMENT FORCES IN STRIATED MUSCLE.
T. C. Irving and B. M. Millman, Biophysics Interdepartmental Group, Dept. of Physics, University of Guelph, Ont., Canada. N1G 2W1.

Filament lattice spacings as a function of applied osmotic pressure have been determined for the A-band of chemically-skinned, frog sartorius muscle at short sarcomere length and low ionic strength (0.024 & 0.038 M). In low ionic strength relaxing solutions, the small-angle meridional and equatorial X-ray diffraction patterns typical of relaxed muscle change to patterns similar to those obtained from rigor muscles. The filament lattice spacings at low ionic strength, are however, greater in relaxed than in rigor muscles indicating that muscles in relaxing solution are not equivalent to muscles in rigor solution under these conditions. As expected from electrostatic theory, the lattice spacings from muscles either in relaxing or rigor solutions swell at low ionic strength. As the ionic strength of the relaxing solution changes from 0.11 to 0.024 M, the change in slope of the osmotic compression curves is the same as that predicted by electrostatic theory (Millman & Nickel, 1980, Biophys J. 32:49). This supports the conclusion of Millman et al. (1983, Biophys J. 41:259) that the dominant repulsive force in the lattice is electrostatic. In low ionic strength relaxing solution, the effective charge radius is increased, a finding consistent with an outward radial movement of the crossbridges as the ionic strength of the solution is decreased. Findings similar to these have been made by (Brenner et al. Biophys. J. 41:33a) on rabbit muscle.

M-Pos139 EFFECT OF CALCIUM BLOCKERS ON E-C COUPLING IN FROG TWITCH MUSCLE.
Valle-Aguilera, R.[+], H. Gonzalez-Serratos and C. Phillips. Dept. of Biophysics, University of Maryland, Baltimore, Md. and [+]Dept. of Pharmacol. Univ. de San Luis Potosi, San Luis Potosi, Mexico.

In a previous report we presented preliminary experiments where several parameters of the slow inward calcium current (I_{Ca}) related to excitation-contraction coupling were measured. It was concluded that there was no clear correlation between I_{Ca} properties and its possible role in e-c coupling. The present experiments were designed to see if the Ca blockers diltiazem and verapamil affect some mechanical characteristics through e-c coupling mechanisms. Experiments were performed on isolated skeletal twitch muscle cells. Diltiazem ($3x10^{-6}$ M) produces an increase in twitch tension (up to 2.5 time the control twitch force) which starts approximately 10-15 sec after the exposure to the drug. In addition, it produces a slight increase in the rate of tension development and a substantial prolongation of the half relaxation time (1.9 times the control value). Partially fused tetanus (11-29 Hz) are potentiated by the drug. Maximal tetanic tension is similar with and without the drug. Verapamil ($1x10^{-6}$ M) has a smaller potentiating effect. Sustained depolarizations (20°C to 1°C) produced with high $[K^+]_o$ under the influence of either drug are similar to their respective controls. K-contractures (95 mM at 8°C) were interrupted during different periods of time by exposure to 2.5 mM-K. The presence of the drug did not affect the redevelopment of tension when the cell was exposed again to 95 mM $[K]_o$. Recovery of twitches and K-contractures after 95 mM $[K]_o$ exposure is slightly affected by these drugs. The above results suggest that these drugs might act on the SR Ca uptake on the contractile proteins.
Supported by grants from the NIH: NS17048-02S1 and SEP: 8304474Y0101 to R.V.A.

M-Pos140 Ca INFLUX AND SR Ca RELEASE IN THE ACTIVATION OF TENSION IN CARDIAC MUSCLE: RELATIVE CONTRIBUTIONS DURING POST-REST RECOVERY WITH CAFFEINE, RYANODINE, Co AND La.
Donald M. Bers and Douglas B. Merrill. Division of Biomedical Sciences, University of California, Riverside, CA.

The recovery of twitch tension (T) and Ca influx after 5 sec to 10 min rest intervals (RI) was studied in rabbit, rat and frog cardiac muscle. In rabbit ventricle, T at the first beat (B1) exceeded T at the second beat (B2). T and Ca influx then increase toward steady state in a parallel fashion. Since Ca influx is small at B1, this beat may be more dependent on Ca stored in the SR and subsequent beats may more closely reflect Ca influx. We have examined this hypothesis using agents which may preferentially inhibit either SR Ca release or Ca influx. Caffeine (5 mM) and Ryanodine (100 nM) (SR inhibitors) changed the pattern of T recovery such that B1 was now less than B2 and more closely paralleled the recovery of Ca influx. Caffeine and Ryanodine decreased steady state T by 27 ± 6% and 22 ± 4% respectively. B1 was also found to be less susceptible to inhibition than B2 when exposed to La or Co (influx inhibitors). These results are consistent with a model in rabbit ventricle where the SR Ca release contributes greatly to B1, that the SR contribution declines while the Ca influx component increases and that at steady state Ca influx can account for a large fraction of steady state T. In adult rat ventricle Caffeine and Ryanodine decrease steady state T by 67 ± 2% and 87 ± 3% respectively. These agents change the T recovery pattern from a monotonic decrease to a monotonic increase. These results are consistent with a model qualitatively the same as rabbit ventricle. However, the SR can account for most of steady state T in the rat and thus its decaying characteristic dominates the control RI recovery. By inhibiting SR Ca release the increasing component ascribed to Ca influx becomes apparent. Similar experiments were done to establish an order of relative dependence on SR Ca release: adult rat ventricle > rabbit atrium > rabbit ventricle > frog ventricle. (Supported by the Amer. Heart Assoc., Los Angeles Affil. and USPHS, HL 28589-01.)

M-Pos141 UNIFORM SARCOMERE LENGTHS IN MAMMALIAN PEELED MUSCLE FIBERS. Christine E. Kasper, Sue K. Donaldson, Daniel Huetteman. Department of Physiology and Department of Medical Nursing, Rush University, Chicago, Illinois 60612.

Previous investigators have found longitudinal non-uniformities of sarcomere lengths in mechanically peeled frog skeletal muscle fibers. The purpose of this study was to measure sarcomere lengths along the entire length of single peeled rabbit adductor and soleus fibers. The skeletal fibers were peeled in an aqueous relaxing solution and mounted in a force transducer at resting length. Bathing solution temperature was 22± 1°C and pH=7.0. All bathing solutions contained variable [Ca^{2+}], 1mM Mg^{2+}, 70mM [Na^{+} + K^{+}], 2mM $MgATP^{2-}$, 15mM CP^{2-}, 15 U/mCPK, propionate anion, imidazole (variable concentration for 0.15M ionic strength). Fibers were then placed in bathing solutions that were 1) relaxing (pCa @ 8), 2) submaximum contracting (pCa 5.4) or, 3) maximum contracting (pCa = 3.6). Fibers were instantly fixed either relaxed or during steady state force generation by making the bathing solution 5% glutaraldehyde; tension was monitored continuously during fixation and did not change. Some unpeeled fibers were fixed mounted in the transducer in the relaxing solution for comparison. The fixed fibers were dehydrated while mounted in the force transducer, tension did not change during dehydration. Longitudinal grey thin sections of the fibers (600-700Å) were cut, photographed end-to-end and measured on a JEOL T-8 electron microscope at (10,000X) magnification. Peeled adductor and soleus fibers were found to have uniform sarcomere lengths (2.15 ± 0.15 μ pCa=3.6; 2.31 ± 0.14 μ pCa=5.4; 2.45 ± 0.15 μ relaxed).

Supported by grants from Muscular Dystrophy Association of American and NIH (HL23128, AM31511).

M-Pos142 OPTICAL DIFFRACTION STUDIES OF SHADOWED FROG THICK FILAMENTS. Robert W. Kensler, Department of Anatomy, The Medical College of Pennsylvania, Philadelphia, PA 19129.

Frog thick filaments isolated as previously described (Kensler and Stewart, 1983, J. Cell Biol. 96:1797) have been shadowed with platinum or platinum carbon (technique: Kensler and Levine, 1982, J. Muscle Res. Cell Motil. 3:349; Vibert and Craig, 1983, J. Mol. Biol. 165:303). The filaments appear highly periodic with the myosin subunits arranged along right-handed approximately helical tracks. Optical diffraction patterns of the filament images are detailed showing a series of layer lines indexing as orders of a 43nm repeat. The patterns show evidence for a slight departure from strict helical symmetry. Meridional reflections not expected from the helical symmetry are frequently present on the 2nd, 4th, 5th and sometimes the 1st layer lines. In addition, along these layer lines, primary maxima at similar radial spacings are frequently present on both sides of the meridian, rather than on one side as expected from simple helical symmetry. Optical filtrations of the images show 5 (sometimes 6) subunits arranged along each half turn of the approximately helical tracks. Comparison of the images to the one-sided appearance of models of 2, 3 and 4-stranded helical filaments shows the images to be most consistent with a 3-stranded arrangement. These results support our previous evidence derived from negative stained images for the presence of 3 cross-bridges per crown.

This work was supported in part by U.S.P.H.S. Grant AM30443 (to RWK).

M-Pos143 INTERPRETATION OF LASER DIFFRACTION PATTERNS FROM SINGLE MUSCLE FIBERS. C.L. Sundell,[1] L.D.Peachey,[1] and Y.E.Goldman,[2] Departments of Biology[1] and Physiology,[2] University of Pennsylvania, Philadelphia, PA 19104.

Fine structure has been observed within the laser diffraction lines obtained from single muscle fibers. We have investigated the possibility that each "fine structure line" is due to a structural domain in the fiber, within which sarcomeres are regularly arranged. The diffraction patterns were recorded photographically or using a Reticon photodiode array during translation of the muscle fiber and masking of the laser beam. When we translate a muscle fiber longitudinally through a laser beam in 100 μm increments, the fine structure lines also move along the meridian by the same amount. As the muscle fiber is translated through many 100 μm steps, individual fine lines appear in the first order diffraction line, they traverse a distance equal to the diameter of the laser beam, and then disappear. In another experiment, a movable mask was placed close to the fiber and in the path of the laser beam to restrict the beam in a controlled way. When this was done, certain fine structure lines disappeared almost completely, while others changed very little. The experiments support the hypothesis that the fine structure in the muscle diffraction pattern is due to groups of sarcomeres which are in localized areas of the illuminated region.

Support: GM7229 (C.S.), HL15835, MDA (L.D.P.), AM26346,AM00745 (Y.E.G.).

M-Pos144 3-D COMPUTER RECONSTRUCTION OF SINGLE SKELETAL MUSCLE FIBERS. W.J. Williams. Dept. of Biology and SDSU Heart Institute, San Diego State University, San Diego, CA 92182.

The orientation of sarcomeres within freshly dissected and chemically skinned frog semitendinosis fibers has been studied using two techniques: computer image analysis of serial optical sections of single muscle fibers and analysis of spectrum of the light diffraction generated by the muscle fiber. Optical sections were obtained using the Zeiss Universal microscope equipped with DIC optics and a high resolution video camera. Sections were then digitized and subjected to analysis algorithms using a UNIX operating system computer with 68000 and 8086 processors. Analysis algorithms include digital subtraction of background noise, image stretch to the full gray scale range, edge detection of sarcomeres and computer generated line superposition over sarcomere edges all within a user defined window on the image. Raw data consist of sarcomere spacing, lattice tilt and position of striations within the window. Data were further processed on a VAX computer running RS/1 statistics and graphics software to generate a 3-D isometric projection. Diffraction spectra were obtained by illuminating the fiber with laser light passed through the microscope's 63X objective and then detecting the diffraction cone with a high dynamic range photodiode array focussed on the back focal plane. Optical sections were taken in the same area illuminated by the laser. Sarcomere orientation data were used to predict the diffraction spectrum from the model of Judy, et al. (Biophys. J. 37:1982. p.475). This analysis indicates that the sarcomeres appear to follow a periodic, spiraling pattern as previously reported by Rüdel and Thaer (J. Physiol. April, 1981. p.28P) and that the sarcomeres occur in domains having relatively uniform tilt and length distributions. (Supported in part by Grant No. 80-S129 to P. Paolini from the American Heart Association, California Affiliate).

M-Pos145 LIGHT DIFFRACTION SUBSTRUCTURES OF STRIATED MUSCLE. Alfred F. Leung, Department of Physics, The Chinese University of Hong Kong, Hong Kong.

The substructures within each diffraction column moved parallel to the muscle fiber axis and retained their shape and intensity when {1} the wavelength of the incident laser beam was varied, {2} the incident angle of the laser beam was varied, or {3} the fiber was stretched slightly. In another experiment, the illumination on the fiber by the laser beam of about 1 mm diameter was translated along the fiber in 0.20 mm steps. During the translation, new structures emerged while others fainted away giving rise to the appearance that the diffraction column was moving in the direction of the translation. During the translation the substructures could be followed until the translation was just greater than the width of the laser beam. The effects on the substructures by decreasing the width of the illumination were also recorded. As the width of the illumination decreased, the substructures began to faint away and broadened. When the illumination decrease to about 0.1 mm, only the brightest substructures usually located in the central portion of the diffraction column remained. The measurements suggest that the diffraction substructures are not independent entities. The substructures are attributed to the interference of light scattered from clusters of sarcomeres of equal length or clusters of myofibrils rather than from bragg planes.

M-Pos146 VARIABILITY OF VERTEBRATE SKELETAL THICK FILAMENT STRUCTURE Santa J. Tumminia and Jane F. Koretz, Biology Dept., Rensselaer Polytechnic Institute, Troy, NY 12181, and Ronald O. Bailey, Dept. of Neurology, Albany Medical College, Albany, NY. (Intro. by J.V. Landau).

Native skeletal muscle thick filaments were isolated from rabbit, normal human, and two types of dystrophic human tissue (Duchenne and fascio-scapular-humeral), and studied using electron microscopy and laser diffraction. Rabbit thick filaments exhibit orders of a 43 nm axial repeat, with a very weak 14.3 nm reflection, and always show an off-meridional reflection indexing at 57.2 nm. Outside the banded region, other reflections are present as well, suggesting a difference in the degree of myosin organization in the distal portion. Normal human thick filaments, in contrast, show orders of the 43 nm axial repeat, including a strong 14.3 nm meridional, but do not exhibit a 57.2 nm reflection. The presence of other weaker off-meridionals which index on a 9/1 primitive helix is consistent with the interpretation of Squire et al. (1983) of a disordered myosin lattice for the thick filament, but the strong 14.3 nm meridional suggests that this disorder is not in the axial direction. AMP deaminase decoration of human thick filaments results in one tetramer per subunit level; diffraction of this structure confirms a 9/1 helical organization. The dystrophic samples give similar, but less ordered, results.

Supported in part by the Muscular Dystrophy Association.

M-Pos147 OBSERVATIONS OF CROSS-BRIDGES IN SKELETAL MUSCLE FIBERS BY THE FREEZE-FRACTURE METHOD. Suechika Suzuki and Gerald H. Pollack, Division of Bioengineering and Department of Anesthesiology, WD-12, University of Washington, Seattle, WA. 98195

Electron microscopic studies by a number of investigators have suggested the possibility that in striated muscle fibers there are interconnections between thick filaments apart from those in the M region (e.g. Hoyle, 1973). We have attempted to ascertain whether or not such interconnections could also be detected using the freeze-fracture, deep-etch, rotary shadowing method (Heuser, 1982), in which no fixatives or embedding media are used. Isolated frog semitendinosus muscle fibers were mechanically skinned in relaxing solution. Fibers at various sarcomere lengths and in each of several physiological states were rapidly frozen with a dual jet liquid propane device. Freeze-fracture replicas were obtained with a Balzer's apparatus. In both relaxed and contracting fibers, interconnections between thick filaments were sometimes but not always observed. They were particularly prevalent in the highly stretched fibers. Such interconnections were rod-like, several hundred Angstroms long and roughly 100 Angstroms wide, similar to those observed by Magid et al. (in press). In some instances at least, rods appeared to be built of opposed cross-bridges projecting from adjacent thick filaments. Such interconnections between thick filaments may serve not only to stabilize the lattice, but as a vehicle for synchronization required to account for stepwise shortening.

M-Pos148 STRUCTURAL STUDIES OF TITIN AGGREGATES Jane F. Koretz, Biology Dept., Rensselaer Polytechnic Institute, Troy, NY 12181, and Kuan Wang, Dept. of Chemistry, University of Texas, Austin, TX 78712. (Intro. by J.C. Salerno).

Rabbit titin (T_2) is a very large cytoskeletal protein associated with the sarcomere. Native T_2 has recently been purified such that it is essentially free of myosin and C-protein as determined using silver staining. The purified native protein was allowed to aggregate by dialysis from 0.5M KCl, 10 mM imidazole, pH 6.5, to 0.1 M KCl, 10 mM imidazole, pH 6.5. The aggregate as observed by negative staining in the electron microscope is thin and filamentous, with narrow fibrous nodes at regular intervals. Laser diffraction of these structures reveals an axial period of approximately 230 nm (16 x 14.3 nm). The titin aggregates can be decorated with AMP deaminase, and under these conditions reveal a strong 14.3 nm periodicity along with the same 230 nm axial period. If titin and C-protein are mixed together before dialysis, there is no apparent change in aggregate appearance in the electron microscope or change in organization as determined by diffraction. If the pH of the solution is raised to 7 or above after titin aggregation, the filaments will themselves aggregate into ordered bundles. These results confirm the unique properties of this unusual protein; further, the 230 nm axial period observed here for T_2 aggregates may be related to the 230 nm cytoskeletal periodicity detected by Cooke and Meek (1983, JCB Abstracts) in frog striated muscle.

Supported by a grant from the Muscular Dystrophy Association (JFK) and NIH grant AM 20270 (KW).

M-Pos149 MASS DISTRIBUTION IN RELAXED AND RIGOR SINGLE RABBIT PSOAS FIBERS WITH SPATIAL RESOLUTION EXTENDED TO 125Å. Leepo C. Yu* and Bernhard Brenner*+. *National Institutes of Health, Bethesda, MD. 20205; +Institute of Physiology II, University of Tübingen, FRG.

Both stiffness measurement and equatorial X-ray diffraction provided evidence that cross bridges are attached in relaxed rabbit psoas muscle at low ionic strength (μ =20mM) and 5°C. In addition, the X-ray study showed that upon lowering μ from 100 to 20mM, I_{10} decreased and I_{11} increased, indicating a mass shift towards the thin filament. To investigate the properties of mass distribution in greater detail, higher order equatorial X-ray reflections beyond [1,1] were obtained from the relaxed and rigor states at μ =20 to 120mM with varying concentrations of KPropionate. Although reflections up to [3,2] were consistently obtained, two dimensional electron density maps were constructed based on intensities of five reflections ([1,0], [1,1],[2,0], [2,1] and [3,0]), since phases of these reflections have been determined (Yu, et al, in press). Preliminary density maps of the relaxed fiber at μ =120mM showed a thick filament backbone surrounded by an annular shell of mass, most likely that of the myosin heads. As μ was lowered from 120mM to 20mM, mass was transferred to the thin filament region, originating most prominently from the neighborhood around the thin filament. The part of the annular shell distal to the thin filament was less effected. However, transition from relaxed to rigor state showed that mass transfer towards the thin filament involved mass originating from the entire annular shell. The crossbridges formed in the relaxed state are thought to be weakly bound, in contrast to the strongly bound rigor bridges. The difference in mass redistribution observed here suggests different modes of attachment in these two states.

M-Pos150 STRUCTURE AND FUNCTION OF EPIMYSIAL COLLAGEN FIBERS IN HEART MUSCLE. T.F. Robinson, S.M. Factor, L. Cohen-Gould, and J.M. Capasso. Cardiovascular Center, Department of Medicine, Departments of Physiology & Biophysics and Pathology, Einstein College of Medicine, Bronx, New York.

We have examined the biphasic length-tension relation in passively stretched cardiac papillary muscle in correlation with the disposition of collagen fibers of the epimysium (sheath of connective tissue surrounding the muscle). Techniques employed are length and force measurements and light microscopy (L.M.) of living muscle; L.M. of silver stained sections; scanning E.M.; and transmission E.M. At slack length, the majority of collagen fibers are biaxially oriented near +/- 45 degrees relative to the long axis of the muscle. The collagen network is dramatically rearranged near Lmax: the collagen fibers are essentially co-linear with the muscle axis. Due to the very limited extensibility and high tensile strength of collagen, the aligned configuration of epimysial fibers can well account for the sharp rise in passive tension of the muscle at Lmax. Protection from over-stretch of the muscle beyond Lmax prevents sarcomeres from being stretched beyond lengths of 2.3-2.4 um. These sarcomere lengths represent the upper limit where most cross bridges are in overlap configuration. The degree of tolerance in coupling between epimysium and inner layers of connective tissue, as well as the role of connective tissue at muscle lengths below Lmax remain to be determined.

M-Pos151 COMPUTERIZED 3-DIMENSIONAL IMMUNOCYTOCHEMISTRY IN SINGLE CELLS. F.S. Fay, K. Fogarty, and J. Coggins, Dept. of Physiology, Univ. of Mass. Med. School, Worcester MA 01605.

The use of fluorescent markers to follow molecules within cells as function changes had led to considerable insights into many cell processes. While such probes allow observations on living cells, the fluorescence microscope has a broad depth of focus (3.0 μm at 63 x, NA = 1.4) yielding considerable spatial uncertainty; in addition, a single image precludes following continuous structures over long distances. To surmount these problems, we developed an approach combining a computerized microscope, low light TV (SIT) camera, and digital image processing techniques. The approach involves taking a picture of fluorescence from multiple focal planes and removing from this 3-D image out of focus information by digital image restoration and segmentation techniques. Images are obtained at 0.25 μm intervals by computer, the SIT images stored in digital form, and several frames at each plane averaged to reduce noise. To correct for the spread of an object within the image, we quanitated the extent of this effect by recording the 3-D image of a 0.1 μm diam sphere labelled with fluorochrome (the point spread function (PSF)). A filter designed utilizing the PSF removed greater than 75% of the spread of out of focus information. The computer then identified stained elements in the deblurred 3-D image by convolution with a template of similar shape and size to that of the stained bodies. The bodies were replaced by a single vector oriented along the long axis of each body. The methods have been used to examine the distribution of α-actinin in single smooth muscle cells (SMC). The 3-D images reveal strings of bodies that run for considerable distances within the SMC before apparently inserting on membrane attachment sites; these strings appear to be the site for force generation. Supported by the MDA and the NIH (HL14523).

M-Pos152 BIPHASIC RELAXATION OF CARDIAC SARCOMERE BY LASER DIFFRACTION.

Y. Lecarpentier, J.L. Martin°, D. Chemla°, J.P. Chambaret°, A. Antonetti° and P.Y. Hatt, INSERM U2, Limeil-Brévannes and °ENSTA Ecole Polytechnique, Palaiseau, France.

Sarcomere dynamics were examined in real-time by laser diffraction in thin right ventricular trabeculae of rat (n = 10). Sarcomere movements were registered simultaneously with force and shortening of the whole trabecula, for various levels of isotonic load. Peak of sarcomere lengthening max.Vr (μm/s) decreased when the isotonic load (expressed in terms of % of isometric total force TF) increased : $max.Vr = -4 \exp(-2.5\ 10^{-2}\ \%\ TF)$, $r = 0.95$. Sarcomere relaxation occurred in two successive exponential phases : a rapid phase (time constant (ms) : τ_1) followed by a slower one (time constant : τ_2). When the total load increased, τ_1 increased and τ_2 decreased as follows : $\%\ TF = 0.2\ \tau_1 + 4.8$ ($r = 0.83$) and $\%\ TF = -0.1\ \tau_2 + 157$ ($r = 0.95$). The relative predominance of the amplitude and of the time course of these two phases depended on the level of load : the rapid one predominated at low load and the slow one at high load. Load clamp steps at a given final level of isotonic load allowed to modify the onset and the time course of the rapid phase without change in τ_2. The load sensitivity of cardiac relaxation requires a well-functional sarcoplasmic reticulum (SR). This argues in favor of the involvement of the SR in the regulation of the time course of the rapid phase. A balance between two mechanisms, i.e. the calcium removal from Troponin C and the Ca^{2+} - uptake by the SR appears to regulate the time course of sarcomere relaxation, according to the loading conditions.

M-Pos153 THE MUSCLE-TENDON JUNCTION IN THE FROG SARTORIUS. Brenda R. Eisenberg and Richard L. Milton; Department of Physiology, Rush Medical College, Chicago, Illinois 60612.

The force produced within a skeletal muscle fiber is transmitted to the bone through the membrane at the fiber's end via a myotendon junction. This region was examined by light and electron microscopy in the sartorius muscles of three Rana temporaria. The intact myotendon was fixed in a stretched position for 1 hour then trimmed away from the pelvic bone for processing. A light microscope was used to make montages of longitudinal sections of the whole myotendon junction at 500x magnification. A digital planimeter was used to measure the taper in fiber diameter starting 100 μm from the tip. Electron micrographs at 25,000x were sampled systematically at the junctional region where extensive membrane interdigitation occurs. A stereological analysis was made using a semicircular test grid to count intersections made with the wrinkled sarcolemmal membrane and also with the smooth line which might have been observed in the light microscope. Orientation tests showed that the caveoli and 40% of the sarcolemmal membrane were isotropic and 60% of the sarcolemma had cylindrical anisotropy. Surface areas of the membranes were calculated using the appropriate stereological equations. The wrinkling and caveoli increase the real sarcolemmal area at the myotendon to 30 times that of a flat disc perpendicular at the zone where the wrinkling begins at about 50 μm from the tip. The additional membrane increases the contact between the muscle and the tendon thereby providing greater mechanical strength. Electrophysiological measurements of membrane capacitance made at the end of the fiber imply a similar large surface area of membrane.

M-Pos154 MUSCLE SOUNDS: OBSERVATIONS WITH IMPROVED TRANSDUCERS. F.V. Brozovich & G.H. Pollack, Div. of Bioeng. & Dept. of Anesth., WD-12, University of Washington, Seattle, WA 98185.

We have recently reported that muscles generate discrete sounds during contraction (Brozovich & Pollack, Biophys. J. 41: 35-40, 1983). These sounds are hypothesized to derive from rapid changes of fiber diameter associated with shortening steps. To explore the properties of the sounds further, we used a piezoresistive sound transducer whose sensitivity (0.33 v/mW) and frequency response (flat between 200 Hz and 16.5 kHz) were improved over transducers used in previous studies. This enabled us to use thinner specimens. We mounted either the whole dorsal head or bundles of 2 - 20 fibers from the semitendinosus muscle of the frog, R. temporaria, in a chamber filled with Ringer's solution at 2-3°C. Sarcomere length was determined by optical diffraction: the beam of a 5 mW He-Ne laser was expanded and focused to a rectangle, 4 mm x 1 mm, onto the muscle, and the resulting first order was projected onto a photodiode array. Sound, sarcomere length and tension were recorded during isotonic twitches. Because of uncertainty in the coincidence of regions sampled by the laser and by the sound transducer, we are as yet unable to draw conclusions as to possible coincidence of steps and sounds. Analysis of sounds reveals more detail than previously reported. High amplitude single spikes of sound, reported earlier, were found; however, in most cases, the sound consisted of several such spikes, or cycles, in close sequence, lasting several milliseconds, but of lower amplitude. The number of cycles ranged from one and 20; bursts with fewer cycles generally had higher amplitude. Fourier transforms of sound bursts revealed principal frequencies of approximately 650 Hz and 2.1 kHz. The sounds occurred most frequently at approximately 25, 50 and perhaps 100 msec after stimulation.

M-Pos155 .URFACE VIEW OF JUNCTIONAL FEET IN FREEZE-DRIED ISOLATED SR VESICLES. Donald G. Ferguson and Clara Franzini-Armstrong (Introduced by A.V. Somlyo). Depts of Biology and Anatomy, University of Pennsylvania.

The junctional feet are evenly spaced structures which span the gap between apposed membranes of T tubules and sarcoplasmic reticulum at triads. In the intact triad they form long rows in which the individual components are tetragonally arranged. We have isolated crude SR fractions from rat and guinea piglegmuscles and suspended them in 10 mM dl-histidine and .25 mM sucrose. Washing with 0.6 M KCl was avoided because it is known to extract the visible component of feet (Campbell, et al., B. B. Acta, 602,97,1980). The vesicles were spread on a freshly cleaved mica surface, stabilized for 5' in 1% uranyl acetate, briefly rinsed in distilled water and frozen in liquid nitrogen. Following freeze-drying to expose the cytoplasmic surface, the vesicles were rotary shadowed with platinum and replicated with carbon. The junctional SR surface is covered by elevated structures which are identified as feet on the basis of their spacing. Each foot is composed of four subunits surrounding a central depression, and its outline has the shape of a four leafed clover. Adjacent feet abut at corners, not along the sides. This structure and disposition is consistent with previous thin section and freeze-fracture images and provides detail of subunit structure not previously described. Supported by an Alberta Heritage Foundation fellowship (to DGF) and by MDA (H.M. Watts Research Center).

M-Pos156 ROLE OF TIGHTLY BOUND DIVALENT CATION IN THE POLYMERIZATION AND DEPOLYMERIZATION OF ACTIN

James E. Estes, Lynn A. Selden and Lewis C. Gershman, Research Service, VA Medical Center, Albany and Dept. of Physiology, Albany Medical College, Albany, New York 12208

We recently reported measurements of the forward rates of polymerization (k^+) of N-pyrenyl-iodoacetimide (N-P) labeled monomeric actin (Selden et al., B.B.R.C., in press) and showed that the critical actin concentration (CAC $=k^-/k^+$) for actin containing bound Ca^{++} (Ca^{++}-actin) is about 20 times greater than the CAC for Mg^{++}-containing actin (Mg^{++}-actin). We also found the ratio k^+_{Mg}/k^+_{Ca} to be in the range of 1.5. From these data it can be estimated that the ratio k^-_{Mg}/k^-_{Ca} should be 0.05-0.1. We have studied actin depolymerization by diluting F-Mg-actin and F-Ca-actin polymers labeled with N-P to concentrations below the CAC and monitoring the time course of fluorescence intensity decrease as a measure of depolymerization. We found the depolymerization of F-Mg-actin to be faster than that of F-Ca-actin under similar depolymerization conditions. Since the initial depolymerization rate is proportional to the product (k^-)(number of polymer ends, m) this would predict that for F-Mg-actin and F-Ca-actin prepared at similar ionic strengths, there are about 15X more polymer ends in F-Mg-actin than in F-Ca-actin. This difference in the number of ends in these solutions correlates well with the larger nucleation rate constant for Mg^{++}-actin than for Ca^{++}-actin (Tobacman and Korn, J.Biol. Chem. 258, 3207-3214, 1983), and with measurements of the rates of actin ATP hydrolysis under these conditions. Supported by the Veterans Administration.

M-Pos157 BOUND CATION EXCHANGE AFFECTS THE LAG PHASE IN ACTIN POLYMERIZATION

Lewis C. Gershman[1], Jay Newman[2], Lynn A. Selden[1] and James E. Estes[1], [1]Research Service, Veterans Administration Medical Center, Albany, NY 12208 and [2] Department of Physics, Union College, Schenectady, NY 12308

The delay or lag phase at the onset of polymerization of actin by neutral salt is generally attributed to an actin nucleation reaction. However, when nucleation is circumvented by the use of phalloidin-stabilized nuclei, a lag phase persists when Ca^{++}-containing actin is polymerized with $MgCl_2$. We (Biophys. J. 41:95a,1983), as well as others (Cooper et al, Biochemistry 22: 2193-2203, 1983), proposed that this nucleation-independent lag was due to a monomer activation step. Since pretreatment of actin with EGTA and/or Mg^{++} shortens or eliminates this lag phase, we considered that exchange of the actin-bound divalent cation might occur during this delay in polymerization, as suggested by Tobacman & Korn (J. Biol. Chem. 258:3207-3214, 1983). Measurement of the actin-bound cation initially and after brief incubation with EGTA/Mg^{++} directly verifies that Mg^{++} has replaced Ca^{++} as the actin-bound cation with a time constant estimated to be on the order of 180 sec. The Mg^{++}-actin produced nucleates and polymerizes more readily than Ca^{++}-actin. It thus appears that bound cation exchange accounts for the difference in polymerizability between Ca^{++}-actin and Mg^{++}-actin and for the nucleation independent lag phase which occurs when Ca^{++}-actin is polymerized with Mg salts. Supported by the Veterans Administration.

M-Pos158 LASER LIGHT SCATTERING STUDIES ON "MONOMERIC" ACTIN: EVIDENCE FOR THE PRESENCE OF OLIGOMERS BELOW THE CRITICAL CONCENTRATION.

Jay Newman, Dept. of Physics, Union College, Schenectady, N.Y. 12308; Lynn Selden, Lewis C. Gershman and James E. Estes, Research Service, Veterans Administration Medical Center, Albany, and Dept. of Physiology, Albany Medical College, Albany, N.Y. 12208.

In earlier work, we reported a value of $7.88 \pm 0.11 \times 10^{-7}$ cm^2/sec for the extrapolated translational diffusion coefficient at 20°C, D°_{20}, for column purified monomeric actin in 0.2 mM ATP, 0.02 mM $CaCl_2$, 2mM Tris, 0.1% NaN_3. New work has confirmed this value and shown it to be independent of the scattering angle to within 3%, as expected for a monodisperse solution. The concentration dependence of D_{20} was such that at 20 µM actin (our standard condition), $D_{20} = 8.25 \pm 0.15 \times 10^{-7}$ cm^2/sec. When the $CaCl_2$ concentration was increased to 0.2 mM, the D_{20} value decreased slightly (~ 5%) probably due to a decrease in the concentration virial, and no significant increase in the ATP hydrolysis rate was measured. With 0.1 mM $MgCl_2$ present, the critical actin concentration (CAC) of N-pyrenyl iodoacetimide labelled monomeric actin was determined to be 22 µM. Under these conditions, at 20 µM actin, there was no polymer detected by viscosity or intensity light scattering measurements. However, under these same conditions at 20 µM actin (below the CAC), the D_{20} value dropped to $4.8 \pm 0.2 \times 10^{-7}$ cm^2/sec within 1h remaining stable for at least 5h, and a corresponding tenfold increase in the rate of ATP hydrolysis was measured. Intermediate ATPase rates and D_{20} values were obtained in the presence of both 0.1 mM $MgCl_2$ and 0.2 mM $CaCl_2$. These results strongly suggest that, in the presence of $MgCl_2$, solutions of actin at sub-critical concentrations contain small amounts of oligomer which may account for the observed ATP hydrolysis. Supported by the Veterans Administration and the Research Corporation.

M-Pos159 PROPERTIES OF MUSCLE ACTIN LABELLED WITH FLUORESCEIN ISOTHIOCYANATE. L.D. Burtnick and K.W. Chan, Department of Chemistry, University of British Columbia, Vancouver, B.C., Canada.

Reaction of rabbit skeletal muscle G-actin in a low ionic strength HEPES buffer, pH 8.8, with fluorescein isothiocyanate (FITC) resulted in incorporation of up to 1.9 fluorescein groups per actin unit. When excited with 365 nm light, the FITC-actin samples were highly fluorescent, exhibiting an emission maximum near 516 nm. Labelling to the extent of one dye molecule per actin caused virtually complete loss of the polymerizability of the sample as monitored by capillary viscometry. The fluorescence of FITC-actin samples was not affected significantly by the addition of KCl or $MgCl_2$ to levels that would induce polymerization of unmodified actin, reflecting the loss of sample polymerizability. FITC-actin samples demonstrated only a mildly reduced ability to inhibit the nuclease activity of DNase I. While FITC-actin does interact with DNase I, addition of DNase I to FITC-actin samples did not alter the fluorescence properties of the samples.

Tryptic digestion of FITC-actin produced a nonfluorescent, protease-resistant core protein and a pool of peptides that did display fluorescence. Fractionation of the peptides on DEAE-BioGel A with a 0.5 to 2.0% ammonium bicarbonate gradient produced only one major fluorescent peak in the elution profile. Amino acid analysis of this fraction showed it to have a composition consistent with that of a possible tryptic peptide of actin that extends from asp-52 through arg-62 of the actin sequence. The major site of FITC reaction under our conditions, therefore,is at lys-61.

Supported by the Natural Sciences and Engineering Research Council of Canada and the B.C. Health Care Research Foundation.

M-Pos160 CATION DEPENDENCE ON THE MECHANISM OF ACTION OF CYTOCHALASIN D ON ACTIN FILAMENTS. Angel Mozo and B. R. Ware, Department of Chemistry, Syracuse University, Syracuse, New York 13210.

Fluorescence photobleaching recovery has been used as a physical technique for the study of the assembly of G-actin into actin filaments. Directly determined parameters include the diffusion coefficient of the non-assembled species, the diffusion coefficient of the assembled filaments, and the fraction of monomers assembled into filaments. We have compared the assembly characteristics with particular attention to the differences that result from the induction of polymerization by either K^+ or Mg^{+2}. Using concentrations of K^+ and Mg^{+2} that induce filaments of similar length, we have then compared the effects of addition of cytochalasin D either before or after assembly has taken place. From these data it is possible to infer whether the action of cytochalasin is the result of filament cleavage or net depolymerization, since the former mechanism would lead to filament shortening without increase in unassembled protomers and the latter mechanism would lead to a distinct increase in unassembled protomers accompanied by a commensurate, generally lesser, degree of filament shortening. Our results indicate that for all conditions examined, and independent of whether cytochalasin D was added before or after assembly, the mechanism of action of cytochalasin D includes a substantial degree of filament cleavage if and only if Mg^{+2} is present. Supported by NSF Grant PCM 8306006.

M-Pos161 STRUCTURE OF F-ACTIN IN SINGLE-LAYERED Mg^{2+} PARACRYSTALS
E.P.Morris, R.Mendelson and E.J.O'Brien
Medical Research Council Cell Biophysics Unit, King's College, London, U.K.

Electron microscope analysis of paracrystals of F-actin induced by Mg^{2+} has usually been complicated by the presence of superimposed layers of filaments, so that the structure obtained may represent a composite (Egelman *et al.*, 1983, J.Mol.Biol.166, 605). At lower levels of Mg^{2+} (25mM) single-layered paracrystals are obtained which appear well suited to image analysis. Optical and computer-generated diffraction patterns indicate that the filament symmetry comprises 13 subunits in 6 turns of the 5.9nm genetic helix. The intensity of the second layer-line in the patterns is relatively strong, about half that of the first. Filtered images of the paracrystals show clearly that adjacent filaments have opposite polarity. Individual filaments in the filtered images were extracted from the arrays and used for helical three-dimensional reconstruction. In the reconstructions the actin subunits have a large elongated region extending to a radius of about 4.5nm and a smaller protrusion extending to about 3.5nm. Connections along the long-pitch helices occur at low radius.

The F-actin reconstructions are consistent with the portion assigned to actin in three-dimensional reconstructions of F-actin + tropomyosin calculated from electron micrographs of paracrystals by O'Brien *et al.* (1983, in "Actin, its structure and function in muscle and non-muscle cells", Academic Press, Sydney). The binding of tropomyosin does not therefore alter the conformation of F-actin greatly. An interesting feature of the F-actin reconstruction is a thin extended region which may form part of the tropomyosin binding site.

M-Pos162 IDENTIFICATION OF A THIN FILAMENT LINKED-35,000 DALTON PROTEIN IN VERTEBRATE SMOOTH MUSCLE. William Lehman and Benjamin Kaminer, Dept. of Physiology, Boston University School of Medicine, Boston, MA 02118

A 35,000 Da actin-binding protein has been purified from chicken gizzard smooth muscle. The possibility that this protein is an isomorphous form of tropomyosin is ruled out, since the two proteins do not copurify and they migrate differently on several gel electrophoresis systems. Furthermore, by means of immunoblotting of SDS gels, antibodies raised against gizzard tropomyosin and the 35,000 Da protein were shown to be monospecific for their respective antigens, showing no cross-reactivity or detectable interaction with other smooth muscle proteins. We also ruled out the possibility that the protein is glyceraldehyde 3 P_i dehydrogenase (an abundant glycolytic enzyme and 35,000 Da protein).

Antibodies to the 35,000 Da protein (and also those to tropomyosin) precipitate intact native smooth muscle thin filaments, suggesting the 35,000 Da protein is a bona fide component of smooth muscle thin filaments. Additionally, co-sedimentation studies demonstrate that purified 35,000 Da protein interacts with actin. Densitometric scans of SDS gels of unfractionated gizzard muscle show the protein is present in relatively large amounts (stain intensity ratio 1:2.1:5.8, 35,000 Da protein:tropomyosin:actin), suggesting it and tropomyosin are equimolar. The protein may not be restricted to gizzard smooth muscle as it is also seen on SDS gels of bovine aortic smooth muscle. The role of the 35,000 Da protein is currently being investigated.

M-Pos163 EFFECT OF CHAIN LENGTH ON THE STABILIZATION AND FORMATION OF TWO-STRANDED α-HELICAL COILED-COILS: SYNTHETIC MODELS OF TROPOMYOSIN. S.Y.M. Lau, A.K. Taneja and R.S. Hodges, Department of Biochemistry and Medical Research Council of Canada Group in Protein Structure and Function, University of Alberta, Edmonton, Alberta, Canada, T6G 2H7.

Synthetic tropomyosin (TM) analogs have been prepared by solid-phase peptide synthesis with the sequence Ac-(Lys-Leu-Glu-Ala-Leu-Glu-Gly)$_n$-Lys-amide, where n varies from 1 to 5. Circular dichroism has been used to determine the length of the peptide chain required for the formation and stabilization of two-stranded α-helical coiled-coils. It was found that TM analogs which have residues of more than 4-heptads will form two-stranded coiled-coils while shorter polymers (3-heptads or less) show little or no α-helix. Gel-filtration high performance liquid chromatography and ultracentrifugation experiments have shown that TM-29 and TM-36 behave as dimers in benign medium while TM-8, TM-15 and TM-22 behave as monomers.

The stability of TM analogs to urea denaturation and temperature denaturation at different pH and KCl concentrations were examined.

Interestingly, all 5 TM analogs can be resolved by reverse-phase high performance liquid-chromtography on a Beckman Ultrapore C_3-300 Å pore column. A linear relationship is obtained when the ln of the monomeric molecular weight is plotted against retention time. These results will be discussed in light of the conformation of these analogs on the reverse-phase column and their conformation in the solvents used for reverse-phase chromatography.

(Supported by MRC and AHFMR)

M-Pos164 PURIFICATION AND CHARACTERIZATION OF A TROPOMYOSIN BINDING PROTEIN FROM CHICKEN GIZZARD SMOOTH MUSCLE. J. Lees-Miller and L.B. Smillie, MRC Group in Protein Structure and Function, Department of Biochemistry, University of Alberta, Edmonton, Canada T6G 2H7.

Using [^{125}I]-labelled chicken gizzard tropomyosin as a probe in the gel overlay technique, several tropomyosin binding proteins were observed on SDS-polyacrylamide electrophoretic gels of extracts of chicken gizzard smooth muscle. While three of these comigrated with calf thymus histones, a unique protein of Mr ~20,000 was also detected and purified to homogeneity by $(NH_4)_2SO_4$ fractionation and ion-exchange chromatography on CM-cellulose. Its interaction with rabbit skeletal troponin-I and brain calmodulin was demonstrated by affinity chromatographic and gel overlay techniques respectively. However, neither its amino acid composition nor NH_2-terminal sequence (30 residues) are similar to any other known protein as established by a computer search of the sequence data bank (National Biomedical Research Foundation). While its location and function in chicken gizzard muscle are presently unknown, the isolation of a tropomyosin binding protein with similar Mr and amino acid composition from bovine aortas indicates its presence in a variety of smooth muscle tissues.

(Supported by MRC of Canada and the Alberta Heritage Foundation for Medical Research)

M-Pos165 TROPOMYOSIN LYSINE REACTIVITIES: RELATIONSHIP TO STRUCTURE. Sarah E. Hitchcock-DeGregori, Tony M-T. Chou, and Stephen F. Lewis. Department of Biological Sciences, Carnegie-Mellon University, Pittsburgh, PA 15213.

We have studied the structure of rabbit skeletal muscle α-tropomyosin by measuring the reactivities of lysines with acetic anhydride using a competitive labeling procedure (Hitchcock et al., 1981, JMB 147, 125). We have isolated peptides containing 38 of 39 lysines, most with an individual lysine or 2 or 3 adjacent lysines in the sequence. The most reactive lysines (5, 6, 7, 65, 189) are about 10 times as reactive as the least reactive (Lys 29, 30, 59, 118, 128, 161, 251). Although the N-terminal half of the molecule is known to be more stable than the C-terminal half, there is no correlation with lysine reactivities. We have analyzed individual lysines in terms of position in the helical net of the coiled-coil structure proposed for tropomyosin by McLachlan and Stewart (1975, JMB 98, 293). Lysines on the outside of the helix (positions b, c, f) range widely in reactivity. When a lysine is in position e or g, it tends to have a lower than average reactivity when there is an acidic residue facing it in the opposing helix (eg. Lys 70, 112, 161). Lysines in the e or g position with high reactivities are in regions of the molecule known to be unstable and/or there are nonacidic residues in the opposing helix (eg. Lys 5, 7, 189). Two lysines in the hydrophobic band between the two helices (Lys 15, 30) were not isolated as individual lysines.

Supported by grants from NIH (GM 28830, AM 00914) and MDA.

M-Pos166 BINARY INTERACTIONS OF TROPONIN SUBUNITS, R.H. Ingraham and C.A. Swenson, Department of Biochemistry, University of Iowa, Iowa City, IA 52242.

The association constants for the formation of the binary complexes of rabbit fast skeletal troponin subunits have been measured for three solution conditons: A) 1 mM $CaCl_2$; B) 3 mM $MgCl_2$ and 1 mM EGTA; C) 2 mM EDTA. The solutions were buffered at pH 7.0 with 10 mM Pipes and contained 0.3 M KCl, 5 mM dithiothreitol and 0.01% NaN_3. Subunits were labeled with extrinsic fluorescent probes (iodoacetamidoeosin or dansylaziridine) as indicated by the Table.

Binary Complex	$K(Ca^{2+})_9$	$K(Mg^{2+})_8$	$K(EDTA)_6$
Troponin C•I	[d]1.7×10^7	[d]1.3×10^7	[a]1.3×10^6
Troponin C•T	[b]4.2×10^7	[a]4.7×10^7	[a]4.5×10^6
Troponin I•T	[c]9.3×10^6	[c]9.8×10^6	[c]8.7×10^6

[a] dansylaziridine-C
[b] iosoacetamidoeosin-C
[c] iodoacetamidoeosin-T
[d] iodoacetamidoeosin-I

This data indicates that the presence of magnesium in the Ca^{2+}-Mg^{2+} sites strengthens the troponin C•T and troponin C•T interactions over that observed in its absence. The presence of calcium in all four Ca^{2+}-binding sites enhances the strength of C•I interaction even further, which strongly suggests the involvement of the Ca^{2+}-specific sites in the troponin C•I interactions. There is little additional effect of calcium on the C•T interaction. As expected, troponin I•T complex formation does involve a reasonably high association constant which is not significantly affected by the presence or absence of Ca^{2+} or Mg^{2+}. (Research supported by NIH grant AM-27554).

M-Pos167 FLUORESCENCE QUENCHING STUDIES OF RABBIT SKELETAL TROPONIN. CHIEN-KAO WANG, Graduate Program in Biophysical Sciences, University of Alabama in Birmingham, Birmingham, AL 35294

Acrylamide quenching of the fluorescence of IAEDANS attached to Cys-98 of TNC was monitored by lifetime measurements at 20°C. Measurements were carried out on labeled TNC, the binary complex TNC-TNI, and troponin reconstituted with TNT, TNI, and labeled TNC. I have obtained the quenching constant Kq for each of these systems by fitting the data to the equation: $1/\tau = 1/\tau_o + Kq[Q]$, where τ and τ_o are the quenched and unquenched lifetimes, respectively.

Proteins	Kq x 10^{-8} (M^{-1} sec^{-1}) -cations	$+4Mg^{2+}$	$+4Ca^{2+}$
TNC	5.35	5.43	5.32
TNC-TNI	5.22	5.30	3.54
TNC-TNI-TNT	5.61	5.96	4.20

Kq provides a measure of the accessibility of the attached probe to collisional quenching. The following conclusions can be drawn: (1) Binding of Mg^{2+} or Ca^{2+} to isolated TNC has no significant effect on the accessibility of the probe. (2) In the binary complex, binding of Mg^{2+} to the high affinity sites of TNC does not lead to protection of the probe from quenching. However, binding of 4 moles of Ca^{2+} to the TNC decreases the accessibility by 35%. This suggests that Cys-98 of TNC is protected from solvent in the TNC-TNI complex in the presence of Ca^{2+}. This effect is likely due to structural changes resulting from Ca^{2+} binding to the low affinity sites since occupation of the high affinity sites by Mg^{2+} has no effect on Kq. (3) In the reconstituted troponin, the accessibility of the probe is not affected by TNT or Mg^{2+}. It is, however, decreased by Ca^{2+} binding to TNC. These results are consistent with the notion that TNT does not bind to TNC at a site adjacent to Cys-98. The Ca^{2+} effect observed with the ternary complex does not appear to be mediated through TNT. (Supported in part by NIH AM-25193).

M-Pos168 CALCIUM-SENSITIVE CHANGES IN THE CONFORMATION OF TNI DETECTED BY PYRENE EXCIMER FLUORESCENCE. G.M. Strasburg, J. Gergely and P.C. Leavis. Dept. Muscle Research, Boston Biomed. Res. Inst.; Depts. Neurology and Biol. Chem. Harvard Med. Sch., Dept. Neurology, Mass. Gen. Hosp., Boston, MA 02114.

TnI was carboxymethylated at Cys 133 and labeled with N-(1-pyrene)maleimide at Cys 48 and 64. The fluorescence spectra exhibit peaks characteristic of the pyrene monomer and an additional peak that results from the formation of excited dimers of pyrene (excimers) (cf. Betcher-Lange and Lehrer (1978) J. Biol. Chem. 253;3757). The excimer is indicative of the proximity of the labeled Cys residues in TnI. Addition of TnC to labeled TnI results in a slight decrease in excimer fluorescence and an increase in monomer fluorescence intensity. Titration of the complex with Ca^{2+} produces a 25% decrease in excimer intensity and a doubling of the monomer peak intensities with a $[Ca^{2+}]_{1/2} = 6.25 \times 10^{-6}$M, indicating that the fluorescence change occurs upon titration of the lower affinity Ca^{2+}-specific sites of TnC rather than the Ca^{2+}-Mg^{2+} sites (cf. Potter and Gergely (1975) J. Biol. Chem. 250;4628). This is consistent with the lack of fluorescence change upon addition of 5mM Mg^{2+} to the complex. Stopped-flow fluorescence experiments in which Mg^{2+}-TnC-TnI is mixed with Ca^{2+} show a rapid decrease in excimer intensity which is complete within the instrumental dead time, followed by a further decrease whose rate corresponds to the rate of Ca^{2+}-Mg^{2+} exchange at the high affinity sites ($k=5.9$ sec^{-1}). Addition of Ca^{2+} to the ternary complex containing labeled TnI produces a decrease in excimer fluorescence similar to that seen in the TnC-TnI complex. These data suggest that N-(1-pyrene)maleimide is a useful probe of TnI conformation.

M-Pos169 THERMAL STABILITY OF COILED-COIL α-HELICAL PROTEINS. Sφren Hvidt, Michael E. Rodgers and William F. Harrington, Department of Biology, Johns Hopkins University, Baltimore, MD 21218

ORD has been used to examine thermally induced conformational changes in paramyosin, tropomyosin, myosin rod, LMM and S-2. Melting curves were determined using three different indicators of the helix content: $[m']_{231}$ ($\alpha_{215}/\alpha_{231}$) and b_o. The melting profiles for all samples showed similar behavior. At 5°C, $[m']_{231}$ is -15,600 ± 400 and increases linearly at a rate of 60 ± 5/°C as the temperature is increased to ~25°C. At intermediate temperatures (30-55°C), $[m']_{231}$ increases markedly as the α-helical structure is disrupted. The midpoint of the transition(s) varies among the different proteins and is also species dependent. At high temperatures, $[m']_{231}$ levels off to a value of 3070 ± 80 at 80°C in each case. Measurements of (b_o) and ($\alpha_{215}/\alpha_{231}$) yielded consistent results (with $[m']_{231}$) in both the transition region and at high temperature. Between 5° and 25°C, however, no change in these parameters was observed. Poly-L-lysine has been studied as a model system for random coils and α-helices. In 50% MeOH at high pH, where poly-L-lysine is an α-helix, $[m']_{231}$ increases linearly at a rate of 59/°C. ($\alpha_{215}/\alpha_{231}$), however, showed only a 1% drop over the range of 5-40°C. Poly-lysine in the random coil form also showed some temperature dependence in $[m']_{231}$. These results are consistent with those observed for the coiled-coil proteins in the low and high temperature regions, respectively. We suggest that the low temperature increase in $[m']_{231}$ (where b_o and $\alpha_{215}/\alpha_{231}$ are constant) may reflect a thermal coefficient of the α-helix without loss of helicity. The temperature dependence of the random-coil form may similarly reflect a thermal coefficient or it could indicate the formation of some slightly ordered structure. Our results show that estimating fraction helicity from [m'] measurements alone may be misleading when measuring thermally induced transitions.

M-Pos170 THE ROLE OF TROPONIN-T RESIDUES 1-70 IN THE INDUCTION OF POLYMERIZATION OF TROPOMYOSIN. J.R. Pearlstone and L.B. Smillie, MRC of Canada Group in Protein Structure and Function, Department of Biochemistry, University of Alberta, Edmonton, Alberta, T6G 2H7, Canada.

Using the methods of Tn-I Sepharose affinity chromatography, Sephadex G-75 gel filtration chromatography and far ultraviolet circular dichroism measurements, fragments spanning the length of the troponin-T (Tn-T) molecule were used to reinvestigate the binding site of troponin-I (Tn-I) or Tn-T under physiological ionic strength conditions. The binding site of Tn-I was found to span an extensive region at the COOH-terminal end of Tn-T, with fragment T2 (residues 159-259) mimicking the strong binding observed with whole Tn-T. However, no binding was observed between Tn-I and the NH_2-terminal fragments T1 (residues 1-158) and CB3 (residues 1-70) of Tn-T, in contrast to earlier findings carried out in high salt buffers.

Further gel filtration studies using Bio-Gel A were carried out to compare the interaction of Tn-T fragments CB1 (residues 1-151) versus CB2 (residues 71-151) to two fragments derived from α-tropomyosin (α-TM), CY1 (residues 1-189) and CY2 (190-284). As found previously (Pato, M.D. et al. (1981) J.B.C. 256, 602-607), no interaction was observed when CY1 was mixed with CY2, whereas a ternary complex resulted when CB1, CY1 and CY2 were present simultaneously. However, replacement of CB1 with CB2 in the latter mixture showed the presence of a CB2/CY2 binary complex and free CY1, and the lack of a ternary complex CB2/CY1/CY2. It therefore appears that the NH_2-terminal portion of CB1 (residues 1-70 of Tn-T) may be required for binding to the NH_2-terminal region of the adjacent α-TM molecule at the head-to-tail overlap region. Direct evidence for such binding is shown in an abstract by J.-R. Brisson et al. (Supported by MRC of Canada)

M-Pos171 **STRUCTURAL CHARACTERIZATION OF THE Z-BAND PROTEIN 85K AMORPHIN.** J.L. Feldman, P.K. Chowrashi, T.F. Kumosinski*, F.A. Pepe, Department of Anatomy, School of Medicine, University of Pennsylvania, Philadelphia, PA 19104, and *Eastern Regional Research Center, U.S. Department of Agriculture, Philadelphia, PA 19118. (Intr. by P. Wachsberger)

The Z band associated protein 85K amorphin was first isolated and purified by Chowrashi and Pepe (J. Cell Biol. 94:565-574, 1982). It has a subunit weight of 85,000 daltons when reduced by dithioerythritol (DTE) in SDS-PAGE. A second band of 170,000 daltons appears in the absence of DTE indicating the presence of disulfide links between some 85,000 dalton subunits. The weight ratio of dimers to monomers is 2:1 on coomassie blue G-250 stained gels scanned with a spectrophotometer at 650nm. In sulfhydryl determinations using DTNB, each native 85K subunit chain has one sulfhydryl group available for reaction. After SDS denaturation, six sulfhydryls are available per chain. Native 85K amorphin exists in an equilibrium between two forms: trimer and hexamer. In spectrophotometric scans of native gradient gels at varying pH, hexamers are favored under neutral conditions and trimers with increasing alkalinity. An average molecular weight of 350,000 daltons, a $S_{20,w}$ of 12.6S, and Stokes radius of 6 nm were measured by analytical ultracentrifugation in 0.1 M KCl, 0.1 M Phosphate, pH 7.9. Electron microscopic examination of negatively stained, linear and rotary shadowed molecules reveals flattened discs 15 nm in diameter and 7.5 nm thick. Discs appear singly and, less frequently in pairs juxtaposed on their flat surfaces. Stacks of these paired discs and side by side aggregates of stacks also have been observed. Highly ordered crystals of 85K amorphin can be grown under low ionic strength conditions and protein concentrations greater than 1 mg/ml. (Supported by NIH grants: HL15835 to the Pennsylvania Muscle Institute and T32-HD07152).

M-Pos172 KINETICS OF CALCIUM DISSOCIATION FROM CALMODULIN BY QUIN-2. Marcia A. Tudor and Howard D. White, Department of Biochemistry, University of Arizona, Tucson, AZ 85721.

The fluorescent calcium indicator, QUIN-2 (Tsien, Biochemistry 19, 2396 (1980)) has been used to measure the kinetics of calcium dissociation from calmodulin. The increase in QUIN-2 fluorescence observed upon mixing with bovine calmodulin in a stopped flow florimeter is biphasic. An initial rapid increase, which has an amplitude corresponding to 1-2 calcium per calmodulin occurs within the mixing time of the stopped-flow and therefore has a rate constant >500 s^{-1}. The rate constant of the second slower phase of the reaction is 7 s^{-1} and has an amplitude corresponding to 2 calcium per calmodulin. The rate constant of calcium dissociation from the two slowly dissociating sites is identical to that measured for dissociation of calcium from the two high affinity sites ($K_d \sim 10^{-6}$ M) by changes in tyrosine fluorescence. The rapid initial fluorescence increase must therefore be a measure of calcium dissociation from the low affinity sites ($K_d \sim 10^{-5}$ M). A minimal kinetic mechanism obtained for calcium binding to calmodulin obtained from this data and previous results obtained in this laboratory (H. D. White et al. Biophys. J. 37, 51a (1982) is:

$$\text{CAM} \underset{\geq 100\ s^{-1}}{\overset{10^7\ M^{-1}s^{-1}}{\rightleftarrows}} \text{CAM-Ca} \underset{7\ s^{-1}}{\overset{\geq 10^8\ M^{-1}s^{-1}}{\rightleftarrows}} \text{CAM-Ca}_2 \underset{\geq 500\ s^{-1}}{\overset{\geq 10^8\ M^{-1}s^{-1}}{\rightleftarrows}} \text{CAM-Ca}_3 \underset{\geq 500\ s^{-1}}{\overset{\geq 10^8\ M^{-1}s^{-1}}{\rightleftarrows}} \text{CAM-Ca}_4$$

Experimental conditions: I = .12, pH 7-9, 20°C. This work has been sponsored by grants from the Muscular Dystrophy Association, AM 25113, and the Arizona Heart Association.

M-Pos173 PROPERTIES OF HIGH-CA^{2+} AND LOW-CA^{2+} FORMS OF THE CA^{2+}-DEPENDENT PROTEINASE FROM BOVINE SKELETAL MUSCLE. Tim Edmunds, William C. Kleese, and Darrel E. Goll, Muscle Biology Group, Univ. of Arizona, Tucson, AZ 85721.

High-Ca^{2+} and low-Ca^{2+} CAF from bovine skeletal muscle autolyze rapidly in the presence of Ca^{2+}, so four forms of CAF can be distinguished: 1) high-Ca^{2+} CAF, which has 80K and 28K polypeptides and requires 10 mM Ca^{2+} for half-maximal activity ($K_{0.5}$); 2) autolyzed high-Ca^{2+} CAF, which has 78K and 18K polypeptides and $K_{0.5}$ = 0.2-0.3 mM Ca^{2+}; 3) low-Ca^{2+} CAF, which has 80K and 28K polypeptides and $K_{0.5}$ = 5 μM Ca^{2+}; and 4) autolyzed low-Ca^{2+} CAF, which has 76K and 18K polypeptides and $K_{0.5}$ = 0.5 μM Ca^{2+} [Nagainis et al., Federation Proc. 42, 1780 (1983)]. Fluorescently labeled monoclonal antibodies show that low-Ca^{2+} CAF is localized at the Z-disk, just as high-Ca^{2+} CAF is. Gradient-pore PAGE indicates that low-Ca^{2+} CAF has a Stokes' radius approximately 0.2 nm larger than high-Ca^{2+} CAF. Mg^{2+} (0.1 μM-15 μM) has no effect on activity of any of the four forms of CAF, whether added singly or in the presence of sufficient Ca^{2+} to produce half-maximal activity. Mn^{2+} alone activates all four forms of CAF; concentrations required for half-maximal activation are approximately: 1) high-Ca^{2+}, 3 mM; 2) autolyzed high-Ca^{2+}, 1-2 mM; 3) low-Ca^{2+}, 0.5-0.8 mM; and 4) autolyzed low-Ca^{2+}, 0.5-0.8 mM. Mn^{2+} activates high-Ca^{2+} and autolyzed high-Ca^{2+} CAF's in the presence of enough Ca^{2+} to cause half-maximal activation, but has no effect on low-Ca^{2+} or autolyzed low-Ca^{2+} CAF's under similar conditions. The physiological significance of the autolyzed forms of CAF is unclear. Both low-Ca^{2+} and high-Ca^{2+} CAF autolyze rapidly in the presence of substrate, so activities measured in vitro are largely those of the autolyzed proteinase. (Supported by NIH Grants AM-19864 and HL-20894 and NSF Grant PCM-8118177.)

M-Pos174 Allosteric Interactions Among the Drug Binding Sites of Calcium Binding Proteins. J. David Johnson, Physiological Chemistry, The Ohio State University College of Medicine, Columbus, Ohio 43210.

The dihydropyridine calcium antagonist (Ca-ANTs) felodipine (Fel) binds to calmodulin (CDR) in a calcium (Ca) dependent fashion and undergoes a fluorescence increase which allows us to monitor its binding. Recently, we have shown that other Ca-ANTs and calmodulin antagonist drugs including prenylamine, diltiazem and R24571 can bind to sites distinct from the Fel binding site on CDR and increase its affinity for Fel by an allosteric mechanism (Johnson, J.D. BBRC 112, 787-793, 1983). We find that other Ca binding proteins including skeletal and cardiac troponin C (TnC) exhibit similar (but lower affinity) Ca induced binding sites for these drugs which are also allosterically related. Drug binding to some proteins was capable of dramatically enhancing their Ca affinity. For example, R24571 binding to CDR increased its affinity for Ca $\sim$ 40 fold at some of its Ca binding sites.

Conclusions: Ca binding to many Ca binding proteins exposes hydrophobic drug and/or protein binding sites which are allosterically related. Drug and protein binding to some of these Ca dependent sites can often dramatically increase their affinity for calcium. These studies are discussed in terms of possible mechanisms of action of calmodulin and Ca binding proteins. Supported by The Muscular Dystrophy Association of America.

M-Pos175 FACILITATED CALCIUM DIFFUSION BY THE SOLUBLE CALCIUM-BINDING PROTEIN, PARVALBUMIN. Joseph J. Feher, Dept. of Physiology and Biophysics, Med. College of Virginia, Richmond, VA 23298.

The calcium flux through an aqueous compartment was determined using a flow-through dialysis cell in which two dialysis membranes isolated the aqueous compartment. Convection in the aqueous compartment was eliminated by gelling with 1% agar. The calcium concentration was at near physiological levels (1 μM). Plots of the inverse of the flux against diffusion distance were linear with a slope equal to the inverse of the apparent diffusion coefficient. In the absence of parvalbumin, the self-diffusion coefficient was 0.81×10^{-5} $cm^2 sec^{-1}$. When parvalbumin was added to the aqueous compartment, the apparent diffusion coefficient increased linearly with the parvalbumin concentration. At the highest parvalbumin concentration investigated, 23 μM, the diffusion coefficient was increased to 3.5×10^{-5} $cm^2 sec^{-1}$. These observations are consistent with the notion that the overall unidirectional calcium flux is the sum of free calcium diffusion and protein-calcium diffusion:

$$J = D[Ca] + D'[CaPr]$$

where D' is the diffusion coefficient of the calcium binding protein, D is the self-diffusion coefficient for calcium, [Ca] is the free calcium concentration, and [CaPr] is the concentration of calcium bound to the calcium-binding protein. The results suggest that enhanced diffusion by the binding protein occurs by translational diffusion of the laden protein and not by a "bucket brigade" mechanism.

M-Pos176 PROPERTIES OF A PROTEIN THAT IS PURIFIED FROM BOVINE SKELETAL MUSCLE AND THAT INHIBITS THE CA^{2+}-DEPENDENT PROTEINASE. John D. Shannon and D. E. Goll, Muscle Group, Univ. of Arizona, Tucson AZ 85721

A protein that inhibits the Ca^{2+}-dependent proteinase, CAF, has been purified from bovine skeletal muscle by using an improved procedure that does not involve heating or denaturing solvents. Purification involves successive chromatographic steps on DEAE-cellulose, phenyl-Sepharose, Ultrogel 34, and DEAE-cellulose columns and requires 7 to 8 days for completion. Four to eight mg of purified inhibitor are obtained from 10 kg bovine skeletal muscle; yields are 30 to 60% of original inhibitor activity and specific inhibitor activity is increased 10,000 to 25,000-fold during purification. Purified inhibitor has a M_r of 125,000 on SDS-polyacrylamide gels, has no detectable carbohydrate, either by direct assay (< 2%) or as estimated on SDS-polyacrylamide gels by using basic Fuschin (< 0.5%), has a Stokes' radius of 6.4 nm, and has very little or no α-helix as estimated by circular dichroism spectra. Antibodies to the purified inhibitor bind to the Z-disk of purified bovine skeletal muscle myofibrils. Purified inhibitor inhibits high-Ca^{2+} CAF, autolyzed high-Ca^{2+} CAF, low-Ca^{2+} CAF, and autolyzed low-Ca^{2+} CAF from bovine skeletal muscle [Nagainis et al., Federation Proc. 42, 1780 (1983)]. One 125 K-dalton inhibitor polypeptide inhibits approximately 6 to 7 high-Ca^{2+} or low-Ca^{2+} CAF molecules but has no effect on trypsin, chymotrypsin, or papain. When CAF is present in excess above that which can be inhibited, the inhibitor polypeptide is degraded by the excess CAF. (Supported by NIH Grants AM-19864, HL-20894, and NSF Grant PCM-8118177).

M-Pos177 THERMODYNAMICS OF THE DAUNOMYCIN-DNA INTERACTION. J. B. Chaires, Department of Biochemistry, The University of Mississippi Medical Center, Jackson, MS 39216

The binding of the anthracycline antibiotic daunomycin to calf-thymus DNA was studied as a function of NaCl concentration and temperature. Van't Hoff plots were used to obtain the enthalpy and entropy of the binding reaction over a NaCl concentration range of 0.1 M to 1.0 M. Observed values for the enthalpy are large and negative, ranging from a value of -16.0 kcal/mole at 0.1 M NaCl to -9.4 kcal/mole at 0.76 M NaCl. The variance of the enthalpy with ionic strength is well beyond the changes anticipated from the predictions of contemporary polyelectrolyte theory. Values of the enthalpy are compensated by changes in the entorpy to produce relatively small changes in the Gibbs free energy over the salt concentrations studied. Such "enthalpy-entropy compensation" may be plausibly explained by a model in which the binding of the drug molecules is coupled to a conformational change in the nucleic acid. Supported by NIH BRSG grant number 55Ø7 RRØ5386.

M-Pos178 ATTRACTIVE LONG-RANGE HYDRATION FORCES CAN CAUSE MACROMOLECULAR ASSEMBLY: the Condensation of DNA by "Cross-linking" Agents. D. C. Rau, NIADDKD, LCP, and V. A. Parsegian, DCRT/PSL, NIH, Bethesda, MD 20205

Extensive measurements on bilayer systems (e.g., Rand 1981. Annu. Revs. Biophys. 10:277), DNA double helices (Rau et al. 1984. PNAS, in press), and coated mica surfaces (e.g., Pashley. 1981. J. Coll. Inter. Sci. 80:153) demonstrate the ubiquity of exponentially varying 3-Angstrom decay constant, repulsive hydration forces between surfaces covered by water soluble groups. We now report strong evidence for the action of attractive hydration forces causing the assembly of DNA double helices into ordered arrays. The thermal properties of this attractive force are such that it could easily have been mistaken for "hydrophobic bonding" between nonpolar surfaces rather than the long-range non-coulombic attraction between polar groups which seems to be the case for DNA.

DNA "cross-linking" agents, cobalt hexamine, spermine, spermidine, chromium, etc., bring the molecules only to a finite, 8-10 Å, separation. Molecules pushed further together by osmotic stress display an exponential, 1.6 Å decay constant, repulsion -- qualitatively and critically different from the usual 3 Å constant for hydration repulsion and from the expectations of 10 Å or more for the constant ion electrostatic repulsion. It fits precisely within the Landau-type formalism of Marcelja and coworkers (e.g., 1976. Chem. Phys. Letts. 42:129) when one recognizes that binding ligands rearrange surface bound water to create regions of hydration attraction (water bridging) between helices.

Should those properties seen in DNA assembly also occur in other systems, then macromolecular assembly and stability, in general, must be recognized as a process of controlled hydration rather than as a competition between hydrophobic and electrostatic effects.

M-Pos179 BASE PAIR SPECIFICITY IN THE INTERACTION OF NAPHTHALENE DIIMIDES WITH DNA. Robert L. Jones, Shau-Fong Yen, and W. David Wilson, Dept. of Chemistry, Georgia State University, Atlanta, GA 30303.

Base pair specific effects in the binding of naphthalene diimides to DNA and polydeoxynucleotides have been investigated using spectroscopic binding measurements as well as ^{31}P and ^{1}H NMR at different field strengths. Areas investigated include base pair specificity in cooperative interactions, in DNA dynamics, and in the local conformational changes induced in the DNA double helix by intercalators. For comparison with the diimide a range of standard intercalators which have quite different base pair specific effects have been used. Because a bulky (relative to an intercalating ring) cationic substituent must slide between base pairs during intercalation, the dissociation of diimides from DNA results in slow exchange on the NMR time scale. In both ^{31}P and ^{1}H NMR, peaks for intercalated and free sites can be separately identified. With ethidium, which has a much larger exchange rate, ^{31}P spectra show a single peak. Ethidium ^{31}P NMR spectra with polydeoxynucleotides exhibit large downfield shifts for alternating and non-alternating base pairs even though the binding constants for these sequences vary considerably. Proton spectra of ethidium-DNA complexes can, however, exhibit slow exchange at high field and low temperature. The imino proton spectra of DNA (10-14 PPM) in the presence of diimides exhibit quite unusual temperature effects at different binding ratios. At ratios near saturation of binding sites and 30°C, peaks for bound and free sites can be identified. In the 30 to 50°C range, A·T sites apparently go into fast exchange with diimides while G·C sites remain in slow exchange with the diimide. As the temperature is increased above 50°C, the A·T peak broadens and disappears while the G·C peak remains. With ethidium the exchange rate at A·T and G·C base pairs is much more similar. Naphthalene diimides have higher binding constants to G·C than A·T base pairs while monoimides have similar binding constants for A·T and G·C base pairs.

M-Pos180 THE ENERGETIC CONTRIBUTION OF THE 2-AMINO GROUP IN ADENINE IN THE BASE-PAIRING INTERACTION WITH URIDYLIC ACID. Philip D. Ross and Frank B. Howard (Lab. of Molecular Biology, NIADDK, NIH, Bethesda, MD 20205).

The thermodynamics of melting to single strands of helical duplexes formed between poly(U) and homopolymers of poly(A), poly($2NH_2A$) and several random poly($2NH_2A$,A) copolymers have been studied by differential scanning calorimetry. In 80 mM NaCl, pH 8, the melting temperature, T_m, increases from 55.7°C for poly(A)·poly(U) to 89.2°C for poly($2NH_2A$)·poly(U). The plot of T_m vs. mole fraction of $2NH_2A$ is curved downward in agreement with the earlier report by Muraoka et al. (1980, Biochemistry 19, 2429-2439). The enthalpies of transition, ΔH, are 8.4 kcal/2P for poly(A)·poly(U) and 14.7 kcal/2P for poly($2NH_2A$)·poly(U). The large difference in the values of ΔH for these two homopolymer complexes reflects the profound contribution of the 2-amino group to the energetics of base pairing. Bold extrapolation of thermodynamic data for the poly(A)·poly(U) system to 90°C shows that the $2NH_2A$·U base pair is about 4.5 kcal/2P more stable in ΔH at this temperature where there is little or no self-structure of the single strands of either poly(A) or poly($2NH_2A$). The values of the ΔH of melting of the poly($2NH_2A$,A) copolymer complexes with poly(U) increase linearly with $2NH_2A$ content in contrast to the curvilinear behavior found for T_m. The entropies of melting calculated from $\Delta S = \Delta H/T_m$ are also linear in copolymer composition. Thus, if one were to begin with a system in which both ΔH and ΔS are linear in copolymer composition a curvilinear plot for T_m vs. composition will naturally result.

M-Pos181 DNA REPLICATION IN SYNCHRONIZED CHO CELLS: DISTRIBUTION BETWEEN REPETITIVE AND NONREPETITIVE SEQUENCES IN EARLY, MIDDLE AND LATE S PHASE. Leo J. Grady, Center for Laboratories and Research, New York State Department of Health, Albany, N.Y. 12201

Suspension cultures of Chinese hamster ovary (CHO) cells were synchronized by isoleucine deprivation for 36 hr, followed by a 10 hr exposure to hydroxyurea (HU). This procedure arrests the cells in the very earliest stage of S when no more than 4% of the DNA has been replicated. Upon release from the HU block, the cells were labeled with 5-bromodeoxyuridine (BUdR) during either the early (1.0-2.0 hr), middle (2.5-4.0 hr), or late (4.5-6.0 hr) portions of two successive S phases. The DNA replicated during the same interval in the first and second S phases contained BUdR in both strands and was isolated by two cycles of centrifugation in CsCl gradients. Next, DNA representing each interval was radiolabeled in vitro by nick-translation using ^{3}H-dCTP and sheared by sonication to give an average piece size of 300 nucleotides as measured by gel electrophoresis. The distribution between repetitive and nonrepetitive sequences of the DNA replicated during the different portions of S phase was then determined by reassociation kinetic measurements with the labeled DNAs. Reactions were run in the presence of 1.0 M NaCl and 45% dextran sulfate; these conditions give reaction rates approximately 1000-fold greater than those which occur in 0.12 M phosphate buffer (R. Wieder and J. Wetmur, Biopolymers 20, 1537 (1981)). Under these circumstances, complete reassociation curves could be obtained with very small amounts of DNA. The results show that nonrepetitive sequences comprise about 85%, 73%, and 45% of the DNA being replicated in early, middle and late S phase, respectively.

M-Pos182 INTERFERON INDUCTION IN VITRO BY POLYNUCLEOTIDES. James M. Jamison, Peter H. Koo, and Chun-che Tsai, Department of Chemistry, Kent State University, Kent, Ohio 44242 and Department of Microbiology/Immunology, Northeastern Ohio Universities College of Medicine, Roostown, Ohio 44272

A systematic study of the interferon (IFN) inducing capacity of poly r(A-U) was performed using the 50% cytopathic effect endpoint in a human foreskin fibroblast-vesicular stomatitis virus (HFS-VSV) assay system as a measure of IFN induction. Interferon activity was based on the activity of NIH human fibroblast interferon reference standard and poly (rI)·poly (rC) reference standard. Poly r(A-U) was co-incubated with the HFS cells for 1, 2, 3, 4 or 5 hour(s) at 37°C in phosphate buffered saline (PBS) containing 1 mM $MgCl_2$. Subsequently, the HFS cells were incubated at 37°C in minimal Eagle's medium for 17 hours and were then exposed to VSV for 48 hours. The results of these studies indicate that 3 hour co-incubation of poly r(A-U) with HFS cells produced optimal IFN titers characteristic of superinduction. The role of the Mg^{2+} ion in modulating the IFN inducing ability of poly r(A-U) was examined by experiments in which the poly r(A-U) concentration was fixed while varying the $MgCl_2$ concentration to produce variable Mg^{2+} ion/poly r(A-U) ratios or both the $MgCl_2$ and the poly r(A-U) concentrations were adjusted to maintain a constant Mg^{2+} ion/poly r(A-U) ratio. The effects of the addition of 1 mM EDTA or the removal of 1 mM $MgCl_2$ in PBS were also examined. In our recent studies, the Mg^{2+} ion was replaced by ethidium bromide (EB) which was added to a fixed concentration of poly r(A-U) in a series of EB/polyr(A-U) ratios ranging from 1:20 to 4:1. An adjuvant effect on the IFN inducing ability of poly r(A-U) was observed when the EB/poly r(A-U) ratio exceeded 0.25. (Supported by NIH Grant GM 31257)

M-Pos183 VARIANT FORMS OF CLOSED CIRCULAR DNA. K. Multhukrishnan and D.L. Vizard. Dept. of Physics, The University of Texas System Cancer Center, M.D. Anderson Hospital and The Graduate School of Biomedical Sciences, Houston, Texas 77030.

Covalently closed circular DNA (cccDNA) exhibits numerous forms that can be resolved by gel electrophoresis; the froms include types I, II, III, concatenates and topoisomers, depending on how the DNA has been treated. Other forms have been observed and have been attributed to reassociation products of circular, single-stranded DNA. We have observed additional, electrophoretically discrete froms that can be produced from type I cccDNA (plasmid) by partial denaturation or irradiation. The production of the variant forms depends on the DNA sequence inserted into the plasmid (pBR322). The relative mobility of the variants is critically dependent upon the temperature at which electrophoresis is performed. The mechanism of variant production appears to be an equilibrium process with a high activation energy. We suspect that the conversion to these variant forms is associated with alternate DNA conformations.

M-Pos184 ALTERNATE CONFORMATIONS IN RIBOSOMAL RNA FROM E. COLI STUDIED BY ELECTRON MICROSCOPY. B. K. Klein and D. Schlessinger. Division of Biology and Biomedical Sciences, Washington University School of Medicine, St. Louis, MO 63110

Long range secondary structure interactions in rRNA from E. coli can be studied using partial denaturation mapping. In these experiments rRNA is prepared for electron microscopy using a hyperphase containing 50% formamide, 10 mM Tris (pH 8.0), and varying concentrations of monovalent and divalent ions. By varying the ion concentrations the amount of structure in the molecules can be adjusted. The loop patterns of many molecules can then be analyzed in detail. Using these techniques we have mapped the positions and sizes of the most stable loops in 16S and 23S rRNA from E. coli. At moderate Mg^{2+} concentrations (0.5 to 2.0 mM) the consensus loop patterns fall into discrete loop location domains of approximately 500 nucleotides along the contour of the molecule. These results agree with the models for unique secondary structure predicted on the basis of phylogenetic comparison. However, a different set of structural features are observed if the rRNA molecules are subject to more denaturing conditions either before or during preparation for electron microscopy. These new features are not consistent with the domain structure seen in the presence of moderate Mg^{2+} concentrations and most are long range loops which cross the individual domain boundaries of current models. The relation and interconversion of these conformers of rRNA are currently being investigated in detail.

M-Pos185 UNUSUAL PROPERTIES OF A LONG INTERSPERSED REPEATED SEQUENCE OF MOUSE DNA. D. L. Vizard and J. Yarsa, Dept. of Physics, The University of Texas System Cancer Center, M. D. Anderson Hospital and Tumor Institute and The Graduate School of Biomedical Sciences, Houston, Texas 77030.

A long interspersed repeated DNA sequence of the mouse genome (called MIF-1) is segmentally heterogeneous; i.e., it contains conserved and non-conserved regions of nucleotide sequence. The length of the repeat seems to be one of its most conserved properties, which suggests that this DNA sequence may serve a structural function in mouse genomic organization. In support of this concept, the nucleotide sequence of a region of MIF-1 is non-coding and contains "structured" sequences possessing numerous symmetries. Cloned sequences of the same region of MIF-1 disagree with the consensus sequence of the corresponding genomic fragment, indicating that the procaryote "processes" the mouse DNA in selected regions of the nucleotide sequence. Consequently, the MIF-1 repeated DNA, although segmentally heterogeneous, may be far more homogeneous than clone-sequencing studies imply.

M-Pos186 CONSECUTIVE CONFORMATIONAL TRANSITIONS OF POLY(dAdT)·POLY(dAdT) INDUCED BY COBALT(III) COMPLEX. Y. A. Shin, S. Feroli, and G. L. Eichhorn. National Institutes of Health, National Institute on Aging, Gerontology Research Center, Baltimore, MD 21224.

We have previously reported (Eichhorn et al., Cold Spring Harbor Symp. Quant. Biol. (1983) 47, 125) that the treatment of poly(dGdC)·poly(dGdC) with $[Co(NH_3)_6]Cl_3$ can lead to several consecutive conformational transitions, in which the B-form is first converted to Z, which in turn is converted into an "A" like form that eventually yields a $\psi(+)$ structure, i.e., B → Z → "A" → $\psi(+)$. We now observe that the $[Co(NH_3)_6]Cl_3$ reagent also induces a series of conformational changes in poly(dAdT)·poly(dAdT). The B-form is first transformed into a conformer with reduced ellipticity in the 270 nm region; this first intermediate is then transformed into an "A" like conformer, with CD maximum ∿ 280 nm. At high polymer concentration the "A" like structure is converted to $\psi(+)$. At low polymer concentration it is converted into a conformer with a negative CD with minimum ∿ 280 nm, a CD similar to that obtained by Vorlíšková et al. [Nucleic Acids Research (1982) 10, 6968] by treatment of poly(dAdT)·poly(dAdT) with CsCl. Still higher Co(III) concentration at low polymer concentration leads to $\psi(-)$. Thus, if we assume that the conformer with a CD minimum ∿ 280 nm is the same as that of Vorišková et al., at high concentration B → first intermediate → "A" → $\psi(+)$, and at low concentration B → first intermediate → "A" → "X" → $\psi(-)$. The regions of stability of these conformational states (all of which, except B, are aggregates) is thus highly dependent upon polymer concentration. The "A" type and $\psi(+)$ structures are stabilized at high concentration, whereas "X" and $\psi(-)$ are stabilized at low concentration. There appears to be some correlation between the tendency to form an "A" like structure and $\psi(+)$, on the one hand, and "X" and $\psi(-)$, on the other.

M-Pos187 THERMODYNAMICS OF DNA BASE STACKING. Luis A. Marky, Beth Buono, and Kenneth J. Breslauer, Department of Chemistry, Rutgers University, New Brunswick, NJ 08903. Ronald Frank, Helmut Blocker, Gesellschaft fur Biotechnologische Forschung mbH, Abteilung, DNA-Synthese, D-3300 Braunschweig-Stockheim, West Germany.

We have characterized the helix-to-coil transition of 14 self-complementary deoxyoligonucleotides using differential scanning calorimetry (D.S.C.) and temperature-dependent ultraviolet absorption spectrometry. The specific sequences studied all form double helices with terminal GC base pairs and between 0 and 50% AT base pairs. The melting temperature data (t_m's) of these oligomers allowed us to define the role of base sequence on duplex stability. Comparison of the model-dependent optical data and the model-independent calorimetric data allowed us to assess the applicability of the two-state model to each thermally-induced transition. We used the calorimetric and spectroscopic data for all oligomers that melt in a two-state manner to calculate thermodynamic profiles ($\Delta G°$, $\Delta H°$, $\Delta S°$) for each of the following six average base stacking interactions: GG/CC, AA/TT, (AT/TA, TA/AT), (CT/GA, TC/AG), (AC/TG, CA/GT), (GC/CG, CG/GC). The oligomer results will be presented and compared with those of parallel studies on synthetic polydeoxynucleotides. This work was supported by NIH GM23509.

M-Pos188 CONFORMATION OF 2',5' POLYNUCLEOTIDES: THEORETICAL COMPUTATIONS OF ENERGY, HELICAL AND BASE-STACKING PARAMETERS. A. R. Srinivasan and W. K. Olson, Chemistry Department, Rutgers, The State University, New Brunswick, New Jersey 08903.

A detailed theoretical analysis has been carried out to probe the conformational characteristics of 2',5' polynucleotide chains. The present approach includes semi-empirical energy estimates and computations of helical and base-stacking parameters over a wide range of conformational combinations. Torsional variables include the pentose pseudorotation, the backbone torsions ω"(O2'-P), ω(P-O5'), and ψ(C5'-C4'), and the glycosyl torsion χ(C1'-N9). Limited rotations around ϕ"(C2'-O2') are also considered. Computed base-stacking data indicate an abundance of intercalation structures and a limited number of base-stacked conformations. This is primarily due to the extended nature of the 2',5' nucleotide repeating unit. Current results also reveal a possibility of forming stacked single stranded 2',5' polynucleotide helices. Studies of base-paired double-stranded 2',5' structures are also in progress. (Supported by USPHS Grant GM-20861).

M-Pos189 DEPENDENCE OF THE 8C-H EXCHANGE RATE OF PURINES ON NUCLEIC ACID STRUCTURE. J.M. Benevides and G.J. Thomas, Jr., Department of Chemistry, Southeastern Massachusetts University, N. Dartmouth, MA 02747.

Raman spectroscopy provides a convenient means of measuring the rate of deuterium exchange of purinic 8C-H groups in D_2O solutions of polynucleotides. We have measured 8C-H exchange rates in a variety of polynucleotide structures, including single and multi-stranded helices. In poly(dG-dC)·poly(dG-dC), the deuterium exchange rate (measured as the pseudo-first-order exchange rate constant, k_ψ, at 50°C) exhibits values of 0.00782 and 0.0114 h^{-1} for B (low-salt) and Z (high-salt) structures, respectively. The 50% faster exchange of guanine in the Z-DNA structure is attributed to substantially greater exposure of the base along the helix exterior to solvent D_2O molecules, when compared with the relative inaccessibility of 8C in the minor groove of B-DNA. On the other hand, both B and Z helices generally exhibit more rapid 8-CH exchange than A helices. Among different polynucleotide structures within a given helix family, great variability can occur for the rate of 8C-H exchange. For example, the four-stranded helix of poly(rI) exhibits a sevenfold lower rate constant (0.00116 h^{-1}) than single-stranded poly(rI), though both structures contain presumably only C3'-endo-anti conformers of inosine. We find that retardation of k_ψ for $[poly(rI)]_4$ corresponds linearly to the percentage of quadruplex formation.

Supported by N.I.H. Grant AI 18758.

M-Pos190 DIRECT TEM VISUALIZATION OF DNA WRITHE, COMPLEX 3-D SUBSTRUCTURE AND DISK-LIKE SHAPE OF FREEZE ETCHED REPLICATED HYDRATED DNA TORUSES. K.A. Marx, G.C. Ruben (Intr. by M. Lubin) Dartmouth College, Dept. of Chem. & Dept. of Path., Dartmouth Medical School, Hanover, NH 03755.

The in vitro polyamine-condensed DNA torus represents a model system for bacteriophage and viral DNA organization. High-magnification TEM of low Pt/C metal deposition (9 Å thick at 45° angle) deep etched replicas of hydrated 1mM spermidine-condensed ØX-174 linear and circular DNA toruses clearly exhibit circumferential wrapping of single DNA double helix size surface fibres. This mode of torus organization is consistent with a continuous circumferential DNA wrapping model (Marx and Reynolds (1982) PNAS, USA 79, 6484-6488). Two dimensional analyses of inner and outer torus circumference and horizontal annulus thickness also support the circumferential model and allow identification of monomolecular collapsed toruses which appear to be organized into disk shaped structures by a minimum hexagonal packing of DNA. To understand the 3-D microscopic details of DNA writhe we have analyzed high-magnification stereomicrographs of a few DNA toruses. Using a mirror stereoscope with "floating" mark stereometer we have mapped relative 3-D heights of surface DNA double helices. While largely circumferential these DNA surface strands reveal an irregular path that suggests a less than crystalline hexagonal DNA packing. Extensive tilting of the objects along the metal shadow direction axis is advantageous since more direct and more precise information is available on DNA writhe from widely separated tilts (50-90°) in a micrograph series where each picture is separated by 10° of tilt. When the edge of the torus plane is at an angle less than 75° to the shadow direction, the torus view tilted end-on can directly reveal the vertical annulus thickness corroborating the less direct stereographic measurements of torus thickness and disk-like torus shape. Res. Corp. 8859, NIH GM 25886, NIH AI17586, BRSG RR-05392 & NCCC CA23108 NCI.

M-Pos191 STRAIN-INDUCED NONLINEAR EXCITATION AND B-Z TRANSITION IN DNA. A. Sarai, S. Miyazawa and R.L. Jernigan. Laboratory of Mathematical Biology, DCBD, NCI, NIH, Bethesda, MD 20205.

Transitions between B and Z forms in DNA can be represented with a bistable energy function dependent on the twisting coordinate. Such a bistable system is expected to undergo a nonlinear structural transition upon twisting. Here we study the strain-induced transition in a circular DNA. DNA is regarded as a linear chain of units with a double-well potential along the twisting coordinate, together with a harmonic potential for nearest-neighbor interaction. We restrict the chain so as to conserve the total helical turns. The minimization of total energy leads to a set of nonlinear balance equations, which can be solved numerically. Suppose a circular chain is twisted from its intial B form. The chain will be deformed uniformly, but when the twist exceeds a certain value a nonlinear solution appears, forming a Z region with two B-Z junctions. We have examined the B-Z transition behavior as a function of twist, together with effects of an asymmetric potential and sequence inhomogeneities. We analysed available experimental results, in which various lengths of alternating G-C sequence were inserted into a plasmid and conversions to Z DNA were observed upon changing linking number. This was performed with a mechanistic model to estimate the magnitude of model parameters. From this analysis, if the length of the insert is less than a certain value, the entire insert converts to Z form at a critical linking number. The critical linking number increases as the length of insert increases, consistent with experimental observation, but decreases if the insertion exceeds certain length. If the insertion is much longer, the B-Z transition exhibits a different behavior, in which part of the insert flips to Z form and the Z part expands linearly upon changing linking number. We have also made a statistical mechanical treatment of the B-Z transition and compared it with the mechanistic analysis.

M-Pos192 DIFFERENCES IN THE CIRCULAR DICHROISM AND THERMAL MELTING OF TWO 147 BASE PAIR RESTRICTION FRAGMENTS OF pBR322. Nancy C. Stellwagen, Anne Stellwagen, and John Stellwagen, Dept. of Biochemistry, University of Iowa, Iowa City, Iowa 52242.

The circular dichroism and thermal melting of two 147 base pair DNA fragments generated by the restriction enzyme MspI from the plasmid pBR322 have been studied. In solutions with salt concentrations ranging from 10 mM Tris buffer to 0.5 M NaCl, the fragment with the higher G-C content, 12B, melts at temperatures 3.0°C higher than the other fragment, 12A. The difference in their melting temperatures predicted from their differing A-T contents is 3.7°. In 1 mM Tris buffer, the melting temperatures of the two fragments are nearly equal. At still lower Tris buffer concentrations, the melting behavior reverses and fragment 12A becomes more stable than fragment 12B. Fragment 12A also migrates anomalously slowly on polyacrylamide gels and exhibits an apparent permanent dipole moment in an electric birefringence experiment. The circular dichroism of the two fragments, in 1 or 10 mM Tris buffer, is very similar. However, marked differences are observed in the B → A transition induced by ethanol. Fragment 12A exhibits a "pre-melting" phenomenon, accompanied by a decrease in ellipticity. The B → A transition, accompanied by an increase in ellipticity, is very sharp, with a midpoint at 78% ethanol. A biphasic transition is observed for fragment 12B, with the midpoint of the first subtransition at 73% ethanol and that of the second subtransition at 79% ethanol. This biphasic transition may represent the conversion of separate domains of fragment 12B from the B conformation to the A conformation; the ends of this fragment have a higher G-C content than the middle. No time dependent effects are observed in the transition region for either fragment.

M-Pos193 LASER RAMAN STUDIES ON ALTERNATING PURINE PYRIMIDINE POLYMERS: UNUSUAL SUGAR-PHOSPHATE STRUCTURES. Stephen P.A. Fodor, Philip A. Starr, and Thomas G. Spiro, Department of Chemistry, Princeton University, Princeton, N.J. 08544.

In low salt solution, the alternating purine pyrimidine polymer poly (dA-dT)·poly(dA-dT) has been postulated to exist in an alternating B structure where the deoxyribose attached to the adenine residues are in a C3'-endo type configuration, while the deoxyribose rings of thymine residues maintain a C2'-endo pucker. This alternating B structure would explain the ^{31}P NMR splitting found in the solution species of poly(dA-dT)·poly(dA-dT). CsF enhances the ^{31}P NMR splitting, and causes a near CD inversion both in poly(dA-dT)·poly(dA-dT) and poly(dG-dT)·poly(dA-dC). Raman spectra of poly(dA-dT)·poly(dA-dT) and poly(dG-dT)·poly(dA-dC) in high and low salt solutions as a function of temperature are reported. We present convincing evidence that the alternating B structure is the correct form of poly(dA-dT)·poly(dA-dT) in solution, and identify a C3'-endo marker band for the deoxyribose attached to the adenine residues and a C2'-endo Raman marker to the thymine deoxyribose rings. A temperature dependent splitting of phosphate vibrations occurs for poly(dG-dT)·poly(dA-dC) in CsF. Structural implications of this splitting will be addressed.

M-Pos194 EVIDENCE THAT C·C^+ BASE PAIRS CAN COEXIST WITH WATSON-CRICK BASE PAIRS IN AN OLIGONUCLEOTIDE DOUBLE-HELIX. Donald M. Gray, Tao Cui#, and Robert L. Ratliff.* Program in Molecular Biology, The University of Texas at Dallas, Box 830688, Richardson, TX 75083-0688, and *Genetics Group, Life Sciences Division, Los Alamos National Laboratory, Box 1663, Los Alamos NM 78545. #On leave from the University of Science and Technology of China, Hefei, Anhui, The People's Republic of China.

In previous work, it has been shown that hemiprotonated C·C^+ base pairs form in poly[d(C)] at neutral pH (Inman, R.B. (1964) J. Mol. Biol. 9, 624-637) and in the alternating polydeoxynucleotide poly[d(C-T)] at pH 5 (Gray, D.M., Vaughan, M.R., Ratliff, R.L., and Hayes, F.N. (1980) Nucl. Acids Res. 8, 3695-3707). In both of these self-complexes, it seems likely that the base pairs would be formed between parallel strands. In order to test whether C·C^+ base pairs might form between parallel strands, we have studied the CD spectra of a hexadecamer, $C_4T_4A_4C_4$, which we synthesized by the phosphite triester method. A·T base pairs can form between antiparallel strands of this oligomer, but not between parallel strands. The CD spectrum of this oligomer at pH 6 and 7 (0°C, 0.5 M NaCl) shows an enhanced negative band at 250 nm as a result of A·T base pairs. At pH 6, a strong positive CD band simultaneously appears at 285 nm which results from C·C^+ base pairs. Even at pH 7, there is a shift of the positive CD band of the hexadecamer to longer wavelengths, which we interpret as evidence for the formation of C·C^+ base pairs. Base pairs do not form in the oligomers C_4 or C_8 at pH 7. Thus, we conclude that C·C^+ base pairs are formed between antiparallel strands of the hexadecamer, which are joined by Watson-Crick base pairs.

Supported by NIH Research Grant GM19060 and Grant AT-503 from The Robert A. Welch Foundation.

M-Pos195 FLEXIBILITY OF DNA INTERCALATION SITES: V.N. Balàji, J. Scott Dixon, D.H. Smith and R. Venkataraghavan. Lederle Laboratories, Pearl River, N.Y. 10965

Intercalation geometries within a B-DNA helix have been studied by minimization of conformational energy of a DNA tetramer duplex. The variables optimized included the base-base twist, shift, tilt and roll, glycosidic torsional angles, sugar puckerings and main chain torsional parameters. The flexibility of the intercalation sites in the twist-shift plane has been searched systematically. The energy differences between the native B-DNA conformation and different sequence combinations at typical intercalation sites will be outlined. Stereoviews of some of the geometries will be presented. These geometries will be useful in the design of intercalating anticancer drugs.

M-Pos196 ENERGETIC AND STRUCTURAL ASPECTS OF THE INTERCALATION OF THE ANTICANCER DRUGS MITOXANTRONE AND BISANTRENE INTO DNA: V.N. Balaji, J. Scott Dixon, D.H. Smith and R. Venkataraghavan. Lederle Laboratories, Pearl River, New York, 10965.

Structural features of the anticancer drugs mitoxantrone and bisantrene intercalated with DNA were evaluated by computer graphics, electrostatic molecular surface compatibility and energy minimization methods. Mitoxantrone intercalates DNA favorably from both minor and major grooves. The side chain OH or NH groups can hydrogen bond with the main chain phosphate groups of DNA, cross linking the complementary strands. In the minor groove intercalated complex, the side chain OH groups can hydrogen bond with phosphate oxygens of another DNA duplex, thereby agglomerating DNA helices. Bisantrene intercalates DNA from the major groove. The NH group of the imidazole rings can hydrogen bond with the phosphate groups of the complementary strands of DNA. These model features are consistent with physicochemical data and electron microscopic observations.

M-Pos197 A MOLECULAR MECHANICAL MODEL TO PREDICT THE HELIX TWIST ANGLES OF B-DNA. Chang-Shung Tung, Department of Physics, University of Alabama in Birmingham, Birmingham, AL 35294.

We have developed a simple torsional spring model to examine the relation between helix twist angles of B-DNA and its sequence. Because of the homogeneous nature of the sugar-phosphate backbone and the irregular order of the bases for different DNA molecules, the effects of base-base interactions are treated seperately from those of backbone deformations. In the crystal data, a propagation effect was observed (Fratini, A.V. et al, J. Biol. Chem. 257, 14686-14707 (1982); Dickerson, R.E., J. Mol. Biol. 166, 419-441 (1983)), where the deviation of helix twist angle in one basepair step is compensated by a fractional deviation of opposite sign in the neighboring steps. We include this propagation effect and use one torsional spring to mimic each of the three effects above. The spring parameters for different basepair steps are derived from conformational energy calculations, while those for the backbone and propagation are determined by fitting the model to experiment. The model explains the dependence of helix twist angles on sequence and can be modified to examine the effects of base modification on the helix geometry.

M-Pos198 BASE TILT OF POLY d(A)·POLY d(T) AND POLY d(AT)·POLY d(AT) IN SOLUTION DETERMINED BY LINEAR DICHROISM. Stephen P. Edmondson and W. Curtis Johnson, Jr., Department of Biochemistry and Biophysics, Oregon State University, Corvallis, OR 97331.

Linear dichroism (LD) is a sensitive method of determining the orientation of the bases of polynucleotides in solution. The reduced dichroism (LD divided by the isotropic absorption) of polynucleotides containing only adenine-thymine base pairs depends upon five parameters: the fraction of polymer oriented, the tilt axes of both bases, and the tilt of both bases. A dyad axis between the bases reduces the number of unknowns to four for poly d(A)·poly d(T). Further, the fraction of polymer oriented affects only the magnitude of the reduced dichroism. Therefore, the orientation of the bases of simple polynucleotides in solution can be calculated, provided the LD is measured over several transitions. We have measured the flow linear dichroism and isotropic absorption spectra of poly d(A)·poly d(T) and poly d(AT)·poly d(AT) in 0.01 M Na^+ over the wavelength region of 320-180 nm. The conformation of the bases in these polymers was determined from an analysis of their reduced dichroism spectra.

M-Pos199 PREDICTION OF THE SECONDARY AND TERTIARY STRUCTURES FOR VARIOUS FORMS OF ACETYLCHOLINESTERASE BY CIRCULAR DICHROISM. P. Manavalan and W. C. Johnson, Jr., Department of Biochemistry and Biophysics, Oregon State University, Corvallis, OR 97331 and Palmer Taylor, Division of Pharmacology, M-013, Department of Medicine, University of California, San Diego, La Jolla, CA 92903.

Two species of acetylcholinesterase (AchE) from torpedo, the 11S tetramer of subunits derived from the asymmetric species and the 5.6S hydrophobic dimer, are believed to have subtle differences in their secondary as well as their primary structures. Binding studies show that both molecules have an active center and a peripheral anionic site, and two distinct classes of ligands bind at these two sites. To probe further into the structural details of 11S and 5.6S AchE's we have monitored the changes due to ligand binding using vacuum UV circular dichroism (CD). Edrophonium chloride (EC) and propidium iodide (PI) were chosen as substrates for the active and peripheral sites, respectively. The CD spectra show that both 11S and 5.6S AchE contain α-helix and a mixture of parallel and antiparallel β-sheet. The amount of α-helix is almost the same for both molecules, whereas antiparallel β-sheet is about 7% more for the 5.6S than for the 11S AchE form. The association of EC with 11S AchE increases α-helix but decreases the antiparallel β-sheet, whereas PI increases the amount of β-sheet. The same trend is also observed for 5.6S AchE. This opposite structural change due to ligand binding at two different sites, and the evidence of a 20 Å separation between the sites from fluorescence studies suggest that these sites are located in two different domains. Further, the analysis of CD characteristics of these two molecules indicates that the folding pattern of one or more domains of AchE represent the α/β tertiary structural type.

M-Pos200 CIRCULAR DICHROISM AND HYDRODYNAMIC STUDIES ON THE METAL (Zn^{2+} AND Ca^{2+}) INDUCED CONFORMATIONAL CHANGES IN S-100a AND S-100b PROTEINS: R.S. Mani and C.M. Kay, MRC Group in Protein Structure and Function, Department of Biochemistry, University of Alberta, Edmonton, Alberta.

The effect of Zn^{2+} binding on the circular dichroism spectra of brain specific S-100a and S-100b calcium binding proteins has been examined. In the presence of Zn^{2+}, S-100a undergoes a conformational change and the decrease in ellipticity at 222 nm, as a result of Zn^{2+} addition, was nearly 1300 $deg.cm^2.dmol^{-1}$, whereas with S-100b there was no significant conformational change. Ca^{2+} was able to bind to S-100 proteins in the presence of Zn^{2+} and the two metal ion binding sites on the protein appear to be different. In the presence of Zn^{2+}, K^+ had no significant effect on the conformation of S-100 proteins. Ca^{2+} and Zn^{2+} binding induce different environments around the tyrosine residues in S-100a, whereas with S-100b, similar changes were observed for the single tyrosine residue, using either metal. Zn^{2+} has a pronounced effect on the secondary structure and the aromatic environment of S-100a but with S-100b it has only a subtle effect on the microenvironment of the aromatic groups.

Hydrodynamic properties (gel filtration and sedimentation velocity studies) of S-100 proteins in the presence and absence of calcium indicate that S-100 proteins unfold in the presence of Ca^{2+}, in agreement with our earlier spectroscopic studies. Among the monovalent cations tested (K^+, Na^+ and Li^+) K^+ had the maximum effect on the Stokes radius and S values of S-100 proteins. Since certain functions of the nervous system are accompanied by local changes in ionic concentrations of Ca^{2+}, Na^+ and K^+, it is conceivable that these respective conformational changes induced in S-100 proteins by these metals may be related to their function in the brain.
(Supported by MRC, Canada)

M-Pos201 ALKALINE ISOMERIZATION IN UNFOLDED YEAST ISO-2 CYTOCHROME C.
John J. Osterhout and Barry T. Nall

Relative amplitudes of kinetic phases depend upon both initial and final conditions while time constants depend only on final conditions. Under constant final conditions a variation in the relative amplitude of a kinetic phase with changes in the initial conditions indicates a perturbable equilibrium in the initial state. The fluoresence refolding of yeast iso-2 cytochrome c was studied by stopped-flow experiments in which the pH of the protein unfolded in guanidine hydrochloride was varied while the final conditions (pH 7.2, 0.4M guanidine hydrochloride) were held constant. The relative amplitude of the fast phase (α_2) proved to be sensitive to pH in the initial conditions varying from 0.8 at pH 7.2 to less than 0.2 at pH 10.0. These data indicate that the unfolded state of cytochrome c consists of a pH dependant equilibrium between fast and slow folding species.

M-Pos202 DYNAMIC ACCESSIBILITIES OF SURFACE PEPTIDE NH'S IN BPTI.
Erik Tuchsen and Clare Woodward, Dept. of Biochemistry, Univ. of Minnesota, St. Paul, MN 55108

Hydrogen isotope exchange kinetics have been measured for 25 peptide NH protons on the surface of bovine pancreatic trypsin inhibitor (BPTI). These includes all of the BPTI surface NH's except the C- and N-termini. Hydrogen-deuterium exchange rates were determined for assigned resonances in ^{1}H NMR spectra of specifically ^{1}H labeled BPTI. For each NH the hydrogen exchange rate constant observed at the pH of minimum rate, $K_{min,obs}$, was compared to the rate constant at the pH of minimum rate in a random coil peptide, $k_{min,rc}$. It is frequenty assumed that k_{min} for an exposed proton on the protein surface is equal to $k_{min,rc}$. Contrary to this, we find that the $k_{min,obs}$'s are 4-2000 times slower than the $k_{min,rc}$'s. We also find that the relative dynamic accessibilities, which are given by the ratio $k_{min,obs}/k_{min,rc}$, are incompatible with the relative static accessibilities in the crystal structure. For example, a number of peptide NH's, e.g., Gly12, Ala25, Thr32 and Ala48 have k_{min}'s that are 200-2000 times slower than for model compounds, but have 12-65% of their surface exposed. Other NH's, e.g., Ser47, Glu49 and Asp50, have zero solvent accessible surface in the static structure, but exchange faster than the NH's of residues 12, 25, 32, and 48.

M-Pos203 REAL-TIME ENERGY CALCULATIONS, MOLECULAR MODELLING AND COMPUTER GRAPHICS
N. Pattabiraman, M. Levitt*, T.E. Ferrin and R. Langridge+, Computer Graphics Laboratory, Department of Pharmaceutical Chemistry, School of Pharmacy, University of California, San Francisco, CA 94143.

Molecular modelling using real-time interactive three dimensional computer graphics is a powerful method of understanding interactions between molecules. Techniques such as skeletal representations, distance calculations and surfaces may be used. The main focus of all these methods is "steric". However, steric fit is not the only consideration in intermolecular interaction; the electrostatic component due to partial atomic charges must also be taken into account. We have developed a real-time docking method in which the energy of interaction between the drug and the receptor molecules are computed on a DEC VAX 11/750 and displayed on an Evans & Sutherland Picture System 2 in real-time as the drug is moved in the receptor site. In our method, the whole receptor is enclosed in a three-dimensional cartesian grid of a given size. The electrostatic and non-bonded potential energies due to the receptor molecule are stored at the grid points. As the drug molecule is moved inside the receptor pocket, the total energy of interaction is calculated and updated on the screen in real-time using the potentials at the grid points. We can also very rapidly minimise the energy of interactions while docking. Using this real-time docking method it is now possible to analyse very rapidly the interactions of a large number of drugs with the receptor molecule. As an application, the interaction of thyroid hormone and some analogs with prealbumin is discussed.
(Supported by NIH RR-1081)
*On leave from Department of Chemical Physics, Weizmann Institute of Science, Rehovot, Israel.
+Guggenheim Fellow 1983-84. On leave at Department of Computer Science, Stanford University.

M-Pos204 A MODEL OF COLICIN A MEMBRANE CHANNEL PROTEIN STRUCTURE.
H. Robert Guy, Lab of Mathematical Biology, NCI, DCBD, NIH, 20205.

A structural model of the colicin A channel was developed using the general folding scheme described below and that was proposed previously for colicin E1 (Guy, 1983, Biophy. J.,41: 363A). Sequences of these proteins are very weakly homologous (Morlon et al., 1983, J. Mol. Biol. in press). The models are based on an analysis of colicin sequences with a method developed to optimally position α helices at a water-protein, water-lipid, or protein-lipid interface. This method has been used in designing a model of the acetylcholine receptor channel (Guy,1984, Biophy.J., in press). The colicin model structure is a dimer. The channel lining consists of amphipathic transmembrane helices 1 (residues 416 to 433), 2 (439 to 454), 3 (467 to 484), and 4 (489 to 505) that contain 11 positively and 11 negatively charged side chains per monomer. These helices can be positioned so that charged groups form two salt bridges and are exposed to water inside the channel. Very apolar faces of transmembrane helices 5 (439 to 454) and 6 (467 to 505) are in contact with lipid and their slightly more polar faces contact the apolar faces of helices 1, 2, and 3. Segments on the trans side of the membrane that connect helices 1 to 2 and 3 to 4 contain unbalanced positively charged side chains that may contribute to the voltage dependency of channel formation. Segments on the cis side connecting transmembrane helices 2 to 3 and 4 to 5 and following helix 6 may form short amphipathic a helices that have some contact with lipid.

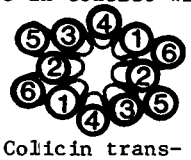

Colicin trans-membrane helices

M-Pos205 A THEORETICAL MODEL FOR PREDICTING THE α-HELIX ALIGNMENT AGAINST β-STRANDS IN PROTEINS, R.S. Bohacek, Department of Chemistry, Rutgers, The State University of New Jersey, New Brunswick, New Jersey 08903

A statistical model to predict the most probable arrangement of an α-helix against a β-strand has been developed. The model consists of the coordinates of an ideal α-helix and β-strand backbone upon which vectors are constructed to represent any desired sequence of amino acid side chain. Different alignments of the α-helix against the β-strand are then simulated by rotating the α-helix against the β-strand. For the various rotations, the side chain-side chain contacts between the α-helix and β-strand are determined. From a set of 33 proteins, frequencies for each type of contact had been previously determined using statistical methods. (Roberts and Bohacek, Int. J. Peptide. Res. 21, 491-512 (1983)). These frequencies are then assigned to the particular side chain-side chain contact predicted by the model for each α-helix β-strand alignment. That orientation of the α-helix against the β-strand which gives the largest sum of frequencies is predicted to be the most probable. The model correctly predicted the position of 9 out of the 10 actual α-helix β-strand cases used to test it.

This model represents an integral part of our efforts to bridge the gap between the predicted secondary structure of a protein and its correct tertiary structure.

M-Pos206 SPATIAL DISTRIBUTION OF SPIN-LABELED COENZYME IN COMPLEXES WITH GLYCERALDEHYDE-3 PHOSPHATE DEHYDROGENASE AS A FUNCTION OF STOICHIOMETRY: NEW INSIGHT INTO THE SEQUENTIAL BINDING MODEL A.H. Beth*,+B.H. Robinson , C.E. Cobb*, J.J. Birktoft[X], W.E. Trommer[†] and J.H. Park*
*Vanderbilt Univ., Nashville, TN 37232, +Univ. of Washington, Seattle, WA 98195, [X]Washington Univ., St. Louis, MO 63110, [†]Univ. Kaiserslautern, F.R.G.

Binding of coenzyme NAD to tetrameric glyceraldehyde-3 phosphate dehydrogenase (GAPDH) exhibits strong negative cooperativity with a substantial decrease in affinity as the four binding sites are progressively saturated. We have synthesized a [^{15}N,^{2}H]-N^{6}-spin-labeled derivative of NAD (SL-NAD) to study the spatial distribution of bound coenzymes in stoichiometric complexes with GAPDH. The SL-NAD exhibited the same negative cooperativity as natural NAD and functioned actively as coenzyme in the enzymatic reaction. At bound stoichiometries of 1:1 (SL-NAD:GAPDH tetramer), the electron paramagnetic resonance (EPR) spectrum was dominated by an immobilized signal from a spatially isolated SL-NAD. As the SL-NAD stoichiometry was increased stepwise to 4:1, there was a progressive increase in a resolved dipolar signal resulting from interactions of pairs of SL-NAD bound to adjacent monomers (R-axis related) but not from the distant monomers across the P,Q plane. Deconvolution of experimental spectra from this titration indicated that subsequent to binding the first SL-NAD, the remaining three coenzymes bound randomly to the adjacent and distant monomers. Molecular modeling from X-ray crystallographic data and computer simulations of the dipolar EPR spectra indicated that the spin-label moieties of R-axis related coenzymes were separated by 12.8A. These data provided new insight into the sequential binding of a cofactor by a multisubunit protein. Supported by NIH GM-07884 and The Chicago Community Trust/Searle Scholars Program.

M-Pos207 ^{13}C-NMR STUDIES OF M13 COAT PROTEIN. Gillian D. Henry, Joel H. Weiner and Brian D. Sykes
Department of Biochemistry, University of Alberta, Edmonton, Alberta, T6G 2H7, Canada.

The major coat protein (gene 8 protein) of the filamentous coliphage M13 is a 50-residue polypeptide chain which spans the inner membrane of *E. coli* during infection. The protein comprises three domains: an acidic N-terminal region, a hydrophobic core, and a basic C-terminal region. Its small size and ease of preparation render it a good model system for the study of the structure and dynamics of an integral membrane protein. ^{13}C-NMR spectroscopy, which offers many advantages to such an investigation, is generally limited by sensitivity problems arising from the low natural abundance of the ^{13}C nucleus. Inclusion of a specifically labelled amino acid in the culture medium, however, yields phage with a coat protein selectively labelled at predetermined sites.

Incorporation of 3-[^{13}C] alanine and 1-[^{13}C] lysine into the phage protein has allowed analysis of protein backbone motions at various points in the molecule. Since the coat protein comprises 20% alanine, which is fairly evenly distributed along the polypeptide chain, this label allows a broad overview of the molecule to be obtained. The N-terminal alanine residue has been identified as a well-resolved downfield methyl signal, by virtue of the pH dependence of its chemical shift. This is a useful environmental probe for reconstituted model membranes. The lysine label, by contrast, is mainly confined to the C-terminal region. Lysine Cl resonances show a marked gradation in chemical shift, linewidth and T_1 values.

Systematic replacement of selected residues with their ^{13}C analogues should ultimately enable us to provide a detailed picture of both backbone and side chain mobility of this protein.

M-Pos208 ^{13}C NMR QUANTITATION OF CIS PEPTIDE BONDS IN THERMALLY UNFOLDED COLLAGEN LABELED WITH [γ-^{13}C]PROLINE. D. A. Torchia, S. K. Sarkar, C. E. Sullivan and P. E. Young*. NIDR, NIH, Bethesda, MD 20205 and *Department of Natural Sciences, York College, C.U.N.Y., Jamaica, NY. 11541.

There is considerable interest in identifying cis X-Pro peptide bonds in unfolded proteins because kinetic data suggest that cis-trans isomerization is the rate limiting step in protein folding when Pro is present. Numerous C-13 NMR studies of peptides and polypeptides have shown that the chemical shift of the pyrrolidine γ-carbon is a reliable means of assigning cis and trans peptide bonds. However, it has not yet been possible to use the NMR method to identify cis peptide bonds in the spectra of unfolded proteins because of the difficulty in identifying cis resonances in the complex spectrum of the protein. We will show that cis X-Pro and X-Hyp signals are readily identified in spectra of [γ-^{13}C]Pro labeled chick calvaria collagen at 43° and 63°C. At these temperatures the collagen triple helix is unfolded, and segmentally flexible single chains are present. The C-13 spectrum consists of four sharp signals at positions (21.6, 24.0, 67.1 and 69.5 ppm) expected for X-Pro and X-Hyp cis and trans isomers. After hydrolysis of the protein, the spectrum consists of two signals at the positions of the γ-carbons in the two imino acids. This result strongly supports the assignments made in the spectrum of the protein. Measurements of the relative areas of the cis and trans signals in the protein spectrum show that 16% of the X-Pro and 8% of the X-Hyp bonds are cis. Since each collagen chain has a total of nearly 250 Pro and Hyp residues, our measurements show that each chain contains 30-35 cis peptide bonds. The implications of this result on the kinetics of molecular assembly will be discussed.

M-Pos209 EFFECT ON BPTI HYDROGEN EXCHANGE KINETICS FROM TRYPSINOGEN-BPTI COMPLEX FORMATION AND FROM TRYPSINOGEN-BPTI-ILE-VAL DIPEPTIDE TERNARY COMPLEX FORMATION. Pamela Brandt and Clare Woodward (Intr. by S. Goldstein), Dept. of Biochemistry, Univ. of Minnesota, St. Paul, MN 55108.

In trypsinogen the activation domain is disordered as compared to trypsin; this change in internal flexibility is suggested to be the basis for the regulation of its enzymatic activity (Huber and Bennett, Symposium on Mobility and Recognition in Cell Biology, 1982). Upon binding to BPTI, trypsinogen assumes a trypsin-like conformation in which the activation domain is rigidly structured. Trypsin binding also causes a marked change in the internal flexibility of BPTI in the vicinity of Tyr35 which is located in the β-sheet in the trypsin binding site region. The binding of trypsin to BPTI selectively slows the NH exchange rate of Try35 by 3 orders of magnitude, but has little effect on other β-core NH's further from the dimer interface. We find that trypsinogen binding also slows the peptide NH exchange rates of Tyr35 and Arg20 by several orders of magnitude. Tyr35 and Arg20 NH's form adjacent H-bonds in the β-sheet of BPTI. In the BPTI complex the tryspinogen activation domain also forms a binding site for exogenous Ile-Val dipeptide, an analog for the N-terminus of trypsin. The ternary complex trypsinogen-BPTI-Ile-Val has an association constant equivalent to the trypsin-BPTI complex. The addition of Ile-Val dipeptide has no effect on the hydrogen exchange kinetics of BPTI NH's. The hydrogen-deuterium exchange kinetics of BPTI in the complex is followed by ^{1}H NMR spectroscopy.

M-Pos210 INVESTIGATION OF BOVINE PROTHROMBIN AND BOVINE PROTHROMBIN FRAGMENT 1 METAL ION BINDING SITES USING TB3+ FLUORESCENCE. L.E. Sommerville and G.L. Nelsestuen, Univ. of Minn., St. Paul, MN, 55108.

The proximity of tyrptophan (Trp) residues to metal ion binding sites, the proximity of metal ion binding sites to one another and metal ion exchange processes in bovine prothrombin (Pro) and bovine prothrombin fragment 1 (F-1) have been studied by measuring fluorescence lifetimes and fluorescence intensity of the lanthanide metal ion terbium (Tb3+) bound to F-1 or Pro. The enhancement of Tb3+ fluorescence due to energy transfer (ET) from Trp residues was shown by Brittian et al. (JACS, 98, 8255, 1976) who reported that, relative to other proteins, Pro showed strong ET while F-1 showed medium ET. We confirmed their results and found that the first three metal ion binding sites on F-1 received very little ET from Trp and are bound by many protein ligands. A second group of bound ions showed the opposite properties. Most of the Trp and Tb3+ ET in Pro arises due to TB3+ ions bound in the non-thrombin portion of the intermediate 1 region (residues 157-582) of the prothrombin molecule. Titrations of the Tb3+-F-1 complex with other lanthanide metals (La3+ and Ho3+) provide evidence of both exchange and close binding proximity, indicated by Tb3+ and Ho3+ ET. The possibility of measuring intermetal ion distances in F-1 and Pro, based on parameters for Tb3+ to Ho3+ ET described by Rhee et al. (Biochem., 20, 3328, 1981) and Snyder et al. (Biochem., 20, 3334, 1981) will be discussed.

(Supported by NIH grant No. HL15728)

M-Pos211 RESONANCE RAMAN STUDIES OF 5'-DEOXY PYRIDOXAL DERIVATIVES; MODELS FOR ASPARTATE AMINOTRANSFERASE. Robert A. Copeland, Michael J. Benecky, Robert A. Pascal, Jr., and Thomas G. Spiro. Department of Chemistry, Princeton University, Princeton, New Jersey 08544.

Pyridoxal 5'-phosphate (PLP) is a ubiquitous chromophore found as a cofactor in many enzymes involved in amino acid and amine metabolism. Recently, our group studied the resonance Raman (RR) spectra of the Schiff bases of this chromophore with various amino acids. Also, we have studied the RR spectra of the PLP containing enzyme aspartate aminotransferase (AAT) in H_2O and D_2O. Based on significant shifts in frequency of the C-N (imine) stretching mode we have proposed that the 4' proton (i.e. on the imine carbon) is labile to solvent exchange in this protein. Here we present RR spectra for the valine Schiff bases of 5'-deoxy pyridoxal, and 5'-deoxy, 4'-deutero pyridoxal at high (9.0) and low (5.0) pH in both H_2O and D_2O. The variations in the spectral patterns among these models closely simulate the changes observed in the AAT spectrum when the solvent is changed from H_2O to D_2O. Data will be presented which strongly suggest that those changes observed in the protein spectra reflect solvent deuteration of the 4' position, as well as the ring nitrogen, in D_2O solutions.

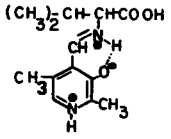

Valine Schiff base of 5'-deoxy pyridoxal.

M-Pos212 FLUORESCENCE DEPOLARIZATION STUDY OF HYDRATION-INDUCED PROTEIN NANOSECOND INTERNAL ROTATIONAL MOBILITY. M. LIMKEMAN and E. GRATTON, Dept. of Physics, University of Illinois, Urbana, Illinois.

The effect of hydration on protein dynamics was investigated using steady state fluorescence depolarization on azurin, which has a single tryptophan residue well-buried in the hydrophobic interior. Azurin was embedded in a thin, solid, water-permeable polymer film. This inhibited whole-protein motion while allowing examination of internal degrees of rotational freedom in the protein as a function of film hydration. In the dry film at room temperature the tryptophan fluorescence emission showed the limiting polarization characteristic of low temperature solutions in which all motion is frozen. As the hydration was increased, the observed polarization value changed sharply at about 0.6 h (h = g H_2O/g film), indicating an increase in the rotational mobility of the tryptophan. The fully hydrated film had a polarization equal to that of an azurin solution measurement extrapolated to infinite viscosity where the rotation of the protein as a whole was hindered. We conclude that the protein internal mobility is linked to the hydration level, and that hydration can turn on the full protein flexibility on the nanosecond time scale accessible by fluorescence techniques.

M-Pos213 CHARACTERISTIC VIBRATIONAL MODES OF γ-TURNS. J. Bandekar and S. Krimm, Biophysics Research Division, University of Michigan, Ann Arbor, MI 48109.

Normal mode calculations have been done on γ-turn structures in order to characterize the vibrational frequencies of this polypeptide chain conformation. The model system used was CH_3-CO-(Ala)$_5$-NH-CH_3, with the Ala CH_3 groups taken as point masses. The force field was a recently refined one appropriate to such a point mass approximation. Three conformations were studied: (a) a γ-turn, (b) a mirror-related γ-turn, and (c) an inverse γ-turn such as is found in thermolysin. Dihedral angles ϕ_1, ψ_1 and ϕ_5, ψ_5 correspond to a β-sheet structure, although other conformations are being studied. In the turn, the amide I mode of peptide group 3 is found to be an isolated mode characteristic of the turn: 1670(a), 1655(b), 1660(c). The amide I modes of the other peptide groups of the turn are mixed: (a) 1655(4), 1663(2,5,6), 1666(5,6), 1675(2,5,6); (b) 1664(4,5,6), 1665(4,6), 1668(4,5,6);(c) 1667(4,6), 1668(4,6), 1655(5). The amide II modes of the turn mix in a different manner for the three structures: (a) 1554(2), 1527(3), 1509(4); (b) 1510(2,3), 1547 (3,2,4), 1544(4,3); (c) 1506(2), 1525(4,3,5), 1541(5,3), 1558(4,3,5). The amide III modes do not allow strong distinctions between the three structures, but the amide V modes do provide for such a possibility. These points will be discussed in greater detail, as will the results of calculations on a model cyclic pentapeptide containing a γ-turn. Also, a comparison will be made with characteristic modes of β-turns and of α-helix and β-sheet structures. This research was supported by NSF grants PCM-8214064 and DMR-8303610.

M-Pos214 STUDIES OF PROTEIN SECONDARY STRUCTURE BY RESOLUTION-ENHANCED FT-INFRARED SPECTROSCOPY. D. Michael Byler and Heino Susi (Intr. by Shu-I Tu), Eastern Regional Research Center, U. S. Department of Agriculture, 600 East Mermaid Lane, Philadelphia, PA 19118.

Fourier self-deconvolution and second derivative techniques have been used to enhance the resolution of the infrared spectra of selected proteins in both D_2O solution and in the solid state. These mathematical procedures permit the inherently broad features observed in such spectra to be resolved into distinct peaks. In the amide I region (1600-1700 cm^{-1}), for example, where absorption is due to hydrogen-bonded C=O stretching vibrations of the peptide linkages, the observed frequency positions of the newly-resolved bands can be associated with specific protein secondary structures. Theoretically, the areas of the overlapping bands which compose the broad, ill-defined features in the original spectra do not change upon deconvolution into the individually resolved constituents. Thus quantitative estimation of the proportion of each conformation in the secondary structure of a protein should soon be possible.

These resolution-enhancement methods are already providing new insights on "turns" and on hydrated peptide linkages in proteins. Such data are not, to our knowledge, presently available by other spectroscopic techniques. Deconvolution and second-derivative spectroscopy can also provide information on amino acid side-groups and on the conformational changes which occur upon denaturation of proteins.

M-Pos215 SIMULTANEOUS ANALYSIS OF MULTIPLE FLUORESCENCE EMISSION ANISOTROPY DECAYS Joseph M. Beechem, Jay R. Knutson and Ludwig Brand, Dept. of Biology, The Johns Hopkins University, Baltimore MD 21218.

It has recently been shown (Knutson, et al., Chem. Phys. Lett. 1983) that simultaneous analysis of related decay curves ("global analysis") greatly improves the accuracy with which decay parameters can be determined. In a similar fashion, it is often possible to greatly overdetermine anisotropy decay parameters. This is accomplished by observing the same hydrodynamic process under a variety of different conditions (change in: excitation wavelength, probe location, timing calibration, temperature, viscosity, etc.). A non-linear least squares algorithm will be described for simultaneous analysis of multiple anisotropy decay experiments which greatly increases the accuracy in recovered multiple rotational correlation times. Analysis of simulated data by this method shows that biexponential decay of the anisotropy with rotational correlation times that differ by as little as 20% can be resolved. Specific examples concerning anilino-napthalene sulfonates bound to horse liver alcohol dehydrogenase will be described. A similar program for analysis of polarized phase/modulation data will be discussed.

Supported by NIH grant No. GM 11632.

M-Pos216 RAMAN SPECTROSCOPY OF HOMOLOGOUS PLANT TOXINS: CRAMBIN, α_1- AND β-PUROTHIONIN SECONDARY STRUCTURES, DISULFIDE CONFORMATION AND TYROSINE ENVIRONMENT, Robert W. Williams* and Martha M. Teeter. *Optical Probes Branch, Naval Research Laboratory code 6510, Washington, D. C. 20375 - current address: Biochemistry Department, Uniformed Services University of the Health Sciences, 4301 Jones Bridge Road, Bethesda, MD 20814. **Department of Chemistry, Boston University, 685 Commonwealth Avenue, Boston, MA 02215.

A quantitative analysis of the Raman amide I spectra of the highly homologous (40%) proteins crambin, α_1- and β- purothionin shows that while the secondary structure content of these proteins is about the same, helical segments in the purothionins appear to be significantly more irregular than those in crambin. An anlaysis of the conformational preferences of the amino acids in these proteins is consistent with this evidence. Based on a combined amide I and sequence conformational analysis we propose that while the overall 3-dimensional structure of the purothionins is the same as that of crambin with the exception that residues 7-12 in the purothionins form an irregular helix or overlapping turns. The disulfide bands for α_1-purothionin and crambin are both at 503 cm^{-1}, indicating that the disulfide bands for α_1-purothionin are not in strained conformations. The α_1-purothionin tyrosine doublet at 830 and 850 cm^{-1} is identical to that of crambin, indicating that the phenolic OH is probably exposed to the solvent.

M-Pos217 INTERPRETATION OF THE "SOLUBILITY LIMIT" OF POLYMERIZING PROTEINS. Judith Herzfeld, Department of Physiology and Biophysics, Harvard Medical School, Boston, MA 02115.

The apparent solubility limit of polymerizing proteins is generally attributed to the formation of helical fibers with multiple stabilizing contacts between monomers: in extreme cases, the relative instability of small aggregates will lead to condensation-like behavior in which monomers "precipitate" at the "solubility limit" into very long polymers. However, protein polymers are not macroscopic in the thermodynamic sense and, except under high centrifugal forces, they remain in solution with the monomers. Except at low volume occupancy, the behavior of this mixture of aggregates and monomers is heavily influenced by packing constraints. Using lattice models, we have shown that a limit in the monomer concentration occurs as a result of packing constraints whether polymerization is linear or helical, although the approach to this limit is characteristically different in the two cases. The limit results from the competition of monomer and polymer for maximum rotational and translational freedom in the solution. Whereas at low volume occupancy solute added to a solution goes progressively more into polymer and less into monomers, beyond a certain point not only does all the solute added go into polymer, but the extra polymer so formed drives monomer already present into polymer. The situation is further complicated by the fact that any other molecules present in the solution also contribute to the packing constraints. Thus, the apparent solubility limit of polymerizing proteins is not generally simply related to the free energy of monomer association.

M-Pos218 MOLECULAR DYNAMICS SIMULATIONS OF THE THIRD DOMAIN OF TURKEY OVOMUCOID. Joe W. Keepers and Ronald M. Levy, Department of Chemistry, Rutgers University, New Brunswick, New Jersey 08903

Two molecular dynamics simulations of The Third Domain of Turkey ovomucoid inhibitor have been completed. In the first simulation, twenty 10ps trajectories each with different initial conditions were calculated, while in the second simulation a single 200ps trajectory was constructed. The dynamics of the protein backbone and the side-chains including the 18 methyl groups in turkey ovomucoid third domain were followed explicitly. For each of the simulations we have calculated the average protein structure, the root-mean square atomic displacements for each of the atoms, and the order parameters S^2 corresponding to ^{13}C NMR relaxation of each of the methyl groups as well as other selected groups in the protein. The results of the analysis of both simulations suggest that: (1) the region of the active site of Turkey ovomucoid third domain (residues 15-21) is significantly more mobile than the rest of the protein and (2) the conformational space accessible to the protein appears to be more efficiently sampled in the series of short trajectories than the single long trajectory. We also discuss the variation in the effective barrier to rotation of the methyl groups in different regions of the protein due to protein packing differences.

M-Pos219 ROTATIONAL BEHAVIOR OF SEGMENTALLY FLEXIBLE MACROMOLECULES WITH RESTRICTED BENDING AND TWISTING. William A. Wegener, Baylor University Medical Center, Dallas, Texas 75246.

A Brownian motion computer simulation is used to generate rotational relaxation curves for bodies composed of two cylindrically symmetric rigid segments connected at their endpoints by a flexible swivel joint. Small angular displacements of the segments involve both random components determined by configurationally dependent diffusion coefficients as well as directed components determined by any internal forces. The diffusion coefficients are calculated using bead model methods and include intrasegmental hydrodynamic interactions, while the restrictions to bending and twisting motions between segments are represented by sharp internal boundaries or elastic restoring forces. For large degrees of flexibility, the simulation results are well described by previously derived expressions for completely flexible bodies. For small degrees of flexibility, wobble models suffice, with rigid body expressions applying as the extent or rate of flexible motions vanish. Specific relaxation techniques treated include fluorescence depolarization, transient birefringence and depolarized light scattering. These restricted flexibility models are used to interprete data on myosin. Supported by NIH grants HL-26881 and GM-32437.

M-Pos220 CALCULATION OF THE EFFECTIVE DIELECTRIC CONSTANT IN THE INTERIOR OF PROTEINS. B. Honig, M. Gilson, R. Fine* and A. Rashin, Dept. of Biochemistry, and *Dept. of Biological Sciences, Columbia University, New York, New York 10032, and *10027.

The effective dielectric constant (D) for the coulombic interaction between pairs of atoms in a protein is a variable that frequently arises in studies of protein structure and function. Force fields used in energy minimization and molecular dynamics studies generally use constant values, in the range of D=2-5, or a distance dependent dielectric. Most calculations of the electrostatic potential in the interior of proteins, for example, at the active site, have employed a small, constant dielectric constant. Small values of D implicitly assume that buried charges and polar groups are effectively shielded from the solvent. However, the extent of shielding is clearly dependent upon the location of the atoms within the protein and on their depth from the surface. Thus, the effective dielectric constant should be different for each pair of atoms in the protein. Most current treatments of solvent screening are based on the Kirkwood theory which represents the protein as a spherical cavity of low dielectric constant embedded in a high dielectric solvent. The theory has been shown to provide a successful account of pH-dependent phenomena on the surfaces of a number of proteins. We have applied the theory to the interior of proteins and have found that the effective dielectric constant can vary by two orders of magnitude. One unique aspect of our approach is the application of the theory to polar as well as to charged residues. Our results have important implications for a wide range of problems. Among these are calculations based on empirical force fields and considerations of long range vs. short range electrostatic effects in proteins.
Supported by NIH Grants GM 30518 (to B. Honig) and RRO-0442 (to Cyrus Levinthal).

M-Pos221 CAN DETAILED STRUCTURAL PREDICTIONS BE MADE FOR HELICAL PROTEINS? A. Rashin, B. Honig, R. Fine* and Cyrus Levinthal*. Dept. of Biochemistry, Columbia University, N.Y. 10032, and *Department of Biological Sciences, Columbia University, New York, N.Y. 10027

Secondary structure prediction schemes have achieved a considerable degree of success, especially for α-helices. The prediction of tertiary structure, for example in membrane proteins which are often found to be helical, requires the design of algorithms for the packing of fragments of secondary structure. Although general packing patterns have been extensively studied, the successful achievement of detailed predictions has not been reported. A simple predictive scheme (the "evolvement" method) based on use of the two-dimensional representations of ideal α-helices has successfully accounted for packing patterns and conformations of many side chains (at the level of rotational isomers) involved in the interactions of helical pairs in myoglobin and hemoglobin[1]. However, a survey of α-helices in known structures has revealed both significant deviations from ideality and the presence of many 'kinks'. These factors complicate the detailed prediction of structure at atomic resolution. A stepwise strategy to explore the possibility of accurately predicting helix packing patterns, based on a computerized three-dimensional version of the evolvement method, is outlined for helical proteins. Progress is reported on the "prediction" of side chain conformations in known structures. Extensions to unknown structures are discussed.

[1]A. Rashin, In: Biomolecular Structure, Conformation, Function and Evaluation. Volume 2, R. Srinivasan, ed., Pergamon Press, Oxford (1980).

[2]Supported by NIH Grants GM 30518 (BH) and RRO-0442 (CL).

M-Pos222 MODELS OF THE COLICIN E1 CHANNEL; SALT BRIDGES IN THE LIPID. R. Fine, and C. Levinthal, Department of Biological Sciences, Columbia University, New York, NY 10027.

We present a possible molecular model of the bacterial membrane channel-forming protein Colicin E1. The sequence of the coding region for this protein has been published (Yamada et al. PNAS). A C-terminal fragment consisting of 152 Amino Acids has been isolated by CNBr cleavage in our laboratory and has been shown to form a voltage-dependent ion channel in a lipid bilayer in the Finkelstein laboratory (Cleveland et al. 1983 PNAS 271: 3706-3710). The channel is known to have a lumen diameter of approximately 7-9 Angstroms. Using a combination of cardboard cylinders and helical wheels, computer graphics, energy minimizations, and CPK space filling models, two classes of models consistent with the sequence and with requirements of close packing, large lumen size, and neutralization of the charges in the C-terminal fragment are examined. The general procedures for determining helix packing and the lumen size in a membrane channel model will be discussed. In addition, calculations will be presented indicating that a salt-bridge between a positively charged and a negatively charged amino acid is energetically acceptable if both amino acid residues are within the lipid region of the membrane where the dielectric constant is low. The salt-bridges in a region of low dielectric constant account for about half of the 41 charged residues and the remainder are either facing into the lumen or outside the membrane. Supported by NIH grant RR00442.

M-Pos223 EFFECTIVE INTER-RESIDUE CONTACT ENERGIES FROM PROTEIN CRYSTAL STRUCTURES. S. Miyazawa and R. L. Jernigan, (Intr. by M. Kanehisa), Lab. of Math. Biol., NCI, NIH, Bethesda, MD 20205

Contact energies for proteins in solution are estimated from the numbers of residue-residue contacts observed in crystal structures on the basis of the quasi-chemical approximation with an approximate treatment of the effects of chain connectivity. A protein is regarded as a close-packed mixture of unconnected residues and effective solvent molecules whose size is the average size of a residue. The quasi-chemical approximation, that contact pair formation resembles a chemical reaction, is applied to this system with the basic assumption that the average characteristics of residue-residue contacts formed in a large number of protein crystal structures reflect actual differences of interactions among residues, as if contacts among residues and solvent molecules in each protein were in quasi-chemical equilibrium. The number of effective solvent molecules for each protein is chosen to yield the number of residue-residue contacts equal to its expected value at Flory's $\theta/T=0$ condition. A residue is represented by the center of its side chain atom positions, and contacting residues and effective solvent molecules are defined to be close pairs within a distance of 6.5A; nearest neighbor pairs along a chain are explicitly excluded in counting contacts. Coordination numbers, for each type of residue and solvent, are estimated and used to evaluate the numbers of residue-solvent and solvent-solvent contacts. Estimated contact energies have reasonable residue-type dependences, reflecting residue distributions in protein crystals; non-polar-in and polar-out are seen as well as the segregation between these residue groups. There is a linear relationship between the average contact energies for non-polar residues and their hydrophobicities reported by Nozaki and Tanford. The relevance of results to protein folding and other applications will be discussed.

M-Pos224 PROTEIN FRACTAL DIMENSIONS AND THE DENSITY OF LOW FREQUENCY VIBRATIONAL MODES. J. T. COLVIN, G. C. WAGNER, J. P. ALLEN, AND H. J. STAPLETON, Depts. of Physics and Biochemistry, University of Illinois, Urbana, IL 61801.

The fractal dimension, $\bar{d}$, of a polypeptide chain can be accurately estimated from the x-ray crystallographic coordinates of the α-carbon atoms. This structural parameter has been computed for the protomer structures of 50 proteins and found to range between 1.20 and 1.81. Proteins of homologous suprasecondary and tertiary structure are characterized by a corresponding agreement in $\bar{d}$. A second parameter, the spectral dimension, $\tilde{d}$, defines a protein's density of vibrational states as a function of frequency, $\rho(\nu) \propto \nu^{**}(\tilde{d}-1)$. Depending upon the off-backbone connectivity of the biopolymer chain, spectral dimensions have been shown (1,2) to range between 1 and $\bar{d}$. For proteins, this upper limit implies a density of vibrational states that varies with a fractional power of frequency. Raman spin relaxation rates in paramagnetic proteins are correlated to this reduced frequency dependence through a reduced temperature dependence, i.e., $T^{**}(3+2\tilde{d})$ rather than $T^{**}9$. Relationships between $\bar{d}$ and $\tilde{d}$ are discussed in relation to the observed dependence of $\tilde{d}$ changes with sample conditions. We also compare a theoretically computed histogram (3) of the 117 lowest frequency ($\nu \leq 2250$ GHz) vibrational modes in bovine pancreatic trypsin inhibitor (BPTI, 58 residues). A fractal dimension of $\bar{d}=1.23\pm0.05$, calculated from BPTI crystallographic coordinates, agrees with a spectral dimension of $\tilde{d}=1.22\pm0.01$, that was obtained from a least squares fit to the histogram data. Supported in part by NIH Grants GM24488 and AM00562.

(1) S. Alexander and R. Orbach, J. Physique-Lettres, 43, L-625 (1982).
(2) R. Rammal and G. Toulouse, J. Physique-Lettres, 44, L-13 (1983).
(3) N. Gō et al., Proc. Natl. Acad. Sci. USA 80, 3696 (1983).

M-Pos225 ON THE MEAN-FIRST-PASSAGE-TIME APPROACH TO THE KINETICS OF DNA CRUCIFORM TRANSFORMATION.
Yi-der Chen and T. Tsuchiya, Laboratory of Molecular Biology, NIADDK, NIH, Bethesda, MD 20205.

Recently, the kinetics of disappearance of cruciform conformations in relaxed palindromic DNAs has attracted considerable attention in relation to the study of rate constants of branch migrations at the Holliday junction. In many cases, the kinetic data was analyzed in terms of a simple two-state model,

$$C \xrightarrow{k} L \qquad (1)$$

where C and L refer to the cruciformed state and the linear (noncruciform) state, respectively, and k is equal to the reciprocal of the mean first passage time of a random walker between a reflection and an absorbing barrier. In fact, the full kinetic scheme of cruciform transformation should be written as

$$N \rightleftharpoons N-1 \rightleftharpoons \cdots\cdots \rightleftharpoons 2 \rightleftharpoons 1 \longrightarrow L, \qquad (2)$$

where the numbers 1,2, $\cdots$, N represent the number of paired base pairs in the extruding arm of the cruciform. It is not obvious that Eq. (2) can be reduced to Eq. (1). In this study, the differences between these two equations were calculated for a number of cases. It is found that the mean first passage time approach is not a bad approximation for cruciform formation kinetics.